

THE TRANSPORT OF RADIOISOTOPES BY FINE PARTICULATE MATTER IN AQUIFERS

A THESIS

Presented to

The Faculty of the Graduate Division

by

Jerry B. Francis Champlin

In Partial Fulfillment

of the Requirements for the Degree

Doctor of Philosophy in the School of Nuclear Engineering

Georgia Institute of Technology

December 1969

THE TRANSPORT OF RADIOISOTOPES BY FINE PARTICULATE MATTER IN AQUIFERS

Approved:

Chairman

Date approved by Chairman Dec 11, 1969

In presenting the dissertation as a partial fulfillment of the requirements for an advanced degree from the Georgia Institute of Technology, I agree that the Library of the Institute shall make it available for inspection and circulation in accordance with its regulations governing materials of this type. I agree that permission to copy from, or to publish from, this dissertation may be granted by the professor under whose direction it was written, or, in his absence, by the Dean of the Graduate Division when such copying or publication is solely for scholarly purposes and does not involve potential financial gain. It is understood that any copying from, or publication of, this dissertation which involves potential financial gain will not be allowed without written permission.

A handwritten signature in dark ink, appearing to be "J. J. [unclear]", written over two horizontal lines.

7/25/68

ACKNOWLEDGMENTS

The support of the Schools of Nuclear and Civil Engineering, Nuclear Sciences Division, Engineering Experiment Station, Georgia Institute of Technology, and the United States Department of the Interior, Office of Water Resources Research made this investigation possible and their aid is gratefully acknowledged. The work was administered through the Water Resources Center of the Georgia Institute of Technology as authorized under the Water Resources Act of 1964 (P.L. 88-379). The donation of the clay used in the study by the J. M. Huber Company of Wrens, Georgia, aided much in bringing the research to fruition.

The author would like to express his appreciation to Dr. G. G. Eichholz for his interest, cooperation and advice. Special thanks are due to Ekkehart Gasper and John Clark of the Biology Department for aid in isolating the bacteria so that their images might be photographed with the electron microscope. The special attention and care in the preparation of those images by John Brown's electron microscope group at the Engineering Experiment Station, Georgia Institute of Technology was especially appreciated. The laser scattering patterns were photographed by David Fellows of Felcraft Enterprises and his care and concern about them helped immeasurably in the preparation of that section of the thesis.

Permission was granted by the Graduate Division for special pagination and margins so that this dissertation could be published as a Water Resources report.

TABLE OF CONTENTS

	Page
I. INTRODUCTION	1
Migration of Radioactivity with Suspended Matter	
The Source of Fine Particles in Groundwater	
Penetration of Packed Sand Beds by Suspended Matter	
The Potential Transport of Pollution by Particles	
II. THEORETICAL CONSIDERATIONS	14
Water	14
The Water Interface	
Hydration of Ions and the Dielectric Constant	
The Magnitudes of Physical Interactions	24
Thermal Forces and the Kinetic Energy of Particles	27
Diffusion Coefficient	
Mean Particle Velocity and Momentum	
Gravitational Interactions	
Radioactive Atom Recoil	
Van der Waals Reactions	
The Presence of Charges in Water	
Submicron Particles in Water	
Van der Waals Interactions Between Particles and Grains	61
The Particle Charges	
The Particle Charge and Ion Exchange	
Chemical Complex Formation and Surface Ion Exchange	76
Ion Exchange and the Silica-Silicate Surface	80
Particle-Particle Charge Interactions	
Particle Interactions between Unlike-Charged Particles	
The Removal of Suspended Particles from Water by	
Porous Media	
Straining	
Sorption	
III. EXPERIMENTAL PROCEDURE	102
Apparatus.	105
Sand Container	
Vibrator Packer	
Side-scanning Radioactivity Detector (GM)	
Side-Scanning Radioactivity Detector (Scintillation Crystal)	
Detector for Radioactivity in the Effluent	

LIST OF TABLES

	Page
1. Diffusion Coefficients of Particles in Water Involved in Experimental Work (300°K).	34
2. Comparison of Molecular Interaction Energies at Different Distances.	53
3. Comparison of Hydration and Lattice Energies for Monovalent Ions.	55
4. Summary of Interaction Energy Ranges	56
5. Bond Energies Between Adsorbed Cations and Charged Lattice Sites	71
6. The Bond Energies of EDTA and Various Cations at Normal Temperatures.	79
7. Free Energy of Hydration of Monovalent Cations	85
8. Comparison of Hydrated to Crystal Ionic Radii for Selected Cations.	87

LIST OF ILLUSTRATIONS

Figure		Page
1.	Van der Waals Interaction Energy for Particles and Grains	66
2.	Effects of NaOH Addition to Clay	77
3.	Energy of Interaction Between Kaolin Plates	92
4.	Container for Packed Sand Model Aquifer	106
5.	Photomicrographs of Soil Bacteria	118
6.	Combined Energy Spectrum of ^{46}Sc , ^{86}Rb , ^{140}La	126
7.	Deposition of Radioactivity Relative to Aquifer Construction	127
8.	Relative Deposition of ^{46}Sc , ^{86}Rb , ^{140}La in Sand Bed	129
9.	Similarity in Radioactivity Retention of First 40 cm for ^{46}Sc , ^{131}I , ^{140}La	131
10.	Displacement of ^{131}I in Sand Bed by NaCl Solutions	132
11.	^{131}I Displacement Relative to NaCl Molarity	134
12.	^{46}Sc Redistribution in Sand Bed as a Result of NaCl Solution Leaching	135
13.	Bromide-Bacteria Release Profile	137
14.	^{82}Br Recovery in Effluent Water	138
15.	Iodide-Kaolin Release Profile (NaCl Eluent)	140
16.	^{46}Sc -Kaolin Displacement by Sodium Tetrphosphate Solutions	142
17.	^{46}Sc -Kaolin Front Showing Near Parallel Displacement After Each 20-Liter of Influent	143
18.	Symmetric Displacement of ^{46}Sc -Kaolin	144

LIST OF ILLUSTRATIONS (Continued)

Figure		Page
19.	Laser Scattering (Angular Dependence) by Aqueous Suspensions	146
20.	Laser Scatter Patterns of Aqueous Suspensions	147
21.	Scattering Intensity of ^{82}Br -Bacteria Effluent Samples at 3°	150
22.	Fractional Distribution of Particle Sizes in Kaolin Suspensions	151
23.	Bacterial Particles in ^{82}Br Effluent	153
24.	Electron Photomicrographs of Filter Surfaces, ^{131}I Labeled Influent and Effluent Clays	154
25.	Comparison of ^{131}I -Kaolin and ^{46}Sc -Kaolin on $5\ \mu$ Membrane Filters	155
26.	Electron Photomicrograph of ^{46}Sc -Kaolin Effluent Suspensions on Membrane Filters	157
27.	Energies of Interaction Conformed to Mean Particle Size of Kaolin Used in Sand Bed	168

SUMMARY

The information required to explain the long-range movement of radioactive fission products from waste pits, fallout, and underground nuclear explosions, as well as that of other environmental pollutants, is sought in this thesis. Both theoretical and experimental investigations of the various phenomena that pertain to ion transport or retention by soils are included.

The theoretical section delves into the interactions between solids in water that result from thermal forces, electrostatic charges, and van der Waals forces. The particle range considered is that of the large colloid to the finest silt. Sources of energy sufficient to cause breakage of adsorption bonds and the importance of the concept of additive bonding in the water are discussed. The important relationship between suspended particles and the "massive" granules making up the model aquifer is explored at some depth.

In the experimental section, factors which influence either retention of radioactivity by the sand bed or transport of the activity through such a bed by micro-particles are considered. Correlation is sought between the phenomena observed experimentally and that predicted in the theoretical section. Casimir's correction to the theoretical van der Waals interactions is proposed to account for major changes in the particle retention ability of the sand bed when dispersants are included in the influent water.

A concluding section is included which discusses the future potential of such research, as well as some of the practical aspects of the results reported here.

CHAPTER I

INTRODUCTION

Considerable concern has been expressed since the inception of the atomic industry about the disposition of the waste radioactivity that results from the reprocessing of the uranium and plutonium fuel elements used in nuclear reactors. These radioactive products are formed for the most part by fission reactions involving ^{235}U , ^{236}U , and ^{239}Pu ^{1,*}. The fuel elements from reactors are scrapped, after only a fraction of their total fissile material is consumed, and reprocessed to recover the fissionable elements. After solution of the fuel elements in strong acid mixtures, the fissionable materials are removed by organic solvent extractions leaving the highly radioactive fission products in the aqueous phase.

Retention of this radioactive concentrate for the period of several generations necessary for the long-lived radionuclides to decay to safe levels of radioactivity requires continuing concern. Over the years that they have been produced, most of these high-level radioactive wastes have been retained in steel tanks or concrete vaults, depending on the final pH of the processed ionic solutions. Realizing that such containers can leak or be ruptured by explosions or earthquakes, other more permanent means of storage have been sought that were not so subject to the whims of politics or of nature. These include storage of sintered or bonded waste solids in salt mines, injection of aqueous waste solutions

*Superscript numbers refer to literature cited in list of references.

into porous formations in the geologic depths, and injection of waste-grout mixtures by hydraulic fracturing into shale beds at relatively shallow depths. However, tanks may leak, and materials injected into sedimentary formations or stored in mines may become subject to leaching by ground waters. Once the release of the high-level radioactive waste to the environment has occurred, whether by accident or design, its migration from the point of origin would follow essentially that about to be described for the low-level waste to be described shortly.

Associated with high-level waste production are intermediate-level wastes consisting primarily of ionic solutions that contain far less radioactivity per unit volume than do the high-level wastes. The former are the wash waters and raffinates that arise from the concentration of the high-level wastes by precipitation into as small a bulk volume as it is economic to make. Over the last twenty years, the intermediate-level wastes have been stored in open pits cut in the surface soils or in buried gravel-filled crypts where the soil was depended on to decontaminate the water carrier as it slowly percolated through into the groundwater. Generally speaking, the volume of the intermediate wastes is so great that it is not profitable to attempt total containment and seepage of the water from the disposal area is a necessary requisite of the industry.

Low-level wastes include reactor cooling waters, wash waters for certain chemical processes, and general low level laboratory wastes. These are very large in volume and after treatment with common water treatment techniques for combined conditioning, adsorption, precipitation and flocculation of the water contaminants, the waste water passes through a

settling basin and out over a weir to the main drainage of the area. There dilution within large streams or other bodies of water is used to reduce the remaining radioactivity to well below maximum permissible concentration (MPC)^{2,3}.

Of greatest concern are those radioisotopes that are produced with relatively high probability in the fission reaction. These include primarily ^{90}Sr and ^{137}Cs , both of which have a half-life of about 30 years, although ^{106}Ru (one year) and ^{144}Ce (285 days) also should be noted⁴. The same group of fission products also may be produced during the detonation of a nuclear device in the atmosphere. They are dispersed from the general shot point location by wind and precipitation run-off. Studies made on the disposition of these explosion-produced fission products in fallout indicate that they follow much the same course in the soil as those released from nuclear reprocessing plants. The interaction of radioactive ions with soil particles is a major factor in the engineering of radioactive waste disposal. The presumption is that once the fission products have reacted with the soil, the radioactivity becomes immobilized or "fixed" and can be relied on to remain well within the confines of the disposal site except for a slow movement due to ion exchange kinetics through the soil at a rate of inches per year⁵.

Fixation or immobilization are terms which infer that the radioactivity, which might have been initially moving with and at the rate of the water, comes to be attached to solid surfaces that are fixed in place. Consequently, this effective removal of the radioactivity from the water as it passes through the soil or porous rock leaves the water containing

less of the radioactive contaminant than it did previously. Such fixation may occur as a direct result of ion exchange on clay surfaces or if the radioactivity is being carried in the form of a suspended particle, the removal may be brought about by physical effects such as "straining" or "sorption". These points will be discussed in some detail in Chapter II.

Treatment of the waste with soil minerals either in place or as additives has been practical in the past because the radioactivity of the water was reduced by the treatment to non-hazardous levels. Unfortunately, the fixation of radioactivity by soils is not 100 percent effective. Special efforts have been made to lower the concentration of certain isotopes known to be present in fission wastes even after a "cooling" period. In particular, workers at Oak Ridge have shown specially prepared vermiculites could be used for cesium-137 stripping and that addition of calcareous phosphates to the wastes would increase the removal of strontium-90 by soil minerals^{6,7}. Similarly, the zeolite-like mineral clinoptilolite was studied at Hanford as a special additive to radioactive waste water that would bond strontium and cesium strongly, thereby reducing the release of radioactivity to the environment⁸⁻¹¹. The chemical methods of precipitation are effective up to about 85 percent removal of the isotopes, and with proper conditioning this may be increased by the addition of adsorbing agents such as clays, lime, special minerals, etc. But there is always a finite fraction of the original radioactivity left for which no further attempt at recovery or retention is economically practical. The remaining waste is released to the soil in the hope that any remaining radionuclides will be taken out of the water there^{3,2}.

Thus, the "leakage" of radioisotopes from aqueous nuclear waste

storage ponds dug in the local soil is an accepted fact at every facility where such storage is practiced. That such "leakage" can be tolerated at all hinges on the fact that the soil is such an effective ion exchanger that almost all of the radionuclides present in the wastes adsorb to the soil surfaces near the boundaries of the disposal ponds and are retained there, migrating only a few inches a year.

The concern with radioisotopes disposal cannot and does not end with environmental dilution to tolerable levels. Radioisotopes of the element ruthenium, for example, are observed to pass through large thicknesses of soil, apparently unaffected by the adsorption characteristics of the soil^{12,3,2}. Christenson and Thomas¹³ noted the migration of other isotopes through the soil under certain conditions, especially those of plutonium and strontium. Various chemical, physical and biological processes tend to reconcentrate the radioactivity to levels which may be hazardous to animal and plant life, especially when maintained in the food chain.

Migration of isotopes from containment sites has been observed for years and a considerable amount of effort has gone into determining why it occurred and what methods could be incorporated into the recovery process to stop the "leakage". For example, the movement of ^{60}Co from a disposal area was shown to be related to its being sequestered by ammonium citrate used in the plant process. Introduction of an ionic exchange resin in the process effluent stream reduced the problem¹⁴. Ruthenium release, however, has been a continual problem that has seemingly defied efforts to tie its migration from waste disposal sites to chemical

chelation or production of anionic complexes as nitrosyl compounds in the plant processes^{15,16}.

Migration of Radioactivity with Suspended Matter

Fletcher¹⁶ investigated the anionic nitrosyl complexes of ruthenium as a possible explanation for the migratory ability of this waste fission product. Others, such as Jones,¹⁷ were able to show that the nitrosyl ruthenium compounds were absorbed to soil particles also and as such were not a satisfactory scapegoat for the leakage problem. Japanese workers observed that ruthenium had an exceptionally high mobility in the soil compared to cesium and strontium even when it originated from fallout¹⁸. This high degree of migratory ability of the ruthenium isotope without the association with chelating chemicals or the high concentrations of nitrate needed to form the nitrosyl complexes makes the chemical chelation theory untenable, at least as the primary cause.

"Flowshare" studies showed the ruthenium from fallout to be almost entirely associated with fine particles of soil that were especially prone to movement with water¹⁹ and particle-separation studies conducted at Oak Ridge on the waste streams showed ruthenium to be concentrated on the finest particles separated by the centrifugal separators²⁰. Studies made in Solway Firth and the Irish Sea off Windscale showed the ruthenium to be associated with particles sufficiently fine to remain in suspension for some time and to be caught and collected in the gills of fish and invertebrates²¹. Champlin⁴ recently showed that ruthenium and a number of other elements could be caused to migrate with the water flowing through a packed sand bed, if previously associated with fine particles

of clay. The results also suggested that bacteria, acting as accidentally participating particles, might be carriers of fission product contaminants in the water. Radioactive ions that react with soil may become attached to mineral, organic, or biological particles that are themselves co-mobile with the groundwater. Changing physical and chemical conditions in the soil may encourage this mobility with the result that the radioactivity is carried far beyond the boundaries of the disposal sites.

Trace element transport by sorption on fine particles suspended in water was noted recently in investigations made by Johnson, Cutshall and Osterberg²² in oceanographic studies off the Columbia River Estuary. They followed the interchange of radioactive ions from particles suspended in the river water with other chemi-physical forms after mixing with the sea water. Eichholz and co-workers²³ followed a somewhat parallel course in their study on trace element fractionation by suspended particles in water. However, their efforts were confined to the "fresh water" portion of many of the nations' rivers. Their studies were limited to bottled samples of river water with which were mixed synthetic radioactive waste mixtures or fission product separates and transference from one chemi-physical form to another under salinity gradient conditions was not included.

Recent papers by Black and coworkers^{24,25} demonstrate the rising interest in the importance of suspended matter in groundwater and the new techniques required to study the physical and chemical reactions of this material. Workers at the Battelle Memorial Institute are applying computerized analytical techniques to the interpretation of waste transport in terms of known or suspected groundwater-flow parameters. Programs

presented by R. W. Nelson²⁶ at the National Symposium on Groundwater Hydrology in San Francisco showed that considerable progress is being made in that regard, at least as far as the Hanford crib-waste disposal areas are concerned.

The Source of Fine Particles in Groundwater

In their studies on the disposal of radioactive nuclear waste into porous, permeable rocks located far below the surface, the U. S. Bureau of Mines Core Analysis Research team at Bartlesville, Oklahoma observed that clouds of clay were released from sandstone by the passage of an ionic front in the infiltrating water²⁷. While realizing the possible hazard to a disposal project from the formation-plugging these particles might cause, they noted that these suspensions remained exceptionally stable except on the addition of strong acid or heavy ions. Later, ultrasonic studies established that the bonding strength of such particles to the sand grains (from which they had been derived in the above) was below chemical bond energies and should be subject to ionic gradient effects as had been observed²⁸.

This mechanism in inverse form appears to be the same as that by which sand and gravel filters function. Most commonly, additives such as alum are placed in water carrying a suspended load to cause the particles to floc together. Once flocced, they will either sediment or be caught by the filter. In his review on the subject, Camp²⁹ notes that the film is collected by the filter through the formation of sheaths about the sand grains. The interspace between the grains is slowly filled but the flow lines are kept clear, by and large. Plugging by large clots of the

floc caused by the actual closing off of a continuous pore does not occur until "breakdown" of the filter occurs. The strength of the physical mechanism by which this floc is attached to the sandgrain appears to be strong enough to resist strong shearing forces caused by rapid fluid flow. In nature this retention of particulate matter apparently happens to a lesser degree without the benefit of strong concentrations of coagulants, such as those used in the waste and water treatment industries. Mineral grains in sandstones from the surface and at depth are often coated with "films" of fine particles that resist removal by normal washing methods.

That the retention mechanism is not well understood has resulted in considerable controversy over the plugging problems in oil field secondary recovery production operations and in the deep-well disposal of industrial wastes. Warner³⁰ made it clear that the appearance of particulate matter sufficiently large to plug a permeable formation is a problem that has yet to be resolved.

Penetration of Packed Sand Beds by Suspended Matter

Davis and Borchardt³¹ concluded that the simple filtration of either algal cells or particulate carbon by sand filters resulted in insignificant removals and that complete removal of the algae was difficult even with the use of coagulant chemicals. Even in the larger size range where the minimal size of algae was on the order of 5-10 microns, it was noted that sand packs were not altogether successful in removing suspended matter. That living particulate matter can penetrate packed granular filtration media was discussed by O'Melia³². His conclusion and that of

Hall³³ and Stanley³⁴ was that the removal of organic or inorganic particulate matter by packed sand beds was essentially dependent on the size of the particles and inversely dependent on the size of the sand grains.

Bush and Isherwood³⁵ working with Cocksackie virus and Robeck³⁶ working with polio-myelitis virus reported considerable penetration of their sand pack filters by these small particles of living matter (10-300 millimicrons diameter according to Pelczar and Reid³⁷). Considerable pre-filtration chemical treatment was required by both groups to substantially enhance the removal of the viruses. Eliassen et al³⁸ described experiments in which the bacterial viruses were followed through soil columns by tagging the viruses with radiophosphorus, ³²P. Important work on the transport of virus-sized particles in simulated aquifers and the general hydrology of porous media was published in the last few years by A. T. Corey and his associates,³⁹ notably Filmer⁴⁰ and Brooks⁴¹. In these publications, packed columns of various kinds of sands were used to correlate the retention rate of particles from suspensions of albumin passing through the columns with the physical parameters of the bulk sand pack.

Champlin and Eichholz⁴² discussed the feasibility of transporting radioactivity through porous formations by adsorption of the activity on particles suspended in the groundwater. They showed the removal rate of the larger particles in the size range was a function of the size of the particle and that finite quantities of kaolin particles had mean travel distances of several meters.

In his Masters thesis, Champlin⁴ pointed out that soft-bodied, rod-shaped particles, about the same order of size as small kaolin particles,

appeared to contribute to the transport of radioactive material through a relatively long bed of packed sand. From their shape, external structure, and what internal structure could be determined in the electron micrographs, he suggested that those unknown particles were probably bacteria. That these microbiologicals are subject to the same physical laws that control the movement of fine mineral particles through filters is evidenced by the discussion of ionic and dipole attractions between soil particles and bacteria by Dvyagintsev,⁴³ straining reactions between sandy soils and bacteria by Krone et al,⁴⁴ and chemical interactions between the soil particles and viruses by Carlson et al⁴⁵.

The Potential Transport of Pollution by Particles

In a series of papers from 1964 to 1968, Bailey⁴⁶⁻⁴⁹ has described the interactions between organic herbicides and pesticides with soil minerals, particularly the clays such as montmorillonite. It is clear from these articles that radioactivity, bacteria, and viruses are not the only potential pollution that may be transported in runoff, stream flow and subsoil drainage. Transport and concentration of toxic chlorinated organics may lead to dangerous accumulations in the food cycle used by man. In a related vein Scalf⁵⁰ reported studies on the fate of insecticides and nitrates in groundwater based on the concern that migration of these materials might result in a toxic accumulation in the public water supply if they were present in surface waters used for forced ground-water recharge. Similarly, Essington⁵¹ and Nishita⁵² were concerned with the facilitation of fission product transport by chemical chelates purposely spread on radioactively contaminated soils to aid the leaching of radioactivity

away from the root zone of plants used for forage or agricultural produce.

Clearly, a study of particulate ion transport phenomena by use of radioisotopes will cast some light on the migration process and have application in a large number of fields. The importance of such organic and inorganic particles to the subject matter of this thesis lies in the fact that their wide-spread abundance provides ample means for transporting radioactive ions and other water contaminants from their places of normal confine.

While the importance of transport of radioactive ions by particulate matter has been of less concern in the past, the anticipated large increase in the number of nuclear power plants and nuclear powered ships will load the capacity of the existing facilities for reprocessing the used fuel elements. Other facilities, no doubt, will be built closer to the new power plants and population centers in order to keep down the cost of shipping the used fuel elements. The expectation is that the risk of radioactivity migration from the disposal areas of the new sites to water supplies of populated areas inherently will be greater than for those isolated plants placed in the western deserts. Indeed, it was in anticipation of this that special arrangements for waste control had to be made for such disposal sites as those of Mallinckrodt in Missouri, Savannah River in South Carolina, and the New York disposal plant in West Valley, New York, all of which are in regions of heavy rainfall.

It is the purpose of this thesis to consider the importance of the various chemical and physical reactions that occur between ions and particles in suspension, and between them and the solid surfaces provided

by the porous matrix that makes up underground aquifers and surface soils. Consideration of the ion exchange processes, van der Waals reactions, ion and surface hydration, effects of ionic fields on the dielectric constant of water etc., will be related to the results of experiments dealing with radioactively tagged particle movement through a packed sand model aquifer. From this will come a better understanding of what factors are important in ion transport by particulate matter through porous media and of the measures that may lead to potential control of this phenomenon for problem areas of the future. Once the factors that control ion transport through aquifers are more clearly understood, it may be possible to use virtually any kind of isotope adsorbed to particles for hydrologic tracing.

CHAPTER II

THEORETICAL CONSIDERATIONS

Water

Since the transport of radioactivity by fine suspended matter is dependent on factors particularly germane to the physical characteristics of water, it is necessary to consider this widely abundant material in some detail. Chemically, water in its simplest form is a combination of two hydrogen ions with one oxygen ion. The interaction energies between the oxygen and the hydrogen ions are of such magnitude that the latter are drawn within the outer electronic "shield" of the oxygen ion. Consequently, the center to center distance between the different types of ions is considerably less than the normal radius of the unreacted oxygen atom⁵¹.

The modern theory of the physical nature of water is based on the observation that the oxygen and hydrogen ions combine sterically at an angle of $104^{\circ} 40'$ ⁵⁴. The resultant three-centered structure leaves the hydrogen ions effectively displaced toward one end and the oxygen ion toward the other. The charge asymmetry that results gives rise to a polar molecule.

The magnitude of the permanent dipole moment produced by the separation of positive and negative charge centers in the molecule can be calculated, from the product of the unit charge ($4.8029\text{E-}10$ esu) and the distance of separation of the charge centers ($4.3\text{E-}9\text{cm}$), to be $2.065\text{E-}18^*$ esu-cm. Actual measurements⁵⁴ put this value between $1.71\text{-}1.97$ E-18 esu-cm with a

*Note that the computer term $\text{E}\pm\#$ will be used to represent $10^{\pm\#}$.

value of 1.88 E-18 esu-cm taken as being the most commonly used ⁵³. The interactions between the dipoles of individual water molecules give rise to many of the common physical characteristics associated with liquid and solid water.

The complexities to be found in aqueous solutions or suspensions and their interdependence on the physical conditions of temperature, pressure and "external" fields that result from the water dipole interactions are nicely summarized by Moeller⁵⁴. For the purposes of this thesis, the more important characteristics of the polar water molecule are that 1) it has a natural permanent dipole with a moment of about 1.88 E-18 esu-cm , 2) it can be polarized and has a polarizability of about 1.48 E-24 cc ,⁵⁶ 3) through the action of its dipole, the water molecule is capable of causing polarization in other molecules and atoms, and 4) the water molecule is tripolar at close range and tends to form tetrahedral associations with other atoms or molecules.

Out of this combination comes the inherent character of water to build networks or chains of molecules that are stable well above the melting point of ice; to hydrate ions and interfaces with solids or gases; to possess an exceptionally high dielectric constant (for molecules of its type); and to act as a solvent for a wide variety of compounds.

Despite the inclination of water molecules to enter into a variety of different reactions based on dipole attractions, few of the products would have more than a transitory existence because of the disruptive nature of the so-called "thermal" forces if it were not for hydrogen bonding. The hydrogen ion may be attracted simultaneously to two electronegative ions and thereby form a relatively strong bond between the two. Moeller⁵⁴

notes that the hydrogen bond between electronegative ions is primarily electrostatic in character and not covalent as had previously been suggested. With its single 1-s electron, the hydrogen atom is incapable of forming more than a single covalent bond, nor can it be said that the hydrogen atom shifts tautomerically from one electronegative ion to the other. This special type of bonding is found only between highly electronegative, polarizable atoms such as fluorine, oxygen, chlorine, and nitrogen, although carbon, highly substituted with negative groups, may enter into hydrogen bonding.

It appears that when a hydrogen atom is chemically bonded to one electronegative element, the strong pull which an atom of that element exerts upon the bonding electrons leaves an effective positive charge on the hydrogen atom. This charge may be sufficient, because of the effective absence of any screening electrons, to attract a second electronegative atom. That more than two such electronegative ions cannot be held together by a single hydrogen ion is due to the limited range of the attractive forces and the restricted space around the comparatively tiny hydrogen ion. The majority of the elements so attracted are non-metals and have in their structures unshared electron pairs; nonetheless, these electron pairs are not directly involved in the hydrogen bond that develops between them.

According to the modern theory of water structure first proposed in the early 1930's by Bernal and Fowler⁵⁷ liquid water is more truly characterized as a highly mobile slush. At a given ambient temperature, the larger part of the water molecules are not free to move individually. Rather, because of the attractive interactions between water molecules, most of them are bonded together in groups, chains, or nets which move past

one another by sliding over the relatively few molecules which, according to the distribution of thermal energies, are free acting.

The structure of water is most clearly seen by observing the structure of ice in which the oxygen atoms are arranged much like they are in the silica mineral tridymite⁵⁴. This arrangement gives the water an open structure which permits the presence of a hydrogen atom between every two oxygens. The overall structure, then, is essentially one of H-O-H units held together by hydrogen bonds.

Through the initial attraction of the dipoles for each other and the hydrogen bonding that results between the oxygen atoms at close proximity of the neutral water molecules, a relatively open structure takes form. Although this structure-development accounts (in the freezing of water) for the lower density of ice compared to liquid water, hydrogen bonding is not complete until a much lower temperature is reached. Finally at -183°C , each water molecule is characterized by the four hydrogen bonds which it is capable of forming⁵⁴. As the temperature rises, polymeric water molecules may result from two or three molecules being hydrogen-bonded together as the structure becomes somewhat disordered by the thermal forces. This disruption continues through fusion of the ice and on to higher temperatures until complete rupture of all hydrogen bonded structures ultimately occurs and the water vaporizes at its boiling point as individual, discrete molecules. Using this concept, the lower limit of energy involved in hydrogen bonding can be estimated at about 0.032 eV under normal conditions.

The maximum in density of water at 4°C is attributed to a change in the equilibrium between the open structure maintained in ice with that of the close packed structure that would result were there no intermolecular bonds. As ice, the water molecules are combined in an open three-dimensional network of molecules with a density of about 0.9 g/cc . A comparable density of water, were it made up of close-packed molecules of dihydrogen oxide, would be in excess of 1.8 g/cc^{58} . Even at 40°C , more than 50 percent of the possible hydrogen bonds still exist. At the room temperatures of concern here, probably 75-80 percent of the water molecules are hydrogen bonded to a large degree and probably even more to a lesser* degree^{59,60}.

At normal temperatures, therefore, a large quantity of the water molecules must still exist in combined form as units of two, three, four or more water molecules bound together in open ice structure. The larger combined forms are theorized to move more or less as a slurry with the smaller combinations or free water molecules acting as the mobilizing medium. The relative quantities of these possible forms affect the rate of movement through shear effects. In fact, the peculiar change of viscosity of water with temperature is attributed to this factor. Consequently, any experimental work with water at temperatures from $17\text{-}27^{\circ}\text{C}$ must be concerned with the effects this substructure of the water may have on the results.

The Water Interface

An interesting thing about this ice structure formation of "macro-molecules" in fluid water is that unless other molecules or micro-structures are highly ionized, polar, or polarizable, so that they can react with

*In this context lesser degree refers to 1-2 hydrogen bonds and large to an average of 2-4 hydrogen bonds per molecule.

water in relatively strong competition with the intermolecular reactions of the water itself, they are forced away by the forming water structures and concentrated in the space between them^{61,53}. A natural consequence of this action, since the polymerized water molecules can no longer act (on a time average) to solubilize other molecules or ions, is that the relative concentration of the solute molecules builds up in the "interstices" between the water molecule aggregates.

Some poignant examples of this type of separation of solutes from solvents are seen in the production of fresh-water ice from sea water in the North Atlantic, in the "upgrading" of hard cider by letting it freeze, and in the setting-up of so-called liquid clays in tank cars left in railroad sidings overnight when it is cold. Hydrocarbons, if present, will most readily orient in the air-water interface; but if that is not available, they will collect as rejections from the water structure and turn inward to form spherical micelles with the most hydrophilic portion of the molecules outward facing the water. Individual molecules may coil up to form the least common surface with the water structure possible. As the rejection process continues the coils may accumulate sufficiently in one place to form the spherical micelles noted earlier.

The problem presented by the topic of this thesis deals with the presumed collection, concentration, and transport of radioactive, relatively heavy-atom ions by fine particulate matter in suspension in groundwater. Since some of these ions are not very soluble in water and are "rejected" by it, they tend to condense at or adsorb to the nearest interface which might be either at the surface of a stream or along entrained

air bubbles in open water. In flow through porous media, however, the most accessible interface may be that between the water and solid particles. This might include the porous matrix itself or the solids of various types suspended in and carried along by the water itself.

Perhaps the most authoritative works on the subject of inorganic ion separations are still the product of consultants to the mineral recovery industry,⁶¹⁻⁶⁵. While much of the previous work^{*} has involved use of organic molecules, the development has been sufficiently general to note parallels in the inorganic physical-chemical reactions of the cations in water. In order to discuss the phenomena of adsorption of radioisotopes on fine suspended particles in a porous medium, it is necessary to consider the physical effects of ions on water, which play integral and important parts in adsorption.

The relatively strong association of water molecules with one another leads to the development of structure that electric charges present in the water may disrupt. The nearby presence of solid surfaces (e.g. suspended particles) sets up a natural competition for the ions between the water and the solid surfaces. Association of the ions with the surfaces inherently reduces their relative presence in the water and such removal favors an increase in the development of water structure.

As is well known in dealing with radioisotopes, one must keep the concentration of the other ions in solution relatively high (acid ions

^{*}Dealing primarily with the separation of valuable minerals by flotation separation methods.

seem to serve best) in order to allay adsorption of the radioactive ions to the container walls⁶⁰. The presence of acid ions in high concentration tends to reduce any adsorption of tracer ions in low concentration to the container walls by competition with all ions for adsorption sites. In addition, the solubility of the ions is increased through the release of free, individual water molecules by the water structure-breaking effect of the high concentration of hydrogen ions. Dilute solutions suffer a steady transport of ions to the container walls and real decreases in concentration in solution can occur over a period of several days or weeks depending on the nature of both the type of ion and the container wall.

Inorganic ions that most commonly accumulate on liquid-solid interfaces may easily be removed from an aqueous solution by the introduction of a powdered solid material that forms strong bonds with most ions in solution, such as clay or lignin. With typical materials used in ion recovery by flotation techniques, advantage is taken of the accumulation of polar molecules at interfaces to attract the ions and remove them from solution⁶¹.

It is important to realize the different situations to be found in the structure of water aggregates when inorganic cations are added in large quantities. Increasing the cation concentration disrupts the formation of water aggregates by breaking more and more hydrogen bonds, literally forcing the water to become more fluid. W. G. Lawrence⁵³ notes that a 0.1 molar solution of cesium chloride is more fluid than pure water and that only ions that are smaller than Cs^+ (1.65 Å) and I^- (2.20 Å) are capable of inducing structure formation rather than its disruption. Thus, the

increase in viscosity of lithium chloride solutions over that of pure water is due to the small radius of the lithium ion (0.6 \AA) making it possible to fit within the water structure and even stabilizing it to some degree by the effects of its electrostatic field⁵³.

Hydration of Ions and the Dielectric Constant

The presence of ions in water tends to alter the ordered structure that water molecule dipoles would tend to build. The presence of some ions in water, however, is inherent. Not only is it virtually impossible to remove all cations and anions from water because of the finite solubility of any material used to contain the water; but a very real contribution of ions comes from the water itself. In the structure building of the water, a large part of the molecular bonding is that of hydrogen bonds. The nature of these bonds is such that the hydrogen ion is virtually exchanged between two water molecules. In a resonance structure of this type, the hydrogen is just as likely to be with one molecule as another at any particular time. The kinetic energy of the system in general is sufficiently close to the energy of the hydrogen bond that a finite number of the intermolecular collisions that take place from thermal motion involve an energy exchange of sufficient magnitude to break hydrogen bonds. The state of the water structure for this reason has been termed "flickering"⁵⁷ and the half-life of a water cluster estimated at 10^{-10} to 10^{-11} seconds⁵³. This half-life is on the order of the dielectric and bulk relaxation time of water but is 100 to 1000 times a molecular vibration period.

The major result of this hydrogen bond breakage is that one part of the cluster is left positively charged and the other part negatively

charged. At normal conditions of temperature and pressure, this reaction yields on the order of 10^{-7} ($\text{H}^+ \cdot n\text{H}_2\text{O}$) ions and the same number of ($\text{OH}^- \cdot n\text{H}_2\text{O}$) ions. This obviously is a natural explanation for the dissociation constant of water⁶⁷. More importantly, it sets a realistic limit to the minimum ion concentration one can expect in a solution carrying radioisotopes. Unless there are other chemicals present (in larger quantity) which tend to alter the 1:1 ratio of the hydrogen and hydroxyl ions, they will be maintained in dynamic equilibrium at a concentration of 0.1 microequivalent per liter in the purest of water. As this is significantly close to the concentration of radioisotopes used in this experiment, or at least to their accompanying stable carrier isotope, it is worth noting the importance of the hydrogen ion concentration, particularly in the competition for adsorption sites.

The presence of these or any other ions in water causes severe re-orientation of the water molecules. The interaction energy of two water dipoles at a distance representing molecular contact is shown in Table 4 to be 0.9 eV while the corresponding energy of interaction between an ion and a water dipole would be 1.5 eV. In addition, the dipole-dipole interaction is subject to change, since it is angularly dependent, and the value of 0.9 eV represents a value determined at optimum orientation of the two dipoles with respect to one another. Only at distances in excess of 10 Å would the dipole-dipole interaction be of equivalent magnitude to the ion-dipole reaction.

This assumes, of course, that the orientation of the water molecules to the ion field is parallel throughout, whereas in fact it becomes

less and less parallel as the water layer around the ion increases in thickness. It is doubtful that even the first layer of water is free of certain disorientating factors. The combination of the rotary motion and the fluctuating electronic field of the water molecules result in a weakening of both ion-dipole and dipole-dipole interactions. The "flickering" electric field that results interferes with the radial field set up in the medium by the ion. Consequently, at a distance of one or two water molecule diameters, the coulombic force of interaction between the ion and any other charge or dipole as calculated for isolated charges must be decreased by a factor of about 80. When measured in the bulk medium, this factor of decrease in the electrostatic force is known as the dielectric constant. However, where the water molecules are subjected to some degree of constraint, as in the vicinity of an ion, the factor is considerably lower and may approach the value of 2.2.

The Magnitudes of Physical Interactions

The experimental portion of this thesis considers the movement of fine particles in suspension through a packed sand bed by means of a gentle flow of water. In particular, it deals with the exchange of those particles between the packed bed and the water. As a model for this system, kaolin particles were chosen to represent the particles and a relatively pure quartz sand packed in a bed of dimensions 0.25 x 1 x 2 meters to represent a horizontal aquifer.

The kaolin particles are taken to be 0.1 micron on a side and $3.3\text{E-}3$ micron thick. The sand is assumed to consist of relatively spherical

particles of 165-micron radius and the packed bed assumed to be infinitely thick, relative to the dimensions of the kaolin particles. To avoid confusion later on, the kaolin and other types of finely divided matter will be called particles, the sand making up the packed bed will be called grains. Ion will refer to any charged atom or molecule, but not to a particle or grain carrying a charge. The latter will be referred to as charged particles or grains respectively on which may be located various charge sites. The grains will be assumed to have homogeneous reacting surfaces while the kaolin particles will be considered to consist of single crystals with two relatively large, parallel, lateral faces of hexagonal outline and six smaller edge faces of rectangular shape. The lateral and edge surfaces have different chemical and physical reactivities.

The mass of a kaolin particle can be estimated from the mineral density of the kaolin and an evaluation of its volume. This mineral has a density that is sufficiently similar to quartz to use the value of 2.65 g/cc for them both. The equation for the area of a polygon is

$$A = \frac{1}{4}n a^2 \cot \frac{180^\circ}{n} \quad (1)$$

where (n) is the number of sides of a regular polygon and (a) is the length of one side. Using $n = 6$ and $a = 1 \text{ E-5 cm}$, the area of one lateral face is

$$A = 2.598 a^2 = 2.598 \text{ E-10 cm}^2 \quad (1A)$$

The volume would be the area times the thickness or

$$V = A\tau = 2.598 a^2 \cdot \frac{a}{30} = 2.598 \frac{a^3}{30} = 0.0866 \text{ E-15 cm}^3 \quad (2)$$

The density of 2.65 g/cc gives an approximate mass to the individual particle of 2.30 E-16 grams.

For the experimental conditions described here, there are essentially three different situations where the effects of physical interactions might be worth considering;

- a) the interaction between particles of the same approximate size and mass, e.g. the suspended particles themselves,
- b) the interaction between particles of the suspension and the grains of the sand bed,
- c) the interaction between the particles of the suspension and the earth itself in the form of gravitational effects.

The first reaction would tend to cause the particles to aggregate into larger more massive particles; the second would tend to remove the particles from the suspension onto the surfaces of the sand grains; the third would tend to cause the particles to drop out of suspension and settle on the bottom of the capillaries of the sand bed.

Forces of attraction that give rise to interaction energies less than the mean thermal energy of the system (about 0.025 eV at room temperatures) must be considered as inadequate to maintain a given juxtaposition between two masses. Attractive forces arise from gravitational, van der Waals, and the opposite charge interactions. Opposing this aggregation

or settling are the repulsive electrostatic forces as well as the mechanical momentum exchange resulting from the so-called Brownian agitation of all molecules and particles. If the forces of attraction give rise to interaction energies significantly higher than the mean thermal kinetic energy of the system, statistical quantities of the aggregates will be maintained against the disruptive effects of the Brownian motion. A large interaction energy relative to the mean thermal energy of the bulk of the particles or molecules gives rise to a high probability that such an aggregate will be maintained. Consequently, the thermal mean energy is commonly used as a criterion of whether the effects of a given interaction between the two masses in question are significant or not.

Thermal Forces and the Kinetic Energy of Particles

The motion of small particles originally described by Brown⁶⁸ and later discussed in detail by Perrin⁶⁹ as Brownian motion is essentially the result of kinetic energy and momentum exchange between the particles and the molecules of the medium in which they are suspended. Under conditions of dynamic equilibrium in such a suspension, there is a mean energy transfer between all particles and molecules for a given temperature.

More formally the relation for free molecules or particles with three degrees of freedom may be written as

$$E = \frac{1}{2} m \overline{v^2} \quad = \frac{1}{2} m' \overline{v'^2} \quad = \frac{3}{2} \frac{RT}{N} \quad (3)$$

(particle) (molecules of)
medium

in which m and m' are the masses of the particle and molecule respectively and v and v' are their velocities. The $\frac{3}{2} RT/N$ or $\frac{3}{2} kT$ term at the right

is the total exchangeable energy. This exchangeable energy is made up of three portions of $\frac{1}{2} kT$, each being the average energy denoted to a given degree of freedom of movement. As Kruyt⁷⁰ points out, "the mean kinetic energy of each freely moving element is therefore completely determined by the temperature." At the temperature of 27°C (80°F) which was the average laboratory temperature during the experimental period, this average energy would be

$$E = \frac{3}{2} \times 8.62 \text{ E-5 eV/}^\circ\text{K} \times 300^\circ\text{K} = 0.0388 \text{ eV} \quad (3A)$$

Perrin⁶⁹ noted, however, that since Brownian motion was merely an extension of molecular motion to particulate matter in suspension, translational motion would not be the only type to be considered. In the 'bombardment' of a particle by other particles or molecules, rotational motion also should be expected. If such an assumption is valid, then at least a portion of the total energy involved in each collision must go into changing the rotational motion of the particle. An estimation of the magnitude of the most probable energy transfers due to rotation of the kaolin particle may begin with the determination of its moment of inertia. This thin, hexagonal prismoid being represented as a typical kaolin crystal may be approximated by a thin circular disc of the same thickness and lateral surface area as the kaolin flake. The moment of inertia of a disc is

$$I = \frac{1}{2} m R^2 \quad (6)$$

if the rotation is about an axis perpendicular to the plane of the disc

and passing through its center, where R is the radius of gyration. By comparison, the moment of inertia about any diameter of the disc is

$$I = \frac{1}{4} m R^2 . \quad (7)$$

Either of these types of rotation may be significant in a random, isotropic exchange of energy and momentum.

Since the area of the hexagonal lateral face of the kaolin flake is 2.598 a^2 (eqn. 1A), the equivalent radius of gyration would be 0.9096 a . The largest moment of inertia and the one most germane to this discussion, will be found with the axis of rotation through the center of the largest surface and normal to it. Hence

$$I = \frac{1}{2} (2.295 \text{ E-16}) (0.9096 \text{ E-5})^2 = 9.49 \text{ E-27 g-cm}^2 \quad (6A)$$

According to Perrin,⁶⁹ the rotation of such a body is quantized and the kinetic energy of rotation may be related to the angular velocity ($2\pi\nu$) by the equation

$$E = \frac{1}{2} I (2\pi\nu)^2 = p h \quad (8)$$

where p is integer and h is Planck's constant. Solving for the frequency, ν , and incorporating the Sommerfeld modification,⁶⁹ a possible value would be

$$\nu = p \frac{h}{4\pi^2 I} \quad (9)$$

This equation implies that the frequencies of rotation of the particle must bear integer relationships to one another and that no intermediate values are possible. Other than having no rotational frequency ($p = 0$),

the next possible value would be at $p = 1$ and

$$\nu = \frac{1}{4\pi^2} \frac{(6.625 \text{ E-27})}{(9.49 \text{ E-27})} = 1.770 \text{ E-2 hertz} \quad (9A)$$

The kinetic energy involved in such rotation would be

$$E = \frac{1}{2} (9.49 \text{ E-27}) (2\pi (1.770 \text{ E-2}))^2 = 5.86 \text{ E-29 ergs} = 3.81 \text{ E-17 eV} \quad (8A)$$

Clearly with the minute requirement of energy such as this, the particle must be in an effective rotational continuum at room temperatures and the probability of obtaining sufficient energy from a thermal encounter to change its frequency of rotation as estimated from the Boltzmann distribution equation⁷⁰ is seen to be

$$\frac{N_1}{N_0} = e^{-\frac{E_{rot}}{kT}} = e^{-\frac{3.8 \text{ E-17}}{2.5 \text{ E-2}}} \simeq e^0 = 1 \quad (10)$$

For normal temperatures, it is obvious that particle rotation should play a part in every collisional energy transfer. Both small (relative to thermal energies) and large changes could be accepted in that energy form with little difficulty.

Brownian motion as a phenomenon has been followed by such notable theorists as Einstein, Smoluchowski, and Perrin. Its study has contributed to such wide ranging subjects as the theories of viscosity and molar quantities. Indeed its use was the means of an early and surprisingly accurate estimate of Avogadro's number. The importance to this research work is that Brownian Motion or Thermal Diffusion is the prime factor in maintaining suspended particles in disaggregation or in resuspending

particles which have "gravitated" to some surface or interface. Since the energy of the molecules and suspended particles follows a distribution about a mean, some consideration of diffusion as typical of large masses of material rather than of single particles or molecules is pertinent.

Diffusion Coefficient

For spherical particles the diffusion coefficient, D_o , can be found by use of the following equation:

$$D_o = \frac{kT}{6\pi\eta r} \quad (11)$$

where k is the Boltzmann constant, T is the absolute temperature, η is the viscosity in poise, and r is the radius of the sphere in cm. Thus, the Stokes equation is not exact in the size range for which this study is being made; but the needed corrections are relatively minor and are due primarily to the relative sizes of the particles and the suspending molecules of water. The correction is primarily an adjustment of the viscosity term. Reasonable assumptions for use of this equation include that the size of the water molecules is negligibly small compared to the diameter (and mass) of the kaolin particles and that the orientation of the water molecules between particles is nearly as random as those in the "bulk" medium. Such approximations are commonly made by colloid chemists who work with particles even closer to the size of the water molecules.

However, it is necessary to correct for the fact that the particles are not spherical. Sheludko⁶⁹ provides an approximate equation which he

attributes to Perrin, that permits a correction for particles whose shape resembles that of an ellipsoid of revolution. By and large, including their adsorbed water and ion envelopes the particles considered for this research can be approximated by ellipsoids of revolution and diffusion coefficients calculated for them. The equation for computing the correction factor in D_o is

$$D/D_o = \frac{(j)^{\frac{2}{3}}}{\sqrt{1-j^2}} \ln \frac{(1 + \sqrt{1-j^2})}{j} \quad (12)$$

where the symbol "j" represents the ratio of the axes of the ellipsoid, (b/a).

The particles observed in the experimental work fell into two general groups, rod-shaped bacteria and flaky, mineral particles of clay. The larger bacteria were approximately 3-5 microns long and 0.5 microns in diameter; the smaller bacteria were 1 micron long by about 0.4 micron in diameter. The clay particles also fell into two groups, the fine grade of commercially prepared kaolin which was added to the sand bed and a rather undifferentiated, flexible clay particle with no identifiable crystal form that was derived from the sand bed itself. Characteristics peculiar to each type of particle are discussed in the section on materials. The size of the commercial clay particles was discussed in the first section of this chapter. The clay particles from the sand bed were about 5 microns in diameter and about 0.2 microns thick. These values for size were taken from electron photomicrographs of the particles in question.

The bacteria had the general shape of a prolate spheroid and the

clay particles that of an oblate spheroid. Taking "a" as the major axis and "b" as the minor axis, then the volume for these two spheroids can be found by the following equations:

$$\text{prolate } V_e = \frac{4}{3}\pi a b^2 \quad (13)$$

$$\text{oblate } V'_e = \frac{4}{3}\pi b a^2 \quad (14)$$

Using equations (13) and (14) in conjunction with equations (11) and (12) the diffusion constants in Table 1 were obtained.

The approximate time between collisions, t , can be determined with the diffusion coefficient of kaolin in Einstein's equation

$$\overline{X^2} = 2 D t \quad (15)$$

where "X" is the particle displacement. Taking the value of 6.1 microns, the average distance between particles for a one mg/l water suspension, as the average displacement between collisions, then

$$t = \frac{\overline{X^2}}{2D} = \frac{(6.1 \text{ E-4 cm})^2}{2 \times 3.147 \text{ E-8 cm}^2/\text{sec}} = 5.9 \text{ seconds} \quad (15A)$$

Thus, from the estimate of the displacement length and the relative frequency of Brownian movement, an approximate value for the time of movement has been determined which can be detected by the eye using the light microscope.

Table 1. Diffusion Coefficients of Particles in Water Involved in Experimental Work (300°K).

Particle	Shape	Axes		Correction	Corrected Diffusion
		a	b	Factor D/Do	Coefficient cm ² /sec
<u>Prolate</u>					
Bacteria	Short Rod	0.5	0.2	0.928	8.79 E-9
Bacteria	Long Rod	2.0	0.25	0.698	3.59 E-9
<u>Oblate</u>					
Kaolin	Flake hex.	0.1	0.1/60	0.312	3.15 E-8
Sand-bed* Clay	Flake flex.	2.5	0.1	0.458	1.38 E-9

*The sand-bed clay also contained some particles about the same size as the kaolin, but with no describable shape. It is assumed that the diffusion coefficient calculation for the kaolin will do for it as well. The sand-bed clays were noted by electron microscopy to appear flexible, or bent in form while the kaolins always appeared in the form of stiff hexagonal prisms. Hence the reference in the Shape column above to Flake flex. for the natural clays obtained from the sand.

The exchange of energy in a collision must be divided between translational, rotational, and internal energy of the particles. Collisional energy is dissipated primarily by subsequent collisional contact with other particles or molecules. For a system, such as is being considered here, little heat is gained or lost from the internal energy of the particle per collision. Consequently, about two-thirds of the collisional energy goes to translational and about one-third to rotational energy ⁶⁹.

Mean Particle Velocity and Momentum

With the mean exchange of energy at 300°K being about 0.039 eV, it is difficult to see how enough energy can be made available at one location in the system to cause major chemical bonds to break. Yet the distribution of thermal energies is given as the principal reason for the dissociation of water and other chemical compounds for which bond energies of an electron-volt or larger are common. In this, an important factor besides the energy transfer itself is the rate of energy transfer.

Consider the model particle of kaolin in equilibrium with the thermal molecular action of water in an aqueous suspension. From equation (3), the average energy involved in a transfer and the average velocity of a particle involved in such a transfer of energy can be calculated. For example, at 300°K, the velocity of a kaolin particle would be

$$\bar{v} = \frac{\sqrt{1.3809 \text{ E-16} \times 3 \times 300}}{2.2949 \text{ E-16}} = 23.27 \text{ cm/sec} \quad (3B)$$

and a small particle of mass = 2.29 E-16 grams traveling at such a velocity has a momentum, $m\bar{v}$, of $5.34 \text{ E-15 gm-cm/sec}$. In contrast, the momentum of a single water molecule calculated from the mass of an individual molecule, 2.98854 E-23 g , and its mean velocity, 6.442 E+4 cm/sec , as $19.25 \text{ E-19 gm-cm/sec}$ is only 3.6 E-4 of the momentum of the particle of the same energy. At that energy a collision of the particle with a water molecule is neither going to affect the momentum or the velocity of the former much, even if all the translational energy and rotational energy of the water molecule were transferred to the particle. Recalling that the Boltzmann distribution provides some molecules of higher energy, an increase in momentum of the water molecule by two magnitudes would be necessary to cause even a minor change in momentum for the particle. This would require a velocity 100 times as great and an energy 10,000 times as great which would be rather rare in this system.

Since it does not appear that the water molecules are directly responsible for the disturbing influences on the suspended particles noted in Brownian motion, the energy transfers between particles and more massive objects than the water molecules must be considered. Those available in the system fall into two categories, 1) other particles of about the same mass and size and 2) the sand grains of the sand bed. Since the maximum momentum transfer in a collision is between particles of the same approximate mass, the first group are by far the most important. With an average mass difference between the kaolin particle and the sand grain of about 10^{10} , no significant momentum transfer is likely to occur between the grains and the particles except for directional changes

in velocity. The primary source of the disturbances noted by Brown⁶⁸ must be from the thermal energy collisions of particles nearly the size and mass as those being examined.

Gravitational Interactions

Perhaps the most neglected interactions between microparticles are those that result from gravitational force interactions between masses. Lappel⁷² showed that these forces take on less importance only for particles of the density of quartz that are smaller than 1 micron. The gravitational potential energy between two masses isolated from other interactions is obtained by integrating Newton's equation for gravitational force over a distance from infinity to some given separation (s).

$$E = \int_{\infty}^s dE = \int_{\infty}^s \frac{G m M}{s^2} ds \quad (17)$$

Using the mass of the kaolin particle obtained above in this equation, the magnitude of the gravitational potential energy between two suspended particles of like size and mass can be calculated at the minimum distance of separation of two water molecules. Assuming the kaolin flakes to be oriented with their lateral surfaces parallel to one another, the total distance between centers of mass would be $0.1/60 + 0.1/60 + 2(0.000136) = 0.0036$ microns or 36 \AA . The energy due to gravitational forces at this distance would be

$$E = \frac{Gm m'}{s} = \frac{6.67 \text{ E-8}}{36 \text{ E-8}} (2.295 \text{ E-16})^2 = 0.976 \text{ E-32 ergs} \quad (17A)$$

Next consider the gravitational potential between an isolated

suspended particle and a quartz sand grain of 165 micron radius (assumed spherical).

$$E = \frac{G m M}{s} = \frac{(6.67 \text{ E-8}) (2.295 \text{ E-16}) (4.986 \text{ E-5})}{165 \text{ E-4}} = 0.463 \text{ E-25 ergs (17B)}$$

And finally, the gravitational potential between a suspended particle and the mass of the earth would be

$$E = \frac{G m M'}{s} = \frac{(6.67 \text{ E-8}) (2.295 \text{ E-16}) (5.983 \text{ E} + 27)}{6.37 \text{ E} + 8} = 14.35 \text{ E-5 ergs (17C)}$$

where (m) and (m') are the masses of the suspended particles, (M) is the mass of a typical grain of quartz 165 microns in radius (assumed spherical), (M') is the mass of the earth, (G) is the gravitational constant, and (s) is the distance between the center of masses concerned. The units are grams for mass, centimeters for distance, and dyne-cm²/g² for the gravitational constant.

The gravitational potential energy between two suspended particles or between a particle and a grain is sufficiently smaller than the thermal mean energy to be considered negligible. The particle-earth reaction, however, is not negligible. It is a reaction in which gravitational kinetic energy must be considered to develop over a very short distance of travel through an almost constant gravitational potential field. This distance would be from the original particle position in the suspension to the nearest sand grain or other particle in suspension. The gravitational force acting on a particle of 2.295 E-16 grams due to the presence of the earth would be

$$F = \frac{G m M'}{s^2} = \frac{14.346 \text{ E-5}}{(6.37 \text{ E+8})^2} = 3.535 \text{ E-22 dynes} \quad (18)$$

At a concentration of 1 mg kaolin particles per liter, the interparticulate distance (assuming a cubic lattice) would be 6.1 microns. Using this distance (s) as the total distance of fall that a given particle could move without being diverted by a collision (and not allowing for viscous effects of the suspending medium), then the total kinetic energy gained by gravitational attraction would be

$$E = F \cdot s = (3.535 \text{ E-22})(6.1 \text{ E-4}) = 21.56 \text{ E-26 ergs} \quad (19)$$

Obviously, for particulate sizes of the magnitude considered here, gravitational attraction cannot significantly compete with the disruptive forces of thermal motion. Consequently, forces that produce aggregation must initiate from some other source than gravity alone. Before going on to the major forces of interaction between suspended particles, one other reaction of relatively minor importance should be noted.

Radioactive Atom Recoil

One of the sources of energy available in this system for counteracting attractive forces between particles and grains is that of radioactive atom recoil. Since the decaying atoms in this experiment give rise only to stable isotopes, the pertinence of the recoil lies in the transmission of its energy to a particle, conceivably in a manner which could account for a change in its state of suspension or adsorption to a surface.

The equation for the recoil energy for gamma decay is

$$E_r = \frac{E_\gamma^2}{2Mc^2} \quad (20)$$

Thus for a 2 MeV gamma emission (E_γ) from an isotope of mass number of about 45 (M), the recoil kinetic energy of the atom (E_r) would be 47.5 eV.

For comparable consideration of relativistic beta particle emission

$$E_r = \frac{E_b(E_b + 2m_0c^2)}{2Mc^2} \quad (21)$$

where the energy of the beta particle (E_b) is 2 MeV, the recoil energy of the same atomic mass would be 71.3 eV. At this energy level, it can be seen that the difference between the two types of emission is relatively small and due largely to the extra energy carried by the beta particle in its rest mass of 0.511 MeV compared to the zero rest mass of the gamma. At higher energies where the rest mass is less significant, the recoil energy would obviously be essentially the same whether due to photon or beta emission.

Most important for consideration here is the general magnitude. While well above the energy of individual chemical bonds (at a few eV per bond), the kinetic energy of the recoiling atoms after radioactive decay is a thousand times greater than the average van der Waals attraction energy. In ideal conditions, then, it is conceivable that a particle 1000 times as massive as the original atom could be broken loose from a point of absorption by radioactive recoil. It is unlikely that such ideal conditions exist in any significant quantity, nor are we concerned with particles in this work only 1000 times more massive than a single atom. Unless several adsorbed radioactive atoms decayed simultaneously on the same particle with the recoil delivered to the particle along the same

direction, even megacuries of activity (representing randomly oriented recoils from decaying atoms) would not remobilize the particle. The heat developed in such a case might be more significant in supplying energy.

Van der Waals Reactions

Next in order of magnitude of the interparticulate force reactions are the so called van der Waals reactions. The van der Waals force is a weak intermolecular force postulated to act at very short range. As applied in systems such as this one, the forces are named van der Waals because of the formal resemblance of their theory to the higher order van der Waals terms in the equation of state. Van der Waals' original theory was designed to describe the reaction of gas molecules, especially the monatomic gaseous elements, in their deviation from the ideal gas law. Van der Waals' explanation of the existence of short range forces gave a reasonable explanation for the liquification of the noble gases.

In the absence of any easy explanation of this force in terms of electric, magnetic or other known effects, London,⁵⁶ Keesom,⁷³ Debye,⁷⁴ and others formulated an alternative approach based on dipole interaction. The expansion of the theory they developed to include interparticulate reactions is due largely to such workers as Hamaker, Casimir, Osterbach, Verwey, Overbeek and Lifshitz. In that many of the contributions of these men were made in the last thirty years, the entire theory of van der Waals forces in an aqueous medium is still relatively new and many of the arguments remain unresolved. As this type of reaction is of particular importance in colloid chemistry, the literature on the subject is voluminous. Since many reviews^{75,63,70,71,76} on this topic are available in literature a

survey of the pertinent basic theory and the extrapolations to particulate matter will be considered here. Calculations of the potential van der Waals energy will be taken up in the next section.

The theory for the interaction of dipoles calls for the determination of the interaction between the dipole moments of the two molecules involved. The dipole moment of molecules is the product of the equivalent negative or positive charge and the distance of that charge from the electrical center of the molecule. In effect, the dipoles interact like fractional coulombic charges; hence the equation for the interaction energy bears a close resemblance to the energy equation relating two isolated point charges in the Coulomb law. By considering the nature of the dipole, however, there are orientation effects to be considered and London⁵⁶ gave the following equation as a good first approximation of the potential energy of interaction between two dipoles at any given orientation:

$$E = \frac{\mu_1 \mu_2}{s^3} (2 \cos \theta_1 \cos \theta_2 - \sin \theta_1 \sin \theta_2 \cos (\phi_1 - \phi_2)) \quad (22)$$

where μ_1 and μ_2 are the dipole moments of the two dipoles and θ and ϕ represent their respective polar coordinates, the polar axis being a line joining the two centers of the dipoles and s is the distance between those centers.

Clearly, in this equation, if all orientations were equally realized, the average dipole moment would be zero and neither attractive nor repulsive forces would be evolved. Realizing this, Keesom⁷³ averaged over all positions and determined that the statistical preference of positioning gave

$$\bar{E} = -\frac{2}{3} \frac{\mu_1^2 \mu_2^2}{s^6} \cdot \frac{1}{kT} \quad (\text{valid for } (\frac{\mu_1 \mu_2}{s^3}) \ll kT) \quad (23)$$

where, as before, kT represents the mean thermal energy. If the quantity E_d is defined as the interaction energy between dipoles that are oriented parallel (by which one obtains the maximum interaction)

$$\bar{E}_d = -\frac{2}{3} \frac{\mu_1 \mu_2}{s^3} \quad (24)$$

At low temperatures and small* distances equation (23) does not hold. Equation (24) is valid for energies much larger than kT . In any case equations (23) and (24) represent the potential energy born of an attractive force, termed the "orientation effect".

Debye⁷⁴ found difficulty with Keesom's results, primarily because the preferred orientation interaction energy of the dipoles was determined relative to the thermal energy of the molecules. If this were the case then the van der Waals forces would show a sharp reduction in magnitude with increasing temperature. Experience showed that this was not wholly valid, nor was an answer to be sought in more complex moment reactions such as quadrupole interactions or evaluations of the charge distribution of the molecules in greater detail since they too would be subject to temperature effects. Seeking a reaction independent of the temperature Debye looked to the physical displacement of the charge distribution that occurs in the presence of another molecule, known as the polarizability, α . The following description is taken largely from London with the symbols conforming to the usage here.

*Small distance of separation where other forces restrict the freedom of the molecules.

In an external electric field of the strength F , a molecule of polarizability α shows an induced moment

$$B = \alpha F \quad (25)$$

(in addition to any possible permanent dipole) and its energy in the field F is given by

$$E = - \frac{1}{2} \alpha F^2 \quad (26)$$

Now the molecule #1 may produce near the molecule #2 an electric field of strength

$$F = \frac{\mu_1}{s^3} \sqrt{1 + 3 \cos^2 \theta_1} \quad (27)$$

This field polarizes the molecule #2 and gives rise to an additional interaction energy according to equation (25)

$$E = - \frac{1}{2} \alpha_2 F^2 = - \frac{\alpha_2 \mu_1^2}{2 s^6} (1 + 3 \cos^2 \theta_1) \quad (26A)$$

which is always negative, giving rise to an attractive force between the molecules. This is true even at high temperatures and since the average of the $\cos^2 \theta$ term taken through all angles is $1/3$ the potential energy of molecule #1 with respect to #2 is obtained from

$$\overline{E}_{1-2} = \frac{-\alpha_2 \mu_1^2}{s^6} \quad (26B)$$

A corresponding value would result for the potential energy of molecule #2 with respect to #1, that is for the action of the dipole moment, μ_2 , on the polarizability α_1 . Hence, a total interaction of the two molecules

is obtained

$$\bar{E} = - 1/s^6 (\alpha_1 \mu_2^2 + \alpha_2 \mu_1^2) \quad (28)$$

If the two molecules are of the same kind ($\mu_1 = \mu_2 = \mu$; $\alpha_1 = \alpha_2 = \alpha$)

then

$$\bar{E} = - \frac{2 \alpha \mu^2}{s^6} \quad (28A)$$

which is the so-called "induction" effect.

London⁵⁶ expressed the criticism of the above "static models" in that they did not explain why in a liquid or solid, the same forces should act simultaneously between all neighboring molecules as between the occasional pairs in the gaseous state. Due to the various physical and energy states of the molecules taken at random, the forces caused by induced or permanent dipoles or multipoles should be greatly diminished or completely cancelled in a dense medium. He noted the complete failure to justify the Keesom and Debye models for use with the rare gases which wave mechanics had shown to be completely spherically symmetric and without any permanent dipole or multipole.

Consequently, London introduced the idea (born of wave mechanical thinking) that now bears his name in relation to van der Waals forces. He proposed that the rare gas elements be used as models on which the analysis of attractive forces be based. He called for two spherically symmetric systems, each with a polarizability, α , consisting of three-dimensional, isotropic, harmonic oscillators with no permanent moment in their rest position. "Classically the two systems in their equilibrium

position would not act upon each other and when brought into finite distance ($s = \sqrt[3]{2} \alpha$), remain in their rest position. They could not influence a momentum in each other." This distance of separation, according to data from Pitzer⁷³ would be on the order of 1-2 Å for the rare gases.

London noted, however, that according to the uncertainty principle in quantum mechanics, a particle cannot lie absolutely at rest at a certain point. Thus the two isotropic oscillators described would possess a certain zero-point motion even in their lowest energy states. For isotropic oscillators, the probability functions describing this motion give a spherically symmetric distribution of configurations around the rest position. An example of this can be seen in the spherically symmetrical distribution for the electrons around the nucleus in the rare gases. In quantum mechanics, the lowest state of a harmonic oscillator has the energy

$$E_0 = h \nu \quad (29)$$

where ν is the frequency and E_0 the so-called zero point energy. From a consideration of three coordinate axes acting for both of the charge centers, there is a total of six degrees of freedom, each of which acts as a separate oscillator. Consequently the internal zero point energy of the two isolated systems is

$$E = \frac{6 h \nu_0}{2} \quad (29A)$$

where $\nu_0 = e/\sqrt{m \alpha}$ and m is the reduced mass. Presuming that $\alpha \ll s^3$, the potential energy of the two reacting systems could be expressed as a power

series in s^{-3}

$$E_0 = 3 h \nu_0 - \frac{3}{4} \frac{h \nu_0}{s^3} \alpha^2 + \dots \quad (29B)$$

Noting that the first term of equation (29B) was simply the internal zero point energy of the two isolated elastic systems, London described the second term as an interaction energy that, being negative, represented an attractive force. This he termed the "dispersion effect". While the correct magnitude for van der Waals forces could be predicted between isolated atoms by London's derivation, the real significance lay in its application to the macro-system. In his own words, "These very quickly varying dipoles, represented by the zero-point motion of a molecule, produce an electric field and act upon the polarizability of the other molecule and produce there induced dipoles, which are in phase and in interaction with the instantaneous dipoles producing them. The zero-point motion is, so to speak, accompanied by a synchronized electric alternating field, but not by a radiation field: The energy of the zero-point motion cannot be dissipated by radiation" ⁵⁶.

Several "periodic dipoles" can exist between a number of molecules and the interaction potentials between each pair of the group are simply to be added. Each of the induced dipoles always has an orientation that produces an attraction by the dipole that generated it while other dipoles, not correlated by phase relationships, give rise at most to a periodic interaction and contribute nothing on the average to the interaction energy. Therefore, the simultaneous interaction of many molecules can be built up simply as an additive superposition of single forces between

pairs. For molecules that are not the same kind, the interaction energy between molecules p and q is

$$E_{p, q} = - \frac{3}{2} \frac{h}{s^6} \cdot \alpha_p \alpha_q \cdot \frac{\nu_p \nu_q}{\nu_p + \nu_q} \quad (30)$$

where $\nu_{p, q}$ is the characteristic frequency of the given molecules that give rise to the interaction. As a first approximation, the substitution of the first ionization energy for the $h \nu$ terms has found some acceptance.

Ultimately, London was able to show that the classically derived equations of Keesom and Debye could both be obtained by quantum mechanical analysis and that the orientation, induction, and dispersion effects making up van der Waals interactions were indeed separate reactions that could be summed for a total overall effect.

$$\bar{E} = -\frac{1}{s^6} \left(\frac{2}{3} \frac{\mu_1^2 \mu_2^2}{kT} + \mu_1^2 \alpha_2 + \mu_2^2 \alpha_1 + \frac{3}{2} h \alpha_1 \alpha_2 \frac{\nu_1 \nu_2}{\nu_1 + \nu_2} \right) \quad (31)$$

which for identical molecules gives three simpler terms

$$\bar{E} = -1/s^6 \left(\frac{2}{3} \frac{\mu^4}{kT} + 2 \mu^2 \alpha + \frac{3}{4} \alpha^2 h \nu_0 \right) \quad (31A)$$

(I) (II) (III)

For water molecules, London lists the following values at 293°C:

$$\mu = 1.84 \text{ E-18 esu-cm}$$

$$\alpha = 1.48 \text{ E-24 cm}^3$$

$$h\nu_0 = 18 \text{ volts}$$

for which the terms in equation (31A) work out to the following

$$\text{I} = 190 \text{ E-60 erg-cm}^6$$

$$\text{II} = 10 \text{ E-60 erg-cm}^6$$

$$\text{III} = 47 \text{ E-60 erg-cm}^6$$

$$\text{TOTAL} \quad \overline{247} \text{ E-60 erg-cm}^6$$

Hence the overall potential energy between water molecules due to van der Waals forces

$$\bar{E}_w = \frac{247 \text{ E-60}}{s^8} \text{ ergs} \quad (31B)$$

is still very small compared to the energy derived by repulsive Coulombic forces until s gets very small. For free, charged water molecules (e.g. two hydronium ions) there is no separation distance, short of actual penetration of one another, which would give rise to a van der Waals force in excess of the Coulombic repulsion. Van der Waals effects have been noted between large monovalent ions, such as cesium, however.

The Presence of Charges in Water

Ions in solutions and their equivalents, the charge sites on the particles and grains, play a very important part in the development of the forces and structure of the system of suspended particles passing through porous media in water. The forces that develop between ions are essentially those that develop between isolated charges and follow the Coulomb law

$$F = \frac{e_1 e_2}{\epsilon s^2} \quad (32)$$

where e_1 and e_2 represent the quantity of charge per ion (generally the valence, s is the separation distance of the two centers of charge and ϵ the correction factor* for the interaction of the medium, in which the ions are dissolved, with the ionic field. For completely isolated charges, $\epsilon = 1$. In real systems, however, the medium itself interacts with the ions or charge sites and changes the force relationships. The correction factor, ϵ , when

*Actually the permittivity of the medium ($\epsilon = 1$ in cgs system).

considered for bulk media is known as the dielectric constant. In essence, ϵ is a measure of the polarizability of the intervening medium. The water dipoles tend to orient parallel to the generally radial field around the ion. Thermal agitation tends to keep the dipoles disoriented. The potential energy that is changed in this way to mechanical work has the effect of diminishing the force of interaction between two ionic centers. Since the alignment of the intervening water molecules is the resultant of the electrostatic forces acting against thermal, random, disorienting forces and intermolecular viscous forces, the "dielectric constant" is temperature dependent. Its normal value at room temperatures for bulk water is about 80.

Not only does the presence of the water dipoles change the effective range of the ionic field but it also may change the relative size and mobility of an ion by the process of hydration. The presence of any ion in solution in water or present as a charge site on a surface causes a more or less radial electromagnetic field to exist in its general vicinity. Regardless of the valence of the ion (i.e. + or -) water dipoles will be attracted to it and tend to orient along the lines of force with the portion of the dipole opposite in charge to that of the ion toward the center of the field. All such orientations are subject to disruption by thermal agitation and, with the force field of the ion weakened by the dielectric effect, this orientation of the dipoles is a fleeting thing. Like other dipole reactions, it is temperature sensitive, as shown in the following equation:

$$\overline{E}_{i-d} = \frac{\frac{1}{3} e_1^2 \mu_2^2}{\epsilon s^4 kT} \quad (33)$$

As in the previous discussion on dipole interactions, the $(\frac{1}{3})$ factor in the equation would be prone to decrease as the orientation of the dipole became more fixed. Consequently, the ion-dipole energy approaches zero and is less important to a dipole in close proximity of an ion than it is farther away where thermal forces are able to maintain its random orientation relative to the ionic field.

One interaction of the water molecule with the ion, however, is not subject to orientation effects, that is, the interaction of the ion and the polarizability of the water molecule. While still subject to the diminution of the effective field range of the ion by the dielectric, the force that develops is capable of maintaining a layer or two of water molecules around the ion in a relatively permanent spacial relationship. The energy for such a relation may be found from

$$E_{i-m} = \frac{e_1^2 \alpha_2}{2\epsilon s^4} \quad (34)$$

where e_1 represents the charge of the ion and α_2 the polarizability of the water molecule.

As the water molecules attracted toward the ion center become more and more fixed in orientation relative to the ionic field, their ability to distort the radial field of the ion becomes less. Consequently the water dipoles have a decreasing effect on the strength of the field the closer they are to its center. The result of this is that the correction factor, ϵ , normally determined for the bulk medium, can be no longer considered a constant but must be adjusted downward as the distance of separation decreases. The subject of dielectric constant adjustment is

considered further in the section on the energy of ion exchange. Table 2 shows theoretical values of interaction energies calculated for isolated charges, dipoles, and polarizable molecules at different distances of separation. In parentheses the energy is calculated again after allowing for the effect of the dielectric correction factor (assuming the charges (as ions), dipoles, and polarizable molecules to be present in water). The values used for the dielectric correction are shown in the row labeled ϵ . These typical values from the literature represent the effort of various authors to account for a varying degree of orientation of the water molecules at different separation distances between test charges.

The values for the dipole reactions are probably not realistic in this close range. Nonetheless, the values were calculated so the relative values of ionic and polarizability reactions could be compared to it. The values in the table were calculated assuming sodium ions and water molecules were interacting. As may be seen in the column at the far right, even with the weak van der Waals forces, the potential energy at contact is markedly higher than the thermal mean energy and a considerable degree of stability would be expected to result. Note that the comparable reactions, i.e. ion-ion versus dipole-dipole etc., are about the same magnitude. Minor contributions from one or another factors could counter-balance the resultant force with apparent ease. In like manner, under the proper circumstances, several of the reactions shown in Table 2 might be expected to add together resulting in a stronger force than expected.

Once oriented by the dipolar attraction to an ion, and at close range attracted even more by ion-molecule reactions, the strength of the cation

Table 2. Comparison of Molecular Interaction Energies at Different Distances.

Reaction	@10 Å	@7.38 Å (~2 H ₂ O)	@4.62 Å (~1-H ₂ O)	@2.29 Å (~contact)
E _{i-i}	1.4 eV (1.8E-2)*	2.0 eV (2.9E-2)	3.1 eV (3.1E-2)	6.3 eV (1.3)
\bar{E}_{i-d}	4.2E-2 (5.3E-4)	1.43E-1 (2.2E-3)	9.3E-1 (9.3E-2)	1.5 (3.1E-1)
E _{i-m}	1.6E-3 (2.03E-5)	3.58E-3 (5.4E-5)	2.3E-1 (2.33E-3)	3.9E-1 (7.7E-2)
E _{d-d}	1.3E-4	8.0E-4	1.3E-2	9.0E-1
\bar{E}_{d-m}	3.3E-6	2.0E-5	3.3E-4	2.3E-2
E _{m-m}	1.3E-5	8.5E-5	1.3E-3	9.6E-2
(ϵ)	(80)	(66.4)	(10)	(5)

Where $E_{i-i} = \frac{e_1 e_2}{s}$; $\bar{E}_{i-d} = \frac{\frac{1}{3} e_1^2 \mu_2^2}{s^4 kT}$; $E_{i-m} = \frac{e_1^2 \alpha_2}{2 s^4}$;

$$\bar{E}_{d-d} = \frac{2}{3} \frac{\mu_1^2 \mu_2^2}{s^6 kT} ; \bar{E}_{d-m} = \frac{\alpha_2 \mu_1^2}{s^6} ; E_{m-m} = \frac{\alpha_1 \alpha_2 V_1 V_2}{s^6 (V_1 + V_2)}$$

The subscript letters refer to ion (i), dipole (d), polarizable molecule (m).

The subscript numbers identify the properties of a given ion or molecule.

(e) = ionic or lattice surface charge, statcoulombs (esu)

(μ) = dipole moment, esu-cm,

(V) = ionization potential of the molecule (approximate equation), stat-volts.

(s) = distance between the interacting molecules or ions, cm,

(α) = polarizability, in cm³ ($\sim 10^{-24}$)

*Values in parentheses are the energies corrected for the value of ϵ shown at the bottom of the columns.

attraction for the oxygen portion of the water molecule may exceed the attractive forces between water molecules. In such cases virtual ionic reactions may occur with the water becoming literally bonded to the ion. Table 3 lists data taken from Klassen,^{7,8} converted to energy units in electron volts, for hydration energies of various cations. Comparable lattice energies of the halides of certain cations are also included for comparison.

As may be seen in the table, the hydration energies of these free ions are in the range of chemical bonds and compare in magnitude with the lattice energies of the halides. The capability of water to dissolve minerals or salts is based largely on the relative magnitude of the hydration energy to the crystalline bond energies in the mineral itself. Considering that the values in Table 3 represent averages subject to the thermal distribution of energies, the relative overlap of the hydration and lattice forming energy distributions must strongly affect solubility. The significant change in solubility with temperature change is a verification of this.

Of greater importance than the actual values for hydration and lattice energies in the Table 3 is the relative magnitude. Table 4 is a brief summary of energies to be expected in three general ranges of interaction between ions, dipoles, and molecules in the aqueous environment. While the energy of interaction between a water molecule and an ion may be influenced by a number of factors, the point to be made is that the energy is sufficiently high, compared to other interactions, for the water to be considered a permanent part of the ion. Consequently, calculations

Table 3. Comparison of Hydration and Lattice Energies for Monovalent Ions

Ion	Hydration Energy, eV ¹	Lattice Energies of the Alkali Halides, eV ²			
		Fluoride	Chloride	Bromide	Iodide
H ⁺	9.76				
Li ⁺	5.68	10.41	8.63	8.17	7.55
Na ⁺	4.21	9.25	7.94	7.57	7.11
K ⁺	3.34	8.23	7.17	6.91	6.54
OH ⁻	3.90				
F ⁻	5.33				
Cl ⁻	3.60				
Br ⁻	3.17				
I ⁻	2.73				

¹Klassen,⁷⁸²Chem Rubber Handbook, 45th edn, p.F95,⁵⁵

Table 4. Summary of Interaction Energy Ranges

Energy Range	Type of Interaction
1-10 eV	Ionic and covalent chemical bonds, including hydration and silicate lattice bonds
0.1-1 eV	Electrostatic interactions including hydrogen bonding, normal ion adsorption and some chelation energies
0.025-0.1 eV	Weak interactions including van der Waals and water orientation effects

involving ions must take into consideration the hydrated radius rather than that obtained from crystallographic studies alone (Pauling,⁵⁹ Goldschmidt⁷⁹).

This is particularly true in the consideration of ion exchange. Klassen⁷⁸ pointed out that ion exchange takes place in two forms, physical and chemical adsorption. The former describes the ion situated in an attractive electrostatic field where the attractive force is somewhat stronger than the force resultant from thermal displacement can overcome. It can be, however, subject to changes brought about in the solution by the condition of the water such as flow, agitation, temperature, salt concentration etc. Chemical adsorption is, on the other hand, the result of chemical bonding in which the ion, as such, is removed from solution onto the substrate by exchanging or sharing electrons. This type of adsorption is virtually irreversible under the conditions of groundwater ion exchange and falls into the chemical or lattice bond category of Table 4.

The physical adsorption type of ion exchange is similar to the reactions that take place in the hydrogen bonding of water molecules. The magnitude of the attractive force depends largely on the field strength. In turn, the field strength depends on the relative valence of the ion and the distance between the adsorption site and the ion center. The degree of the hydration of the ion plays a large part in the determination of the maximum force of attraction because it affects the minimum distance of approach to a charge site.

Submicron Particles in Water

Since this thesis is primarily concerned about the transport of radioisotopes by means of mobile submicron particles, it is particularly

germane at this point to consider the interactions of these particles with the water in which they may be suspended, or with the sand grains to which they may be adsorbed, or with each other as agglomerates. For this particle size range the overall physical reactions give rise to resultant forces which are of the same general magnitude as those arising from the chemical reactions. The size range lies between what might be termed true-colloidal on the one hand and that which is visible under the microscope (light). Being on the order of a few hundredths to a few tenths of a micron in diameter, there is no good way to distinguish them from the colloids on the one hand and the macroparticles on the other except to note that the effects of surface forces are especially pronounced in this in-between range. The particles exist as discrete entities which show little tendency to react with the surrounding molecules on any permanent basis; yet they are active both physically and chemically. Perhaps the best way to distinguish them would be to say that they lie in the range that is well resolved by the electron microscope, but below the range that is well resolved by the light microscope.

The presence of a suspended particle in water does two things. It may disrupt or build water structure, and it forms a solid-liquid interface where, spacially speaking, one did not exist before. The degree to which the particle disrupts or builds water structure depends on many factors that also typify ions in solution. In the particle, lattice distortions resulting from elemental substitutions, physical defects, broken

valence bonds etc. give rise to the effective charge centers or sites on the particles.

The form of the electric field over the surface of a particle differs from that of free ions in that there is a fixed and reasonably homogeneous distribution of charge centers along that surface. At charge sites, water molecule dipoles are attracted with essentially the same energy as they would be with free ions and a decrease in the dielectric constant of the water near the charge center would be expected (Stern⁸⁰). By comparison to free ions, the particles act more like charged flat or slightly curved plates than point charges except at considerable distances. Examination of suspensions of finely divided quartz and kaolin with an electric field has shown that these particles (and indeed all of the silicates) have an overall negative charge. Careful determination of the heat of wetting of carefully dried particles can be used to measure the total charge or charge density of these materials.

The distribution of charge sites, whether due to broken bonds or lattice vacancies, on quartz grains can be considered relatively homogeneous over the entire surface. With kaolin, however, the internal structure is such that bonds are only broken as more edges are created, not when lateral faces are freed from the bulk structure of the mineral. In pure kaolin there is considerable doubt that substitution of aluminum for silicon in the silica layers exists in sufficient amounts to give rise to any significant numbers of charge sites on the lateral surfaces. Various experiments have been performed to show the presence of lateral face charge sites, but most of the evidence now seems to indicate that only

the charges formed by broken bonds along the edges are significant to account for the reactions of the mineral in bulk. Consequently, it will be assumed here that the charge sites are exclusively on the mineral edges and the large flat surfaces of kaolin are composed of polarizable oxygen atoms strongly bonded to the silicon below them.

Mineral surfaces such as that of quartz and the silica layer of kaolin have a natural lattice spacing called the tridymite structure which is not only tetrahedral, like that of water, but for which the oxygen spacing is almost identical to that of the hydrogen-bonded water structure. With essentially no ions or charge centers to distort the structure along the lateral surfaces of the kaolin flakes, the polarizability-polarizability interaction which takes place between the oxygen portion of the water molecule and the oxygen portion of the silica molecules in the clay surface results in the production of a water net with the same approximate steric pattern as the underlying oxygen atoms in the mineral.

The resulting structure for this water layer is essentially hexagonal like that of ice, especially that obtained at quite low temperatures. This ice-like layer is held firmly in place by a combination of the polarizability reactions and the dipole interactions that develop between adjacent water molecules on the mineral surface. Once the positioning of the water molecules is well established, the steric matching of the water molecules in the net and the oxygen atoms of the silica surface is so close that hydrogen ion exchange can take place between the two oxygen layers, resulting in a virtual hydrogen bonding of the water to

the silica surface.

This water net with its open spaces about the diameter of a water molecule plays a large part in the formation of many minerals of the clay type where fundamental mineral layers such as silica, brucite, alumina etc. are held together by ions that fit within this netlike water structure without abnormally distorting it (Grim,⁸¹ Lawrence,⁸³ van Olphen⁸²). Indeed in the mineral montmorillonite, which has a structure similar to that of kaolin except for considerable substitution in the silica layer, many of the physical and ion exchange characteristics arise from this combination of water network and exchangeable cations between the lateral sides of the clay flakes.

Van der Waals Interactions Between Particles and Grains

To study the van der Waals interaction between suspended particles and the sand grain matrix of the packed bed, it is useful first to consider the interaction between two identical particles. Hamaker⁸³⁻⁸⁶ assumed that the potential energy between suspended particles, attributed to the attractive London-van der Waals forces, could be considered additive. With that assumption, it became possible to extrapolate the interaction of individual atoms to the overall interaction of finite-sized particles by integration. Kruyt⁷⁰ performs this integration and the following equation is adapted to the terms used here from his work:

$$E_p = -\frac{\pi}{12} q q' \beta \left(\frac{1}{S_0^2} + \frac{1}{(S_0 + 2\tau)^2} - \frac{2}{(S_0 + \tau)^2} \right) \quad (35)$$

where q and q' are the atom number or molecule densities of the two particles respectively; β is the London coefficient (about $E-59$ erg-cm⁶); S_0 is the minimum distance in cm between any two atoms, each in its own plate; and τ is the thickness of the particle in cm. This equation was developed for two parallel, infinitely large, flat plates and gives the potential energy per unit of effective area in cm². In the literature, this equation takes the form

$$E_p = - \frac{A}{48 \pi} \left(\frac{1}{d^2} + \frac{1}{(d + \tau)^2} - \frac{2}{(d + \frac{\tau}{2})^2} \right) \quad (36)$$

where the magnitude of A , Hamaker's constant, $= \pi^2 q^2 \beta \approx E-12$. In this equation it is assumed that q and q' are equivalent and that d = the half-distance between the particles.

Equation (36) suggests that the actual energy of interaction between infinitely wide, flat particles attributable to London-van der Waals forces varies as $1/s^2$, rather than as $1/s^6$ as it is purported to do with individual atoms or molecules. It also shows that beyond a certain thickness, the particles involved can be considered as infinitely thick without materially changing the results of the calculations. When the distance between the two interacting layers is small compared to the thickness of the particles, then the equation (35) can be reduced to the simpler form

$$E_p = - \frac{\pi}{12} \frac{q q' \beta}{S_0^2} \quad (35A)$$

where E_p has units of ergs/cm² in the cgs system.

The general equation can be applied to three special cases of interaction between masses that pertain to this experimental work.

- a) that between two kaolin particles, essentially of the same size,
- b) that between a kaolin particle and a sand grain, much larger than the particle,
- c) that between two very thick particles or between two sand grains.

In general, the equation (36) is used with a very approximate value for A , Hamaker's constant,⁸⁵ because the equation, as it stands, does not account for the interplay between the molecules of the medium suspending the particles and the particles themselves. To account for this, Hamaker visualized a more complex equation that included energy terms between two imaginary particles occupying the space in which the real particles were found. These imaginary particles had the same nature as the fluid and their interactions with the real particles tended to reduce the force of attraction between the original particles. In reality, these interactions seem to be quite difficult to assess in mixed systems, since the polarizability and characteristic potentials of the atoms or molecules involved must be known for a given system. Generalizing, Hamaker pointed out that the constant, A , will vary between the extreme limits of $E-14$ to $E-11$ ergs with an effective mean lying between $E-13$ and $E-12$ in most cases. He noted, for particles suspended in fluids, the value of A will have the same order of magnitude, although somewhat smaller than that of the same system taken in vacuo.

Examination of equation (35) shows that it is necessary to multiply by the common area of the two particles to obtain the total interaction

energy between them. Using the approximate figure of $A \approx E^{-12}$, van Olphen⁸² calculated the van der Waals attraction energy between two unit layers as a function of half-distance for clay particles. In the appendix to his book, he shows a curve from which van der Waals energy per unit area can be determined at any half-distance between 12 and 75 Angstrom units. The range of energies indicated for these distances varies between 0.1 to 0.0001 ergs/cm² respectively.

The fact that the interaction energy depends very strongly on the distance between individual atoms or molecules in their respective particles implies that the total energy of interaction will be dependent primarily on the effective area of the smaller particle involved in the reaction. Consequently, the range of the forces involved will be most dependent on the smaller particle breadth and not that of the larger one. In the second special case, the quartz grains are nearly one thousand times the size of the kaolin particles and their radius of curvature is such that the surface corresponding to the area of a kaolin particle is essentially as flat as the kaolin particle itself. The reaction between the kaolin flake and the quartz grain, therefore, will be about the same magnitude as that between two kaolin flakes at distances small compared to the particle thickness.

Equation (35A) may be considered valid as long as the thickness of the particles exceeds ten times the distance of separation between them. For the kaolin particles in question, the thickness is approximately 1/30 the length of an edge, 0.033×10^{-5} cm or about 33 Å. It would be better, therefore to use the more complex equation (35) for this interaction.

Since the interaction between a kaolin particle and a quartz sand grain is essentially the same as that between two flat plates (one thin and one thick) equation (35) may be re-evaluated for this case where δ is the thickness of the sand grain

$$E_p = - \frac{\pi}{12} q q' \beta \left(\frac{1}{(S_0 + \delta + \tau)^2} - \frac{1}{(S_0 + \tau)^2} - \frac{1}{(S_0 + \delta)^2} + \frac{1}{S_0^2} \right) \quad (35B)$$

If the grain thickness, δ , is much greater than either the thickness of the particle or the distance between the particle and the grain, then equation (35B) reduces to the following:

$$E_p = - \frac{\pi}{12} q q' \beta \left(\frac{1}{S_0^2} - \frac{1}{(S_0 + \tau)^2} \right) \quad (35C)$$

Again, if S_0 is much smaller than the thickness of the particle, τ , equation (35C) reduces to the simpler form of (35A) and the total energy involved is proportional to the face area of the small particle, not to that of the grain. Evaluation of equations (35) and (35C) for particle-particle and particle-grain at different distances will provide a useful comparison for interaction energies. Assuming that the value for q is essentially the same for both kaolin and quartz, $q = 2.65 \text{ E} + 22 \text{ atoms/cc}$ (Robie and Bethke)⁸⁷ then $q^2 = 7.02 \text{ E} + 44$ and if the polarizability of the surface atoms of those minerals in water is essentially that of water, then $\beta = 47 \text{ E}-60$ (London) and $\frac{\pi q^2 \beta}{12} = 86.378 \text{ E}-16$. Figure 1 shows the evaluation of the London van der Waals attraction energy for the three cases of infinitely thick plates, one thin and one thick, and both thin. These cases are effectively those of grain-grain, grain-particle and particle-particle, where the points of contact of the grains are to be about the same

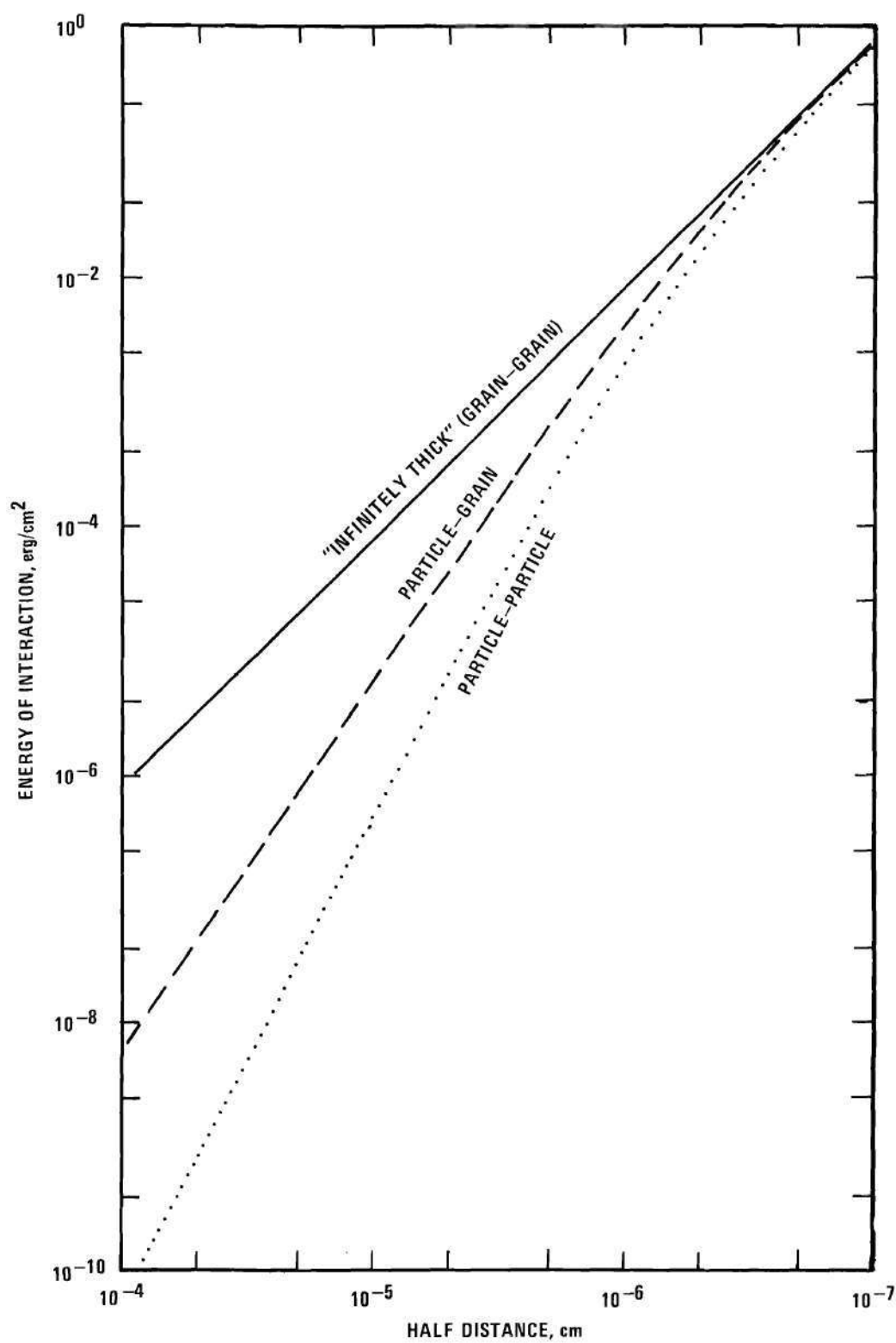


Figure 1. Van der Waals Interaction Energy for Particles and Grains

diameter as the particles.

For the typical grain and particle being considered here, if a common area of 2.60 E-10 cm^2 applied to all three curves in Figure 1 at a separation distance of one micron, then values of 2.24 E-14 ergs for grain-grain, 1.47 E-18 ergs for grain-particle, and 1.45 E-20 ergs for particle-particle would be typical values of interaction energy. As may be seen by comparison with the gravitational interactions, the van der Waals forces are definitely worth consideration even at a distance of a micron.

The Particle Charges

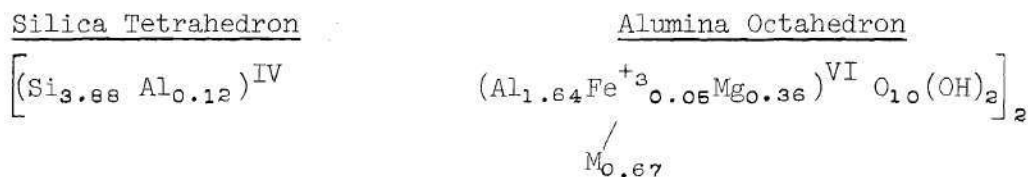
Opposing the long range interactions between particles that result from the summation of London-van der Waals forces is the electrostatic repulsion of like-charged particles. Lawrence⁵³ reasoned that the overall charge that develops on a particle is due to individual unbalanced charges that result from substitutions and lattice deficiencies within or broken chemical bonds at the edges of crystalline minerals.

In the kaolin mineral there are essentially two layers basic to the structure that could give rise to charge locations, one composed of silica tetrahedra and one of alumina octahedra. In the former, the surface oxygen atoms are arranged in an open sheet-like network, whereas in the latter, the surface hydroxyl atoms are arranged in a close packed sheet. Substitution possibilities for the primary cation in the two layers also differ. Replacement of silicon in the silicate layer apparently is quite rare in such pure mineral forms as kaolin or quartz, with aluminum being the most common substitute when replacement does occur. Substitution

of ferric iron or magnesium for aluminum in the alumina layer is apparently much more common.

Unfortunately, the ion exchange capacity of kaolin or quartz, which is a direct measure of the total particle charge, is so low that surface contamination of the finely divided minerals by other materials, even more finely divided, that have much higher ion exchange capacities such as lignin, montmorillonite, sesquioxides of transition metals etc. may account for most of the measurable ion exchange for kaolin or quartz and still be below detection limits by present day techniques.

An estimate of the surface charge distribution as it might appear for kaolin can be made by examining some data on montmorillonite. The latter is also made up of tetrahedral and octahedral sheets of silica and alumina. Van Olphen⁸² gives the formula for a typical montmorillonite as follows:



where M represents the exchangeable cations that give the mineral its peculiar characteristic of expanding in the presence of water. For comparison with kaolin, however, even in this mineral where the substitution in the alumina is so strongly developed, the substitution in the silica layer amounts to only 3 percent.

The cross-sectional area of the unit cell at the oxygen surface of the tetrahedral sheet of kaolin is about 54 \AA^2 , while the actual surface area covered by oxygen atoms is only about 37 \AA^2 or 68.6 percent of the

flat surface. In normal conditions of water suspensions, these oxygen locations represent the only part of the kaolin surface where charges can exist if a substitution or dislocation of the silicon ion below has occurred. If substitution in the silica layer was assumed to exist to the extent of 1 percent (Weaver)⁸⁸ then only 0.00686 of the total area would be available for cation exchange. Assuming that this value represents the fraction per cm² of silica surface layers of the clay then there are

$$\frac{6.86 \text{ E-3 cm}^2/\text{cm}^2}{6.16 \text{ E-16 cm}^2/\text{O-atom}} = 1.115 \text{ E} + 13 \text{ unsaturated oxygen bonds per cm}^2 \text{ silica surface.}$$

With a surface area of the lateral face of the kaolin crystal of 2.6 E-10 cm², this amounts to 2.9 E + 3 unbalanced charges per particle face.

Lawrence⁵³ seems to favor the development of ion exchange at the broken bonds found at the edges of the crystals. There, he points out, are four possible types of crystal sites where ions could be adsorbed. The cations could be adsorbed to O⁻ and OH⁻ while the anions are adsorbed to Al^{+1.6} and Si⁺² assuming these crystal ions are half-coordinated from within. Certainly, a comparable area is available there to that of the larger flat face surfaces. The two areas for the model kaolin flake being considered here would be 0.2 E-10 cm² for the edges and 5.2 E-10 cm² for the total face area of the crystal. For particles that are not as thin relative to the face area as this one, the difference would be even smaller.

Taking Lawrence's value of 7.8 E + 14 unsaturated bonds per cm² of edge surface for kaolin and assuming them to be equally divided between positive and negative charge centers, for a particle of edge area of

$0.2 \text{ E-}10 \text{ cm}^2$ this would be $1.56 \text{ E} + 4$ negative sites. In addition, these negative sites are assumed divided between O^- , $\text{O}^{-\frac{1}{2}}$, $\text{OH}^{-\frac{1}{2}}$, the ratio between (-1) and $(-\frac{1}{2})$ valences being 6:4.

Table 5 lists the estimated bonding energies of certain cations on charged lattice sites. The distance of separation listed was obtained by Lawrence who calculated the hydrated radii of the two ions involved (cation and O^- charge site) and added them to get the distance. An evaluation for the dielectric constant was obtained by using the following equation

$$\epsilon = \frac{s + \ln Z}{2 Z^2} \quad (37)$$

where Z is the valence and s is the distance of separation. This equation was derived by the empirical fitting of Hasted's model #1 for determining the dielectric constant as a function of distance from an ion⁸⁹. In making this determination, the basic requirements placed on Hasted's curve were

- 1) the combination of factors leading to the bond strength estimate had to follow the general replacement series given by Lawrence ($\text{Li}^+ < \text{Na}^+ < \text{K}^+ < \text{NH}_4^+ < \text{Mg}^{++} < \text{Ca}^{++} < \text{Al}^{+++} < \text{H}_3\text{O}^+$)
- 2) the bonding energy of Li^+ had to exceed that of the mean thermal energy (0.025 eV at room temperature).
- 3) the bonding energy of Al^{+3} had to be less than a hydrogen bond (taken nominally to be about 0.5 eV).
- 4) it had to account for some change in water molecule orientation which partially offsets the increase in water layer thickness for

Table 5. Bond Energies Between Adsorbed Cations and Charged Lattice Sites

Adsorbed Ion	Separation Distance, Å	Full Bond Energy, eV	Full Bond Sites Free, %	Half Bond Energy, eV	Half Bond * Sites Free, %
Li ⁺	5.05	0.0534	11.80	0.0267	34.4
Na ⁺	4.65	0.0646	7.55	0.0323	27.5
K ⁺	4.45	0.0754	4.90	0.0377	22.1
NH ₄ ⁺	4.35	0.0922	2.50	0.0461	15.82
Mg ⁺²	5.75	0.0532	11.90	0.0266	34.5 ** (11.9)
Ca ⁺²	5.55	0.0617	8.48	0.0308	29.17 (8.5)
Al ⁺³	3.20	0.7487	----	0.3743	3.14 E-5 (abt 0.0)
H ₃ O ⁺	2.76	0.8973	----	0.4492	1.57 E-6 (abt 0.0)

** Numbers in parentheses (xx.x) represent probability of multiple bond breakage.

*It is assumed that the surface ions on the Kaolin flakes are half-coordinated from within the crystal hence the term Full Bond = 0⁻ and Half Bond = OH^{-1/2} or O^{-1/2} as designated by Lawrence⁵³.

polyvalent ions.

The empirical equation (37) was designed only to evaluate the electrostatic interactions between ions and charge sites in as close accordance to modern theory as possible.

The calculated values given in Table 5 are at best estimates; but they do permit the calculation of the relative number of exchange sites that should be free at any given time (using an adaptation of the Boltzmann equation). Consequently, the possibilities range from about 35 percent for lithium to 1.6×10^{-6} percent for the hydronium ion, 11.9 percent for both magnesium bonds at once and almost zero possibility for all three aluminum bonds to break at one time. The values given in Table 5 are higher than comparable values given by Lawrence, from whom the general sense of the table was derived. However, he erred by using the square of the dielectric constant in the Coulomb equation during his calculation of interaction energies; nor did he allow for changing dielectric coefficient with distance in this rather critical range.

The total number of negative sites available per particle for cation exchange according to Lawrence's criteria would be $0.6 \times 1.56 \times 10^{24} = 0.936 \times 10^{24}$ full bond sites plus $0.4 \times 1.56 \times 10^{24} = 0.624 \times 10^{24}$ half-bond sites. Treating the half bond site as monovalent (per Lawrence) and the full bond site as divalent, if all locations were loaded initially with sodium ions, then $0.936 \times 10^{24} \times 0.0755 \times 2 = 1416$ plus $0.624 \times 10^{24} \times 0.275 = 1720$ give a total of 3136×10^{24} vacancies at any given moment. Using the previously determined weight per particle of 2.295×10^{-16} grams, the number of particles per hundred grams would be 43.57×10^{16} and the total

number of sites per hundred grams would be 13.66×10^{20} or about 2.3 milliequivalents per hundred grams. This value falls well within the range for ion exchange given in the literature as 1-10 meq/100 g which helps to justify this approach to the charge determination.

Whether the program of assumptions followed by Lawrence (edge charges) is followed or that preferred by van Olphen (flat face charges), the number of charges per particle is very much the same. If just the silica face is involved according to van Olphen's criteria, then the charges per particle are about equal to the values predicted by Lawrence (2900 vs 3136). If both faces of the particles and the edges are active in charge development, the total would be two to three times that predicted by either one alone; but the overall value would still lie in the range of ion exchange capacity known to exist for kaolins measured in bulk.

The Particle Charge and Ion Exchange

Under the assumption that the number of potential charge sites on a flake of kaolin is fixed by the total number of fixed charge sites, then the total charge on a particle may be found by an analysis of how many of those charge sites are unoccupied at any given time. Lawrence^{5a} established that the number of vacant charge sites at any given time in the presence of cations could be found by the Arrhenius equation

$$N = N_0 e^{-E/kT} \quad (38)$$

where N is the number of open sites, N_0 , the total number of sites, E , the energy of the bond, kT , the thermal energy. The energy terms need to be

in consistent units, such as kcal/mol, ergs, eV, etc. Note that this equation was previously used as the Boltzmann relation with the dissociation constant of water to obtain an estimate of the effective hydrogen bond energy between water molecules.

In actuality, if there are several cations present, each will have an equation similar to the equation (38) and the total number of unoccupied sites will be determined by a combination of these equations as follows:

$$N = N_0 \left(A e^{\frac{-E_{H^+}}{RT}} + B e^{\frac{-E_{Ca^{++}}}{RT}} + C e^{\frac{-E_{H^+}}{RT}} + \dots \right) \quad (39)$$

where A, B, and C are constants related to concentration of the various ions in the solution. These constants are required to account for the Gouy effect.

At the concentrations contemplated for this study, it appears that the Gouy theory may be assumed to apply, i.e. that the ratio of the ions in the double layer surrounding the adsorption surfaces is the same as that in the solution. Some alteration of this to account for differences in valence is necessary and some adjustment for differences in ionic radii, as will be considered later, help account for the replacement series of different ions of the same valence. Except for these adjustments, then, the Gouy theory of exchange equilibria is

$$K = \frac{[A]_i [B]_e}{[A]_e [B]_i}$$

where A and B are two monovalent ions and $[]_i$ and $[]_e$ are their concentrations in the double layer and the equilibrium solution respectively

(van Olphen)⁸². The cation-exchange capacity is equivalent to the total charge of the solid surface and is identical with the excess of cations in the double layer under the low electrolyte concentrations, such as will be used here.

A considerable simplification of equation (39) is obtained if the bonding energy for all but one of the ions involved is quite large. Under those circumstances equation (39) reduces to a form of the simpler Arrhenius equation with concentration the controlling line factor.

Button⁹⁰ performed a similar analysis except for considering equivalent concentrations of both cations and anions. If the charge on the particle, σ , is related to N/N_0 by $K\sigma = N/N_0$ where K is a conversion coefficient that includes the hydrogen ion concentration, the following equation can be written for the case of sodium exchange:

$$K\sigma = Ae^{-\frac{E}{kT}} \quad (40)$$

Solving for σ and putting the two constants together, gives

$$\ln \sigma = \ln \frac{A}{K} - \frac{E_{Na}}{kT} \quad (41)$$

If $\ln \sigma$ is plotted as a function of $1/kT$, the slope of the resulting curve (E_{Na}) is independent of the constants involved. Button made particle charge determinations by measuring the particle mobility in an electric field at several different temperatures for each solution concentration increment. Apparently realizing the effect of the hydrogen ion as a competing cation of considerable bonding power, he increased the cation (Na^+) concentration by adding sodium hydroxide. It is unfortunate that he did

not make detailed measurements at concentrations less than 10 meq/100g where he obtained his energy peak of 0.732 E-12 ergs per bond. Had he done so his peak energy might lie even closer to Lawrence's^{9a} corrected estimate of 0.81 E-12 ergs per bond.

It is not possible on a massive scale to try to reproduce Button's method with a large, packed-sand bed. However, temperature is not the only variable that could be manipulated to determine relative energy levels. Concentration also may be used as a variable if the particle charge is known or can be estimated. Realizing that when all the charge sites are unoccupied, $\sigma_0 = 1/K$, then $\sigma/\sigma_0 = Ae^{-k/T}$ and

$$E = kT \ln A \left(\frac{\sigma_0}{\sigma} \right) \quad (42)$$

Some data from Button's paper relating particle charge and concentration are plotted in Figure 2. As might be suspected, insofar as one can estimate from his data, for low concentrations of cations the total charge exposed is rather insensitive to the quantity of cations, other than protons in solution. The σ/σ_0 factor, therefore, becomes little more than a constant in solutions as dilute as those used in the sand bed experiments. Hence, energy can be estimated by a simple calculation using

$$E = C \text{ pA} \quad (43)$$

where $C = kT (\sigma/\sigma_0)$ and pA is the cation equivalent of pH.

Chemical Complex Formation and Surface Ion Exchange

In the previous section it was pointed out that the energy of ion exchange could, under certain circumstances, (notably that of high dilution)

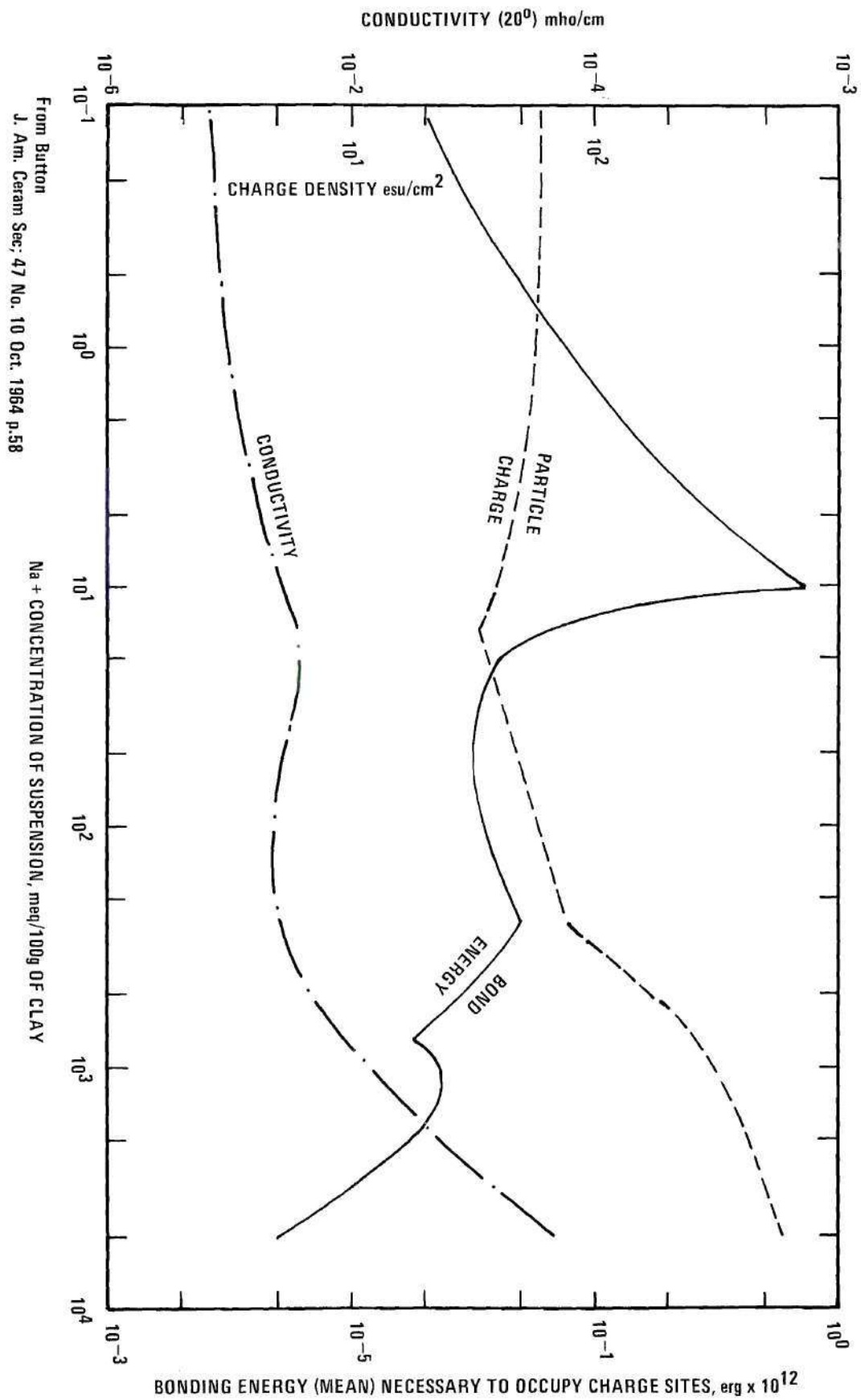


Figure 2. Effects of NaOH Addition to Clay

be found proportional to the pA of the cation involved. A parallel can be seen in this to the chemical complexing of cations by certain organic molecules. In fact, it is useful to consider the latter more fully; for they have been used as tracers in hydrology⁹¹ and as a means of removing trace elements from contaminated soils⁹². Hence, it is useful to evaluate them on essentially the same basis as the ion exchange of the clays.

Welcher,⁹² in his book THE ANALYTICAL USES OF ETHYLENEDIAMINE TETRAACETIC ACID, gives a table of dissociation constants for various cations. Some of these are reproduced in Table 6. While the hydrogen ion bond does not take such a position of dominance in this table it does when combined with the silicate surface, the system of EDTA analyses is based on the constant competition between the cations in question and the hydrogen ions. As may be seen, the general sequence of the cation bond energy is similar to that shown in previous tables for the silicates. The differences are due no doubt to steric matching of some of the ions with the available charge sites on the EDTA molecule. One obvious and important similarity between the data in Tables 5 and 6 is the fact that the general order of magnitude of energy required to complex the cations chemically is approximately that of the energy required in ion exchange with the silica surface.

Thus even active complexing agents like EDTA must undergo stiff competition from the silica and silicate surfaces for the cations they carry. Such competition would cause severe losses from the complexed radioactive tracer. Where a cation is chosen which has a

Table 6. The Bond Energies of EDTA and Various Cations at Normal Temperatures.

Cation	Log K [*]	Bond Energy, eV
Na ⁺	1.66	0.096
Li ⁺	2.79	0.161
H ⁺	10.22	0.588
Mg ⁺⁺	8.69	0.501
Ca ⁺⁺	10.59	0.610
La ⁺⁺⁺	15.50	0.892
Al ⁺⁺⁺	16.13	0.929
Tb ⁺⁺⁺	17.93	1.03
Sc ⁺⁺⁺	23.1	1.33
Fe ⁺⁺⁺	25.1	1.445

*Welcher's⁹² formation constants

high degree of stability with EDTA or some other complexing agent and a low one with the minerals, a relatively long lived tracer for groundwater could be formulated. However, in comparing the data in Table 6 with Table 5, it is obvious that there are no ideal examples that meet this need. Some seem better than others, but on the whole, all of them would be subjected to a significant degree of transfer to the silicate surfaces as long as the latter maintained their overall negative charge.

Ion Exchange and the Silica-Silicate Surface

As noted before, the mineral quartz is composed of a three dimensional, tetrahedral network of silicon ions bonded to oxygen ions that is pure almost to the point of total exclusion of substitution ions. As the original crystals weather out of rock and are fragmented by the movement of wind and water, ionic bonds are broken between the silicon and oxygen each time a new surface is created. These unsatisfied valence bonds determine much of the physical chemistry of the quartz surface.

Presuming that the breaking of the quartz grain occurred in an environment where oxygen or water was present, the broken bonds provide a charge site of attraction for these molecules. Obviously, for every bond broken in the formation of new silica surfaces, there is produced one positive charge site (the silicon) and one negative charge site (the oxygen). Although the silicon is present in the crystal as a $+4$ ion, it is not represented that way at the location of the broken bond because only one of its four bonds is presumed to have broken. The charge at the site, then, is positive and equivalent in charge to only one electron unit.

Water molecules in the vicinity of the free silicon bond would be accelerated toward it by an ion-dipole attraction as well as by an ion-polarization reaction. At contact, the energy of reaction between the 0.42 Å radius silicon and the 1.38 Å radius water molecule would be on the order of 1 electron volt from the ion-polarizability alone. In addition, the proximity of the silicon ion to the water molecule would encourage hydrogen bonding of the latter to other water molecules in the vicinity. Because of the continued presence of the silicon, eventual loss of the hydrogen ion to the general pool of ions in the water probably would occur.

The energy for the normal dissociation of water can be calculated from the general Boltzmann equation

$$N = N_0 e^{-E/kT}$$

where N is the number of free hydrogen ions and N_0 the total number of water molecules, E the activation energy, and kT the thermal energy. Using the hydrogen ion concentration at neutral pH, the activation energy is found to be 0.175 eV. The polarizability-ion reaction energy of silicon with water is nearly ten times this value. From this, it would appear that the silicon indeed should be capable of dissociating the water molecule. Once the hydrogen ion has left the vicinity of the OH^- in contact with the silicon, additional attraction may be found in the ion-ion reaction that develops between the silicon and oxygen ions, tempered by the presence of the one remaining hydrogen ion on the opposite side of the oxygen ion. In essence, the oxygen ion acts to hold the silicon and hydrogen ion together.

The surface produced by the association of a water molecule with a broken silicon valence bond and the subsequent dissociation of the molecule leaving an OH-group on the silicon charge site and the other hydrogen ion taking its place in the pool of ions in solution, must be quite similar to that of the alumina surface on the kaolin particle. Polarized, as it must be away from the silicon, the hydrogen ion remaining attached to the oxygen atom must be bonded somewhat more tightly than it was before. It represents a charge site to which anions and polarizable water molecules will be attracted. Because of the size of the anions, however, the electrostatic attraction between them and these "bound" protons will be weak. Any intervening water molecules due to the momentary hydration of the ions will weaken the bonds even more. A cloud of anions will form around such charge sites and, in order to keep the overall charge per unit volume of the suspension neutral, cations will migrate into the area at a greater distance from the charged surface than that occupied by the anions.

Other charges exist on the broken silica surface, those of the negative valence bonds from the oxygen atoms. Conceivably, attraction of polarizable water molecules to these locations could result in the loss of a hydrogen ion from a water molecule through hydrogen exchange between the two oxygen atoms. In such an event, the surface structure would not be significantly different from that of the silicon and alumina surfaces described above. On the other hand the negative site of attraction may cause migration of cations of all kinds from the solution to the area surrounding the broken oxygen bond. The length of time that any one ion spends in the vicinity of the oxygen bond then would depend on how large

and how abundant it was relative to the hydronium ion.

Van Olphen⁸² points out that the same structures exist at the broken edges of kaolin silica layers as have been described above for quartz. The apparent amphoteric reaction of the broken oxygen valence bond sites may cause the entire edge of the particle to act as a positively charged area resulting in an adsorption of anions, the latter forming a negatively charged counter-ion layer. Apparently, these broken oxygen bonds are so pH sensitive that either anions or cations can be adsorbed to the same surface depending on the relative pH of the environment. This is one of the reasons that van Olphen and others look to the adsorption of cations to substitution sites in the silica sheets on the large flat surfaces of kaolin rather than the edges to explain the natural cation exchange capacity of the mineral in bulk.

The above theories regarding the establishment of ion adsorption sites as a result of the broken chemical bonds at edges of crystals or unbalanced charges along the crystal faces as a result of substitution of ions are both speculative and leave much to be desired in extrapolation to ion exchange, particle charge and ultimately the effect that the presence of ions may have on the attraction between suspended particles and the quartz sand-grain matrix of the packed bed.

Whatever the immediate source of the charge, both quartz grains and kaolin particles are known to be negatively charged in water. It is inherent to such a system that the relatively high mobility and abundance of water molecules precludes any significant number of charge sites being balanced first by free cations. The ion adsorption reaction must

take place through the intermediary of an adsorbed water molecule whether it is one which migrated there by itself or, by being part of the hydration shield of a particular cation, was attracted electrostatically to the site. Therefore, each cation must compete with hydronium ions for the adsorption sites. As can be seen in Table 7, the relative energy of interaction for most ions is so small compared to that of the hydronium ion that exchange with the latter would seem impossible. Even accounting for the finite range of thermal energies, replacement of the hydrogen ion by other cations must require some reduction in its attraction to the bound oxygen on the silica surface. Such a means is found through the activity of the other water molecules nearby through the electrostatic attraction between their oxygen atoms and the adsorbed proton.

Movement of the proton toward the oxygen atom of a passing water molecule would leave the negative charge site of the silica surface at least partially unbalanced. The distance of separation of the proton from the oxygen ion center fixed in the mineral surface layer may be presumed to range from 0.96 to 1.92 Å or more depending on the relative polarization of the two oxygen ions in the vicinity of one another. Any simple cation approaching the negative charge site will have the appearance of a point centered radial electrostatic field in which are oriented water-molecule dipoles. These dipoles will have their oxygen end pointed toward the positively charged center and the other end with the protons oriented outward. Although relatively rigid, this arrangement leads to adsorption which is again effectively that of hydrogen ion exchange.

Table 7. Free Energy of Hydration of Monovalent Cations

Cation	Radius, * Å	Free Energy, ** eV
Li ⁺	0.6	5.0
Na ⁺	0.95	3.9
K ⁺	1.33	3.19
Rb ⁺	1.48	2.94
Cs ⁺	1.69	2.64

*Calculated crystal radii from Pauling⁵⁹.

**Robinson and Stokes⁶⁷.

According to this theory the ability of cations to be absorbed to a given exchange site depends largely on how closely they resemble in size, and to some degree in charge, the simple hydrated proton. In addition, empirical studies on material in bulk suggest that coordination of the water molecules around the ions is an additional factor that may affect the relative ability of one ion to be held more tightly to a charge site than another.

Robinson and Stokes⁸⁷ quote data from Latimer⁹⁴ for the free energy of hydration of monovalent cations. These data (converted to electron volts) are shown in Table 7. As may be seen, the ions that most closely resemble the hydrogen ion in size and might be expected to react most strongly with the exchange site are found to react most strongly with the water molecules. Consequently, the distortion of the water molecules (of hydration) around the small lithium ion is large enough to cause the path, traveled by the oscillating hydrogen ion maintaining the hydrogen bond to the exchange site, to be larger than for that of any of the other monovalent ions. Hence, the mean reaction energy would be weaker to the exchange site. In addition, the thickness of the adsorbed water layer is greater (on a statistical basis) around the smaller cations, affecting not only the distance between the charges but also their relative mobility.

Table 8 lists data accumulated by Lawrence⁵³ showing the hydration radii of several important cations compared to their "normal" crystal radius. The hydrated radii are calculated from the equation

$$r = \frac{0.820}{\lambda^0 \pi^0} \frac{|Z|}{r_s} \text{ (r/r}_s \text{) Angströms} \quad (44)$$

Table 8. Comparison of Hydrated to Crystal Ionic Radii for Selected Cations.

Cation	Cation Radius, Å	Hydrated Radius, Å
Li ⁺	0.68*	3.7
Na ⁺	0.98	3.3
K ⁺	1.33	3.1
NH ₄ ⁺	1.43	3.0
Zn ⁺²	0.74	4.4 (2.2)**
Mg ⁺²	0.78	4.4 (2.2)
Ba ⁺²	1.34	4.1 (2.1)
Ca ⁺²	1.06	4.2 (2.1)
Sr ⁺²	1.12	4.2 (2.1)
Al ⁺³	0.57	1.9 (0.6)
La ⁺³	1.14	4.6 (1.5)

*This data was taken from Lawrence's book with this exception: Lawrence lists the crystal radius of Li⁺ to be 0.78 which is at variance with the data of Pauling (0.60) and of that listed in the Chem. Rubber Handbook. The latter lists (0.68) and Lawrence's figure was assumed to be a typographical variant from this.

**The figures in parentheses are the relative values of hydration radius per ionic charge.

where (r/r_s) is found from a correction chart (Robinson and Stokes,⁸⁷ p 125) r_s is the Stokesian radius, η^0 the viscosity of solvent, λ^0 the conductivity at infinite dilution⁹⁵.

The hydrated radii of the ions obviously follow a very different pattern than do the crystal radii. Of the two, it is the hydrated radius-sequence which most perfectly match the order of exchangeability of the ions quoted by Lawrence ($\text{Li}^+ < \text{Na}^+ < \text{K}^+ < \text{NH}_4^+ < \text{Mg}^{+2} < \text{Ca}^{+2} < \text{Al}^{+3} < \text{H}_3\text{O}^+$). Note especially that the hydration radius relative to the ionic charge follows the sequence very well and ion exchange is in no case a direct sum of the cation crystal radius and the unperturbed diameter of a water molecule.

A third approach to explanation of relative exchangeability of ions is suggested by Pyfe⁹⁵ who notes:

the small Li^+ ion interacts more strongly with the water molecules, and so to free the ion from the solvent requires more energy for Li^+ than Na^+ than K^+ . Thus the ion with the smallest size (Li^+), while being most strongly bound in the solid, is also strongly bound in the liquid through ion-dipole forces. These competing influences, almost always present in such a process, make any detailed calculations or predictions difficult, if not impossible, with our present knowledge.

Whatever model is picked for the theory of individual reactions at the molecular level, it must meet the qualifications required by studies made on bulk material. This is often not easy for a single model to do. Use of the Coulomb law for the energy of electrostatic attractions combined with the hydrated radius of the cations appears to meet the right order of exchangeability. Some ions have hydrated radii so similar in size that other minor changes in a given system may alter the relative order of exchange from that of another. It is necessary to be able to

specify the system as closely as possible, therefore, in order to attempt analysis of experimental data by use of such models.

Particle-Particle Charge Interactions

The previous discussion has dealt with the development of charge on particles of kaolin or on grains of quartz and the concentration of counter ions near their surfaces. Colloid theory holds that the nearest layer of ions to the charged surface is relatively tightly held and moves with the particle wherever it goes. This inner layer, known as the Stern layer, is surrounded by a so-called diffuse or Gouy layer of ions which consists of a rather loose layering of ions of alternating charge. There is, of course, a net counter-ion charge of the Stern layer, σ_s , and a net counter-ion charge of the diffuse layer, σ_d , the two of which summed make up the total effective charge of the particle. In practice, it is this total effective charge that affects the interactions between ions, particles, and/or grains in water suspension.

Dissolved ions move with the water passing through a porous aquifer only to the extent that they escape interaction with the tremendous surface area presented to them along the path of their travels. Since siliceous minerals inherently have negative surface charges in water the interaction of cations with them is particularly strong. These coulombic attractions are relatively long range, especially when the concentration is low and the interference from electric fields of other ions is absent. A rule of thumb for the effective distance over which the electrostatic field acts may be found by calculating the so-called Debye length⁹⁶

$$l = 97/\sqrt{C}$$

where ℓ is in Angstrom units and the concentration of the solution, C , is in millimoles per liter. The Debye length is considered the distance over which the charge or ionic field is effective in attracting or repelling another charge.

The interaction energy between charged particles of any kind can be determined through their effective charge and the Coulomb equation. However, in water suspension and in the presence of many counter-ions at different potentials relative to the surface, the relationship is much more complicated. Van Olphen has summarized some useful techniques for estimating this interaction where the charge density, separation distance, and salt concentration in the solution is known. The following development for the kaolin particles being considered here is taken from Appendix III of his book which deals with electric double-layer computations.

Integration of the force across the complex electrostatic field that exists between two flat interacting double layers can be approximated by a relatively simple equation. So-called weak interactions between particles, for which the distance of separation is substantially larger than the Debye length are found from

$$E_R = \frac{(64 \pi n kT)}{\kappa} \gamma^2 e^{-2\kappa d} \quad (45)$$

in which $\gamma = (e^{z/2} - 1)/(e^{z/2} + 1)$

z = surface potential

$$\frac{1}{\kappa} = \left(\frac{\epsilon k T}{8 \pi n e^2 v} \right)^{\frac{1}{2}}$$

ϵ = dielectric constant of medium ≈ 80

kT = thermal energy $\approx 4E - 14$ ergs

n = number of ions/cc

e = 4.8×10^{-10} esu

v = valence of ion

d = half distance between particles in cm.

For monovalent ions in water

$$\kappa = 10.44 (\eta E+13)^{\frac{1}{2}}$$

where η = normality.

The determination of (z) , the surface potential, is iterative largely from hyperbolic equations. Fortunately, van Olphen has tables of typical values from which an estimate for the energy of interaction between two particles can be made. Figure 3 shows the results of calculations for four NaCl concentrations, E-1, E-3, E-5, and E-7 molar over the range of half distance of E-7 to E-4 cm. These curves are represented roughly over the range from one thickness of a kaolin particle to the mean separation of the particles completely dispersed at a concentration of 1-10 mg per liter.

Since much of the study was made with solutions of E-7 molar NaCl concentration (or its equivalent in ions from dissociated water), the relative constancy of the curve E-7 molar interaction energy with changing

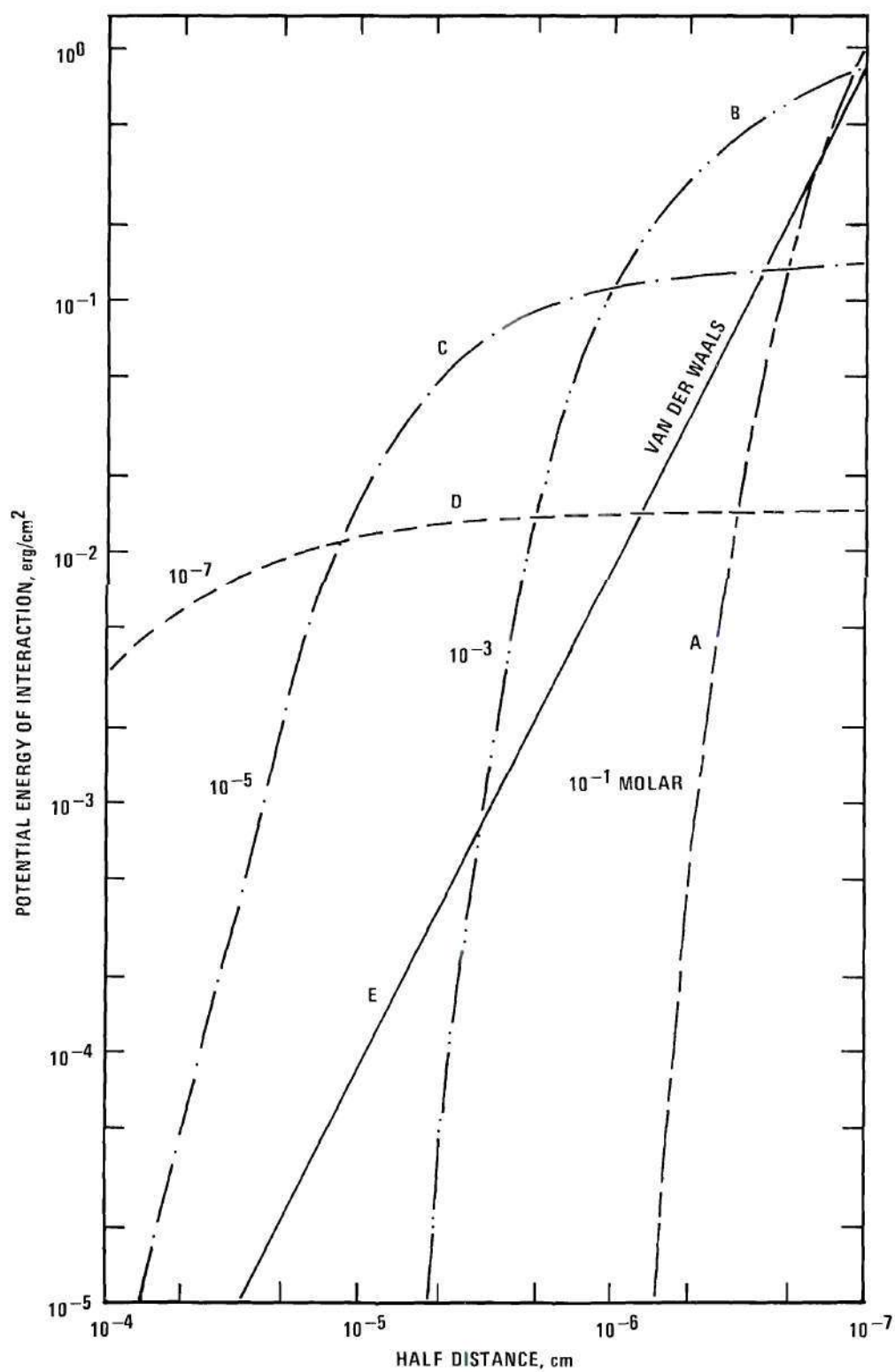


Figure 3. Energy of Interaction Between Kaolin Plates

separation distance is especially pertinent. At this particular ion concentration the London-van der Waals energy representing attractive forces exceeds the energy due to charges on the particles, representing repulsive forces, at about 100 \AA . Curve E in Figure 3 represents the van der Waals energy for the interaction of infinitely thick plates plotted on the same scale as the charge interactions. This curve effectively shows the maximum van der Waals energies to be expected in this system.

While there are probably more complications than those indicated here for this system of ions, particles, water, and grains the curves in Figure 3 do convey the general, theoretical interpretation of modern suspension theory. Comparing curves B and E for example, if B represents the energy of repulsion and E represents the energy of attraction, there are two marked areas of overall attraction between the charged particles even for E-3 molar salt solutions. One is at separation distances less than 20 Angstroms. Similar projections can be obtained for the other curves as well. Even with low concentrations of salts in solution, therefore, there should be an overall grouping together of particles at separation distances of 1 micron, 0.1 micron etc. (depending on the concentration) in a relatively stable form of agglomerate. Such groupings may effect further interactions that lead to tighter packing and eventually lead to different filterability than might be expected from the individual particle size alone.

Particle Interactions between Unlike-Charged Particles

One other point needs to be considered here, if only briefly. That is the interaction between unlike charged particles in this system. In

choosing the materials with which to experiment, an effort was made to select sand and clay which would be charged the same. Both kaolin and quartz are noted in the literature to have overall negative charges in electrodynamic studies with sols of those minerals. However, as van Olphen⁸² points out (and illustrates so beautifully in his frontipiece) the edges of kaolin particles may be positively charged. If conditions of the environment are right, this positive charge may actually dominate the interactions between particles.

Just as quartz grains are noted to be negatively charged in aqueous environments, so ferric hydroxide and other metal hydroxide sols are noted to be positively charged. The quartz sand obtained for this experimental work was nearly pure quartz, having been washed free of fines, and had a very predictable packing characteristic due to its rather clearcut, nominal, grain size range. The grains were noted under microscopic examination to be coated with films of yellow to reddish material which were transparent to translucent and which had no definable particle size themselves (low power optical). Ultrasonic scrubbing of samples of the sand did not remove this material in distilled water suspension. This film on the grains must represent in the experimental system a positively charged sol of iron hydroxides which is firmly attached to the sand grains and, as such, homogeneously distributed throughout the sand pack. Further mention of this film-like material will be made in the Discussion of the Results, Chapter IV.

The Removal of Suspended Particles from Water by Porous Media

The successful transport of radioactive isotopes by particles in

suspension through aquifers depends largely on the rate of removal of those particles by the porous bed. As in the adsorption of the isotopes from solution, the removal of the particles from suspension is a function of the "instantaneous" concentration of particles in suspension at any given point in the bed, assuming that the bed is homogeneous, the flow is essentially isotropic, and recycling is not indigenous to the bed nor practiced experimentally. Two major processes operate to remove particles from suspensions passing through porous media under the above conditions, "straining" and "sorption".

Straining, as used in the literature, refers to the physical removal of particles from a suspension by their encountering passages along the path of flow that are too small for them to penetrate. These may be capillary restrictions or open crevices between the grains. Separation by straining follows the relation

$$C = C_0 e^{-\omega x} \quad (46)$$

where C represents the concentration of particles in numbers or weight units per unit volume of water, C_0 the original concentration, x the distance of penetration into a horizontal bed of sand and ω is a rate factor that is essentially a removal coefficient. This rate factor varies with particle size, but not with position in the bed as long as the conditions of homogeneity and isotropy are approximated³³. An estimate of this rate factor can be made from knowledge of the relative magnitudes of the particles and of the sand grains, as well as the length of path along which the reaction can take place. One such estimate is the following

$$\omega = (D/d)^{\frac{3}{2}} \cdot X/d \quad (47)$$

where D is the effective diameter of the influent particle, d is the effective mean diameter of the grains forming the bed, X is the total length of the bed, or some functional fraction thereof, much larger than d .³²

Sorption, in this context, has to do with a number of processes which arise from the proximity effects discussed earlier. Since the important reactions between the fine particles and the sand grains are dependent on distance as $1/s$, or $1/s^2$ or under certain circumstances $1/s^6$, it is obvious that the region in which reaction takes place between the suspended particles and the sand grains must lie very close to the grains themselves.

In his detailed study of the removal rates of virus-sized particles in porous media, Filmer⁴⁰ showed most of his data, expressing retention of particles versus depth penetration of the sand filter, followed the linear isotherm (that is, a relatively simple exponential) function

$$\theta = \theta_0 e^{-mky} \quad (48)$$

where θ was the concentration of particles (albumin) retained by the soil in grams per gram of soil, θ_0 was the concentration of particles at the soil surface ($y = 0$), y = the depth from the sand surface, k = a proportionality constant, and m was a constant specific for the particular bed.

$$m = \frac{\rho_b}{w \phi S \rho} \quad (49)$$

where ρ_b = the bulk density of the soil, ρ = density of water, ϕ = porosity of the soil (volume of pore space expressed as a fraction of the bulk volume of a porous medium), S = degree of saturation (the ratio of the volume of water to the volume of interconnected pore-space in a bulk element of a porous medium) and w = the thickness of the particle-containing slug or wafer. Only rarely did it appear more complicated functions such as the Freundlich, Langmuir, or B.E.T. isotherms would be required to explain the disposition of the particles in his experimental work.

Filmer set forth conditions required for such a linear adsorption isotherm to apply to porous beds as the following:

- 1) the porous bed initially contains no adsorbed tracer particles
- 2) the particles are carried into the porous bed by the flowing water at the same average velocity as the fluid elements
- 3) (forward) dispersion of the particles by diffusion is negligible
- 4) the velocity of the flow is sufficiently small that there is time for the adsorbed and dispersed phases of the particles to reach equilibrium concentrations, at any given region in the aquifer.

It is also noteworthy that the change in concentration of the suspension, dC , is proportional to the concentration of particles retained by

the soil, θ . That is

$$-dC/dy = m\theta; \quad (50)$$

the effect of this depletion gives a new concentration

$$C = C_0 e^{-mby}. \quad (51)$$

The slope of the corresponding curve would be the same as that expressed in terms of θ . These useful values for the suspension could be determined from the concentration of particles in the effluent, C , and influent, C_0 , of the bed. In like manner the ratio of θ/θ_0 can be determined from the radioactive particle retention in the sandbed. By detection of the radioactivity through the side of the bed, the value of θ_0 can be obtained by projection of the data taken along the bed back to the zero position of the scanner.

In an earlier thesis (Champlin⁴) the decrease in the amount of radioactivity retained was determined to be on the order of a magnitude per meter of distance penetrated into the bed. At $\theta = \theta_0/e$, the value of the exponent can be determined. That is to say when $y^{-1} = mb$, then one can experimentally establish the value of the removal parameter b by using the slope of the plotted data and experimental parameters for m . For Champlin's previous data, which were based on the same parameters by and large as this experiment, $m = 0.965 \text{ cm}^{-1}$ and $b = \sim 43$ for sand and kaolin particles*. Hence the mean free path length for these particles would be predicted to be about 40-45 cm in this bed. At a depletion rate of about a magnitude per meter of travel, the particle load should be completely removed in about 10-12 meters under the conditions of that previous experiment.

*For total removal.

It is useful at this point to show that with an arbitrarily chosen value of about 100 Å for the attractive energy range between suspended particles and the sand grains, a probability for particle removal can be determined. Champlin calculated the mean hydraulic radius for the packed sand being used here as 16.9 microns from the Carman-Kozeny equation

$$(\text{mhr}) = \left(\frac{1 - \phi}{\left(\frac{\phi \times 10^3}{5 p} \right)^{\frac{1}{2}}} \right)^{\frac{1}{2}} \quad (52)$$

where (mhr) = mean hydraulic radius of bed pores in microns

ϕ is the porosity in decimal form

p is the permeability in millidarcies

5 is an arbitrary constant assigned to loose aggregates by Carman.

By using bulk measurements, the bed may be treated as though it consisted of straight frictionless capillaries whose radii are r_c . Assuming that any particle approaching within 100 Å of a sand grain will be removed from suspension within a centimeter path length, then this affected area represents the fraction $\frac{100\text{E}-8}{16.7\text{E}-4}$ of the total cross sectional radius of a capillary whose mean hydraulic radius (mhr) is 16.7 microns⁴. A similar comparison could be made to the "limiting pore" (a measure of the largest sphere that could pass through all the pores of the packed bed), 8.5 microns. The total length of flow path can be taken as 2 meters x $\sqrt{2}$ (a common means to attempt to correct for tortuosity).

Thus, if sorption effects were due to proximity alone, the probability of removal for a particle of this size would be 0.00358 percent per meter. Following Filmer's lead that the sorption process followed an exponential

depletion of the concentration, it is possible to evaluate the proportionality constant, b , by using equations (49) and (51) in combination with established bed characteristics. Using a bulk density of the sand, $\rho_b = 1.63$, a porosity, $\phi = 0.35$, the saturation, $S = 1.0$, the effective wafer thickness, $w = 4.83 \text{ cm}^*$, and the density of water, $\rho = 1.0$, m may be calculated from equation (49) to be 0.965 cm^{-1} . With $m \sim 1.0$, the magnitude of the proportionality constant, b , in equation (51) is essentially the numerical equivalent of the reciprocal of the particle mean free path length (in cm.) through this bed. It is the value of this constant, b , therefore, that will be a measure of the relative particle retention by the sandbed.

Filmer showed in his work with albumin particles in sand packs that "sorption effects provided removal rates of fine particles that were similar in magnitude to the removal rates for coarser particles, assigned to straining" by Hall. Realizing that straining, as a removal mechanism, may have been over estimated in its potential, Champlin indicated that in suspensions of mixed particle sizes (such as with natural clays) both mechanisms might provide significant and possibly comparable rates. He attempted to show that his retention data for radioactively-tagged particles in a sand bed illustrated this contention.

Clearly, if straining is a truly important means by which particles, much smaller than the pores, are retained by a sand pack, then no simple chemical or physical changes such as salinity or temperature increases nor introduction of relatively dilute solutions of different ions should affect the manner in which or the rate with which the particles are

*Determined from the volume of radioactive liquid, porosity and dimension of the bed.

retained by the bed.

On the other hand, if straining does not have the significance assigned to it for fine particle removal by Hall, then sorption must be the principal cause of high retention rates by sands and soils. Sorption effects are subject to changes in temperature, salinity, and anionic type in the water circulating through the bed as shown or indicated by the various calculations and theoretical discussions offered earlier in this chapter. It is the point of this thesis to show that not only is sorption the major means by which fine particles such as clays and bacteria are removed by sand beds (and soils) but also the particles can be displaced chemically from their places of adsorption and caused to move en masse with the infiltrating water.

As suggested earlier in Chapter I, this possible displacement may be viewed in at least two ways. It can be considered as a hazard to the public water supplies and means taken to counteract it. On the other hand, such movement through an underground aquifer, as a direct result of deliberate chemical control of the infiltrating water from the surface, could be a godsend in the field of hydrology.

CHAPTER III

EXPERIMENTAL PROCEDURE

The experimental work to be described here consisted of following the movement or determining the relative retention of radioactivity dissolved in water and that of radioactive particles suspended in that water through a packed bed of sand. The primary purpose for this work was to show that the ability of a sand aquifer to retain either dissolved or particulate matter depends to a large degree on the chemical nature of the infiltrating water. The use of radioactivity in the water can be assumed representative of two field applications which are relatively common. First, as a hydrologic tracer for underground water flow, the ability to use radioactive ions depends on their ability to remain in solution or suspension without being retained by the grains of the bed material. As dissolved ions or suspended particles, if they are poorly retained by the sand pack and, in general, stay with the infiltrating water front, they may be good tracers. If they are strongly retained by the sand bed, then they are poor tracers for the moving water but good indicators for the ability of the sand pack to remove that particular type of contaminant from water. Second, radioactive ions in solution or suspension represent waste products from industry that may be disposed to the environment for natural decontamination and/or dilution by porous soils or rock that make up natural aquifers. Such wastes include nuclear wastes of various kinds, insecticide

and pesticide wastes, paper mill, refinery wastes etc,. The ability of the soil to decontaminate water depends on the partition coefficient for ions between the minerals and the water. The use of radioactive chemicals provides one means of studying these reactions.

One of the principal objectives of this experimental work was to show that relatively minor changes in the chemical nature of the water infiltrating sand horizons could have considerable effect on the ability of the soil to retain particulate matter. In that the ability of quartz sand grains to retain ions directly is quite limited, their ability to form a retentive surface layer of fine particulate matter is important for the latter may, in turn, form a base on which ions will readily adsorb and be retained by the sand pack.

Consequently, the study had to include such factors as the effect of particle size, carrier ion concentration, the adsorption properties of particles and of the sand matrix for the purpose of determining how they affected removal rates and relative mobility of ions or particles through the sand matrix. Minor techniques such as labeling particles of different kinds, scanning the side of the sand pack with radioactivity sensitive instruments, analyzing the effluent for radioactivity, and the nature of and identity of particles etc., also had to be developed in order to conduct the main experimental work.

The basic method used in the experiments was relatively simple in design. All the experimental work centered around a large test box into which a tonne* of sand could be packed. By starting with a freshly packed

*Tonne = metric ton or (000 kilograms).

bed before beginning each major study, no chemical nor particle displacement "memory" caused by conditions in any previous investigation was involved. Each new bed was prepared with a homogeneous composition and the flow of water through it was essentially isotropic. Radioisotopes, used for tracing the movement of the water and its dissolved or suspended components, were either prepared in the Georgia Tech Research Reactor by thermal neutron activation of readily soluble salts of the elements desired or purchased from a commercial vendor in "carrier-free" form. This radioactive material was diluted by a factor of a million with distilled water and then used either directly in the influent water as a dissolved tracer or mixed with a dilute suspension of particulate matter to permit interaction of the tracer with the particle surface through ion exchange prior to introduction into the influent. The movement of these tracers in the packed sand bed fell into three general types; those that traveled virtually unimpeded through the bed, those that interacted with the aluminum manifold, wick, or surface of the sand pack, and those that suffered exponential loss in concentration due to steady removal from the water passing into or through the bed.

These conditions were monitored in essentially the same way as that described by Champlin in his Masters thesis as sampling of the effluent, Geiger-scanning of the sides of the sand pack from the outside and coring of the bed after the end of each run, except that no coring was performed in the two experiments described here. Changes made in choice of radioisotope, particle type and size range, and chemical nature of the influent solution were the only real, planned variables of this basic

experimental procedure. This procedure was essentially that described in detail in the Georgia Tech Water Resources Center Report WRC-0867. Additional information is available in that report.

Apparatus

Sand Container

A large aluminum box was prepared to hold the sand. It had dimensions of 0.5 x 1 x 2 meters with hinged end doors and a removable lid. Figure 4 shows a profile view of the apparatus before loading. The hinged ends served as plenum chambers from which the water solutions or suspensions seeped through a wick into the packed sand. The inner plate of the chamber was perforated with 3/16-inch holes drilled in 1/4-inch aluminum sheet stock spaced hexagonally at 3/4 inch intervals. A manifold constructed from aluminum tubing was connected to the plenum chamber by fittings which penetrated the outer plate. A one-inch thick polyurethane foam wick was cemented to the inner perforated plate at each end of the box to allow good contact between the plenum and the sand. The wick also served to distribute the flow of the water evenly to the sand at the inlet and to collect the water from the entire sand face at the outlet. The inner sides, bottom, and lid of the box were covered with non-permeable neoprene sponge. The porous surfaces of the neoprene and the polyurethane served to interlock the sides of the container with the sand surface to prevent channeling of the water between the sand pack and the smooth aluminum.

A one-inch thickness of plastic bonded, wood-chip plywood was glued

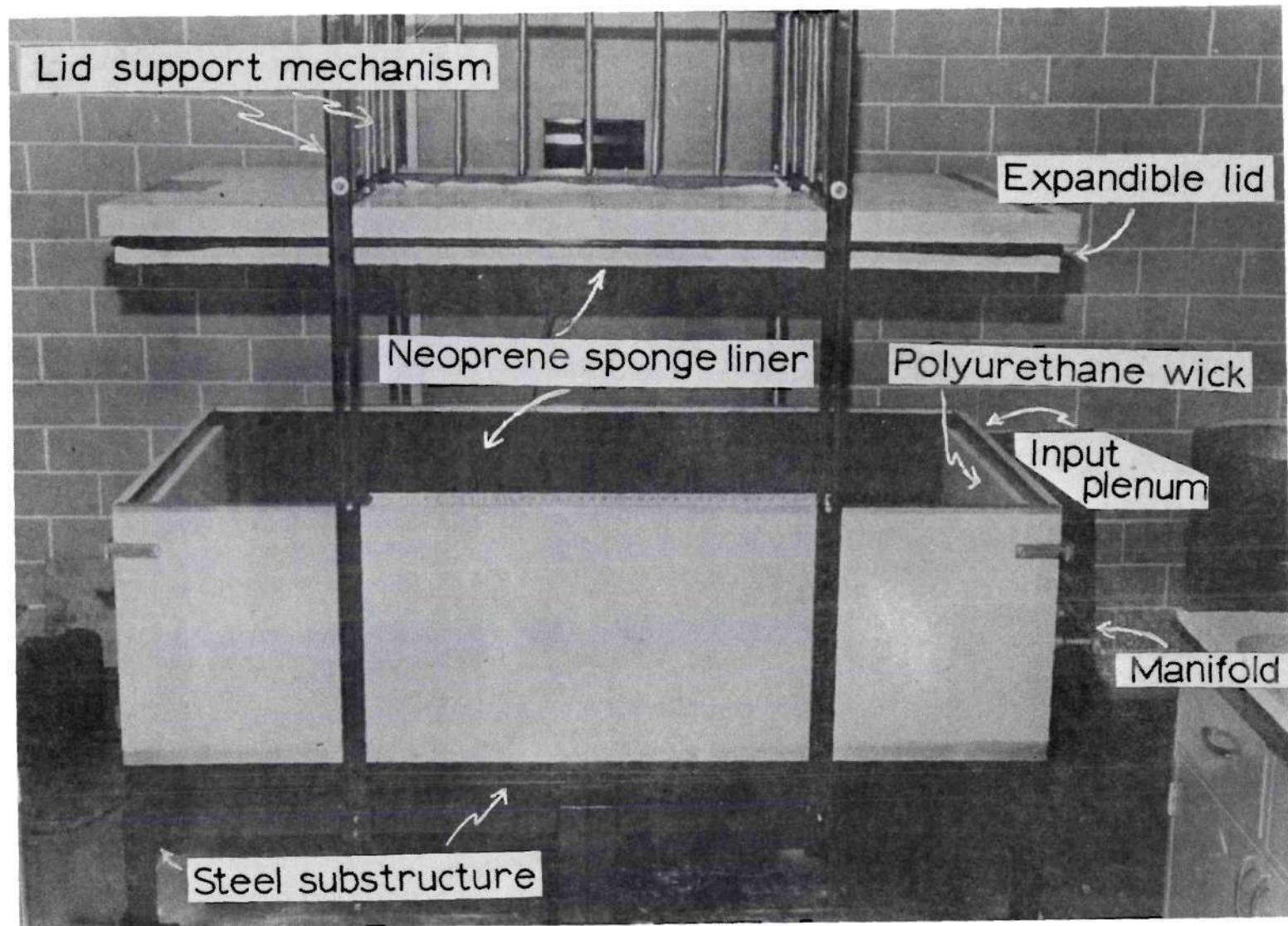


Figure 4. Container for Packed Sand Model Aquifer

to the aluminum sides to support them. Steel channel iron, used to support the lid when raised away from the bed, also served to support the sides. For strength the aluminum sides and bottom (made of 1/4 inch aluminum sheet stock) were welded together at ninety degrees to form the basic box shape. The bottom was supported by one inch of marine plywood backed up by a one-inch layer of wood-chip plywood. A girder system of I-beams and angle iron beneath assured a rigid supporting framework capable of withstanding a possible load up to two tons, with the box filled with wet sand. The lid was constructed in a way similar to that of the bottom except that a section of it could be pneumatically lowered to any position desired in the box to act as a vapor seal for the top of the sand pack. A combination compressed air-vacuum pump was used to seat or raise the pneumatic section of the lid.

The input manifold was connected by means of tygon plastic tubing to a small adjustable diaphragm pump and a ballast bottle. The latter served primarily as a means of introducing the radioactive solutions and suspensions since the flow through the manifold was so slow that the pressure changes introduced by the pumping action were insignificant. Twenty-liter polyethylene bottles and a 20 gallon plastic garbage can were used to store distilled water and to feed water into and collect solutions from the packed bed.

Vibrator Packer

A Syntron Model VH 65-B electrically driven vibrator was mounted on a square of aluminum, 1/4 inch thick, cut to fit the inside of the box closely. Additional support was managed by welding a center strip

to the back of the plate that served as a mounting for the vibrator and minimized torsional modes of the plate. This vibrator was used only during preparation of the sandbed to pack fresh layers after the addition of each 100 pound bag of dry sand.

Side-scanning Radioactivity Detector (GM)

A side scanning device was prepared by placing Nuclear Chicago D-33 or D-34 end window GM tubes horizontally into holes bored in lead bricks to form a vertical array of six detectors. With the sides thoroughly shielded against radiation penetration, the end-windows were recessed into the lead bricks sufficiently so that the cone of sensitivity was restricted to about 20 degrees in front of the window. This arrangement gave such decidedly forward sensitivity that simultaneous detection and quantitative evaluation of the radiation from a given vertical profile of the sand bed was possible, without serious overlap, at spacings as close as 2.5 cm along the side of the bed. The six tubes were arranged so that the lowest was on the level of the bottom of the sand bed and each of the others was sequentially higher with center to center spacings of five centimeters. Each tube was connected through a transistorized circuit by a common lead to a multi-channel pulse height analyzer TMC Model 401. The output of each Geiger tube was taken off a voltage-dividing network yielding a different base voltage fed into the analyzer for each detector. By adjusting the output amplitudes of the detectors to differ by fixed amounts and the TMC gain for spacing between the recording channels on the oscilloscope, the response of all six tubes could be recorded at once. A paper tape printout then gave a permanent record of the six simultaneous readings

and an effective profile of the radioactivity distribution in the sandbed.

Side-Scanning Radioactivity Detector (Scintillation Crystal)

Some of the experimental work required the use of several different radioisotopes in the sandbed at one time. Since the rate of movement relative to the water front was required for each of the isotopes, a mobile shielded unit employing a horizontally-mounted, scintillation crystal was prepared. The main structure was that of an old hospital-tray frame which could be raised and lowered by means of a screw lift. The high platform originally used for the food trays served as a location for the TMC analyzer and printout. A board mounted across the middle supports on the legs served as a platform on which to mount the crystal and preamplifier. A 2-3/4 inch ring of lead, 5 inches long, served as a side shield for this detector. It was sufficiently long that the crystal could be withdrawn into it to cut down on scattered radiation. By moving the frame on its wheels alongside the sandbed and the crystal up or down with the screw lift, the detector could be located at any single position along the side of the bed. The two-inch crystal of NaI(Tl) was mounted as part of beta shielded integral unit with the photomultiplier, Harshaw 8SS-X, and fed its signal through a cathode-follower preamplifier to the TMC pulse height analyzer.

Detector for Radioactivity in the Effluent

Detection of radioactivity in the effluent was accomplished by use of a three inch NaI(Tl) crystal-photomultiplier unit (Harshaw 12S12) mounted vertically in a pile of cylindrical lead-ring shields on a preamplifier. This scintillation counter fed its signal into a TEN decade scaler, Model SA-25Q, obtained from Nuclear Supplies. In cases of mixed radionuclides

in the effluent, the output from the preamplifier was taken to the TMC pulse height analyzer for energy separation of the gamma rays which permitted subsequent analysis from the spectrum printout. Samples collected in polyethylene milk bottles (gallon size) or brown, half-liter, plastic bottles were placed directly on the crystal to be analyzed. The data from the samples were then compared to a standard solution of the same approximate volume in a similar container.

Filtering Apparatus

Standard Millipore or Gelman filter units made of glass and stainless steel respectively were used for all the filtering studies made in conjunction with the analyses of the effluent samples. Membrane filters 47 mm in diameter, composed of cellulose esters exclusively, were used in the pore sizes 5, 1.2, 0.45, 0.10, 0.05 and 0.01 microns. The cellulose composition favored solution of the membrane in organic solvents after shadowing the filtered material so that electron micrographs could be made of the replicated surface.

Devices for Examination of the Particulate Matter

Microscopic examination of the sand grains was made with an American Optical binocular microscope, and sieve analyses over the size range from 25 to 1000 microns previously had been made with a set of stainless steel Tyler screens⁴. By and large, the clay particles were too small to be viewed effectively in the binocular, but studies were made of both the clay and bacteria obtained from the sandbed with a transmission electron microscope and a scanning electron microscope.

An Instrument for Measuring Optical Scattering

Previous attempts to use a nephelometer for measuring the relative concentration of particulate matter suspended in water had proved fruitless because the sensors were arranged in a fixed position to pick up only light scattered at right angles to the original beam. The particles used here, however, were of a size for which forward scattering would be more likely. Fortunately, near the end of the experimental work, Dr. Richard Williams offered the use of a laser he had set up with photomultiplier and nanoammeter for the purpose of measuring scattering angle from suspended particles in air. The laser was a one milliwatt He-Ne University Laboratory, Model 240 placed about two feet from the center of rotation of an angle measuring device on which was mounted a photomultiplier at a radius of about two feet. The Coleman rectangular glass cell originally purchased for the nephelometer work was found to be excellent also for forward-scattering work and it was used to contain the standards and samples in the study. The cell was mounted with long axis parallel to the laser beam directly over the center of rotation of the photomultiplier arm. The readings were taken on a Non-Linear Systems Digital Voltmeter X-3 using the nanoammeter setting after the signal had been detected by a EMI-9558QC (Electronic Musical Instrument) photomultiplier powered by a Fluke 415A power supply. The intensity of the laser was sufficient to give good detail in the forward scattering. Several photographs were taken of the scattering patterns for use in this experiment.

While the scientific potentials of laser scattering from suspended particles are many, one in particular was important to this work. That

was the ability to distinguish between particles larger than a micron and those less than a micron. From a practical standpoint, it was necessary to distinguish between suspensions which were freely divided and those of the same source material in which the individual particles were aggregated. Analysis of the photographs of the scattering patterns showed significant differences between aggregates and finely divided particles. Hence, the laser studies provided a welcome supplement to the electron microscope studies made on the particles caught on filter membranes.

Materials

The Sand

The sand used in the experiments was obtained from the Pennsylvania Glass Sand Company of Columbia, South Carolina. In that the sand is used for the manufacture of glass, the Company customarily screens, washes, and dries the product before packaging it dry in 100 pound paper bags. The grade chosen for these experiments was shown in previous work⁴ to have a grain size distribution mean at 330 microns with very little material smaller than 63 or larger than 1000 microns. Films of fine particles noted earlier to be coating the sand grains did not separate in the screening process. Although the grain-size distribution was peaked mechanically by the manufacturing process, this action did not seem to cause any particular divergence from the log-normal distribution which characterizes such sediments.

The grains of the sand were generally equidimensional, subangular to rounded, non-frosted, clear particles of quartz. Some quartzite and muscovite were present also, each in quantities probably less than two percent of the whole. Gross coatings of the sand grains were not in evidence when viewed by low power microscope, although most grains were coated with a thin transparent film of the color of ochre.

The Clay

A dry-packaged, 100-pound bag of Hydraglos kaolin was obtained from the J. M. Huber Corporation mine and production facility at Wrens, Georgia. The specifications on the bulk clay were that it was 92 percent

smaller than two microns with a mean particle diameter of 0.37 microns. Its distribution of sizes approximated a log-normal and it appeared rather free from chemical as well as mineral contaminants. This clay was placed in dispersion in the summer of 1967 to be used as a stock suspension. It was still well dispersed in the summer of 1969 when the last of the studies reported here were made. Aliquots of this dispersion were used for the experimental work since the uniformity of particle size seemed more likely than for random samples taken from the dry clay.

Chemicals and Radioactive Materials

Other than the salts used in preparing the radioisotopes only two chemicals were used in the experiments. Sodium chloride (Fisher Certified Reagent Grade) was used to build the ionic concentration of the influent solutions for the sandbed. Sodium Tetrphosphate ("Tetrafos" Rumford Chemical Works, Rumford, R.I.) was used as a dispersant in the latter part of the experimentation to effect movement of the clay particles within the sand bed and "calgon", a mechanical mixture of sodium phosphate, soda ash and sodium carbonate, (manufactured by Calgon Corp., Pittsburgh, Pa.) was used in the final part.

The radioisotopes were, for the most part, prepared in the Georgia Tech Nuclear Research Reactor. The amounts were as follows

11 mg NH_4Br to prepare ^{82}Br

5-25 mg Rb_2CO_3 to prepare ^{86}Rb

5 mg $\text{Sc}(\text{NO}_3)_3$ to prepare ^{46}Sc

5 mg $\text{La}(\text{NO}_3)_3$ to prepare ^{140}La .

Except for the rubidium, each of the isotopes was given time enough in the

reactor flux to provide 1-5 millicuries of radioactivity at the time it was placed in the sandbed. The other isotope used, ^{131}I , was purchased from Mallinckrodt, "carrier free" in the amounts of 5 millicuries.

Procedures

The analytical procedures used in these experiments were relatively straight forward and deserve consideration apart from the actual experimental procedures. Aside from the detailed side scanning of the sand bed mentioned earlier, the only other principal data-taking involved means for characterizing the influent and effluent water. Of these, the only quantitative data taking was done with crystal and scaler or the TMC. Determinations were made with each isotope as to whether it was practical to place the collection bottle directly over the crystal rather than to pour out a small aliquot into a Marinelli beaker or some sort of sampling tube. The studies showed that after a milk jug (polyethylene) was more than about one-half full, the reading ceased being particularly sensitive to additional increases in volume and the concentration could be taken as directly proportional to the scaler reading. This proved to be a considerable advantage in time; for by measuring the total volume of a sample and comparing it to a standard of about the same volume, the radioactivity in the effluent could be accounted for quantitatively. Consequently, using fresh sampling containers each time, all other sampling apparatus normally used for transfer, such as beakers, pipettes, vials etc., were dispensed with.

The use of the laser scattering was more qualitative than quantitative since particle size rather than particle numbers was of greater interest

in that portion of the experiment. The technique was almost as simple as that of the radioactivity measurements. The sample bottles were shaken thoroughly, then an aliquot was poured out into a rectangular optical cell 1 x 2 x 2 inches and placed in the light path of the laser. All sample comparisons were made at three degrees of scatter using the intensity reading in nanoamperes as a relative measure of the total number of particles present in the sample. Minor analytical checks were made with the flame photometer, conductimeter, Coulter Counter, pH meter, electron and ultramicroscope etc., and will be presented in the next chapter.

The Procedure

The experimental procedure was divided into Experiment One and Experiment Two, each of which was characterized by a freshly-packed bed of sand. Due to the consistency of results with fresh beds, it was possible to treat the beds as identical for subsequent tests. Experiment One had as an objective the determination of the retention characteristics of isotopes by the sand bed when removed from the influent water as tagged particles (of two kinds) or as dissolved salts. Experiment Two had as its objective the determination of the chemical conditions of the influent water that would reduce the ability of the sand bed to retain radioactive ions, particles, or both.

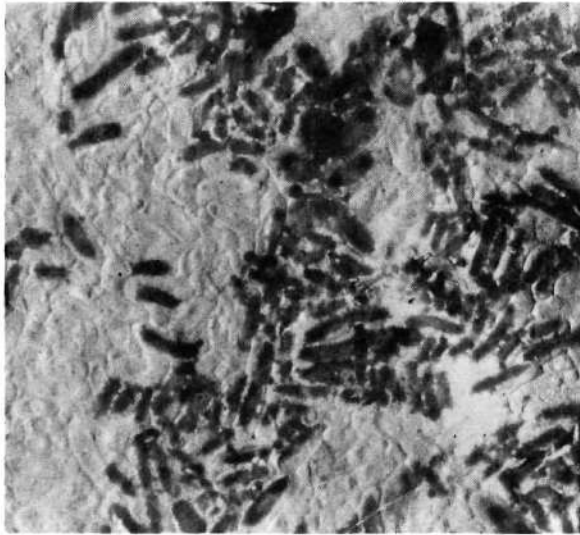
Experiment One

The sand pack developed for this experiment measured 194 cm long, 99 cm wide and 25 cm deep. Water was allowed to seep in at the influent end until the sand had saturated. As more water was passed into the bed by a minor hydraulic gradient, the water in excess of the volume that could

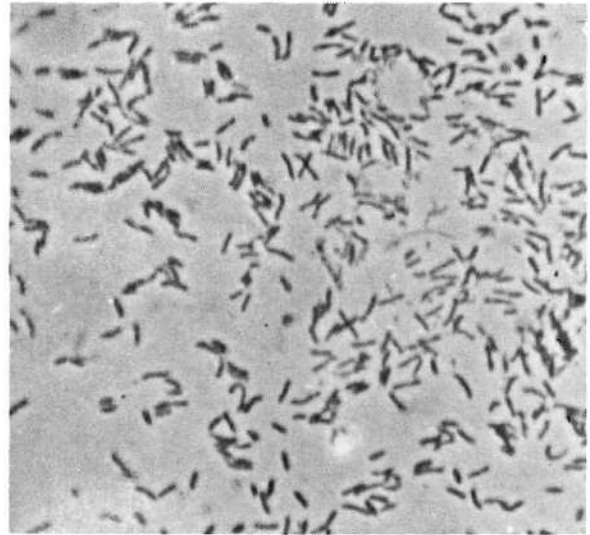
be held in the void spaces of the sand pack drained out through the outlet manifold and was caught as effluent and bottled. As predicted from previous experiments,⁴ the first gallon of water through the bed contained a relatively high concentration of particulate matter, most of which appeared to be bacteria. Figure 5 shows some of these particles by various means such as malachite green staining under the ultramicroscope, internal characteristics by transmission electron microscope, and surface characteristics by scanning electron microscope. The bacteria were noted to be very similar to the slime bacteria characteristic of streams and it was assumed that they had been introduced by the washing procedures during the milling process by the supplier.

The first gallon of water contained the largest quantity of bacteria of the effluent samples. Half of the first gallon was used to dilute 3.3 millicuries (mCi) of ^{140}La , dissolved as the acetate in one-half gallon of water, to a full gallon which was then shaken and allowed to stand until the other isotope mixtures were ready. Next, one-half gallon of the clay suspension containing about 30 mg per liter of Hydraglos Kaolin from the Huber Company, Wrens, Georgia was mixed with a one-half gallon solution of scandium nitrate containing 3.8 mCi of ^{46}Sc , then it was shaken thoroughly and allowed to stand. Finally, 34 mCi of ^{86}Rb in the form of the carbonate was dissolved in one gallon of water and allowed to stand. Thus, the bacteria were labeled with ^{140}La , the clay particles with ^{46}Sc , and the water sample with dissolved ^{86}Rb ions.

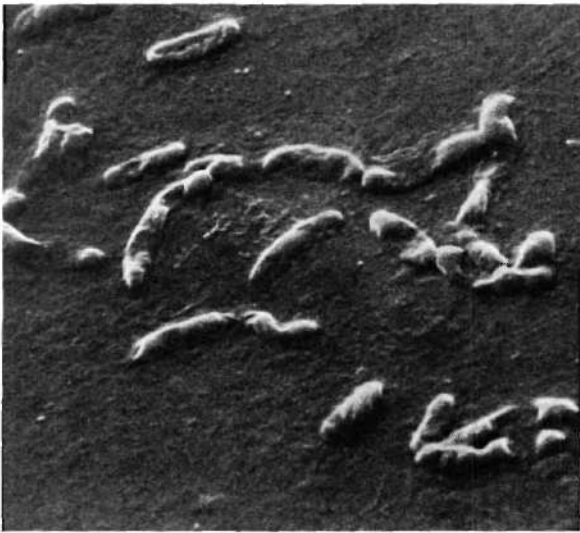
The quantities of cations used in the preparation of these isotopes ranged from 5 mg for the ^{46}Sc to about 25 mg for the ^{86}Rb . In their



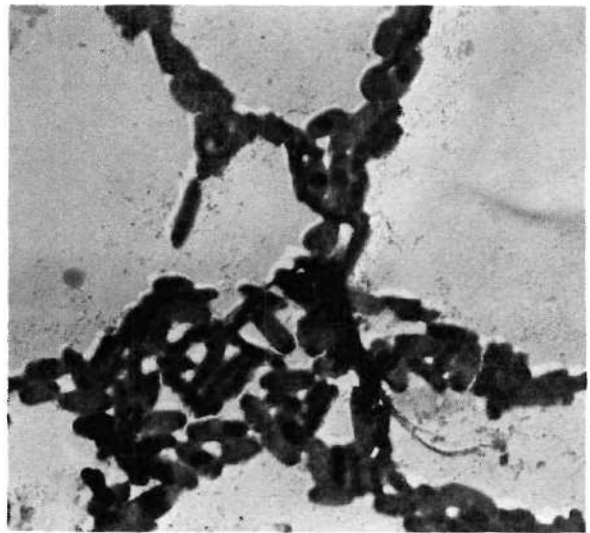
(a) Electron-transmission microscopic view of flagellate forms (effluent).



(b) Ultramicroscopic (optical) view of flagellate forms (cultured).



(c) Electron-scanning microscopic view of flagellate forms (cultured).



(d) Electron-transmission microscopic view of non-flagellate clumping forms (cultured).

Figure 5. Photomicrographs of Soil Bacteria

dilute form before placing in the sand bed, therefore, these solutions represented concentrations on the order of E-4 molar. Further dilution in the sand bed would reduce these concentrations at the most by a factor of 50 if equally distributed throughout the sand bed. The actual dilution in all probability was not more than a fraction of that because the solutions tend to maintain themselves as a piston-like front passing through the sand bed.

The sand bed at this point was saturated with water at a relatively low level of concentration of dissolved salts and dissolved solids in the capillaries of the portion of the sand bed nearest the input. As water enters a newly packed bed, it dissolves salts left there by desiccation of the sand before packaging and carries those salts in solution forward with it as a salinity front. As shown previously,⁴² this salinity front emerges in the effluent with a concentration of sodium at about E-3 molar, potassium E-4 molar, and calcium E-5 molar. This concentration of salts falls off by a magnitude or so after one bed volume of water had passed through the bed. Consequently, the concentration of dissolved salts in the pore spaces of the sand bed for the new experimental work would have been on the order of E-5 molar.

The rubidium was introduced first into the sand as a "slug", or in Filmer's terms, a "wafer" of radioactivity. That is, instead of distributing the activity over a large volume of the influent water, the flow was interrupted, the gallon water containing the radioisotope introduced, then the flow of distilled water was resumed. In this experiment, a rather

high activity of the rubidium isotope (34 mCi) was used because the relative intensities of its gamma emissions are low, on the order of $1/10$ that of the scandium isotope, ^{46}Sc .

Following the introduction of the radioactive rubidium solution, the lanthanum-labeled bacteria were passed into the bed with about two gallons of plain water separating the two isotope inputs. Next, again with the insulating water between, the scandium-labeled clay suspension was introduced to the sand bed. Even though pumping of the input water was suspended briefly to allow introduction of the tracer, movement of the water was continuous in the sand bed due to a small reserve of water in the manifold, wick, and door of the sand container.

Scans were made of both sides of the sandbed with the Geiger-Müller tubes mounted in the lead tower and with the scintillation crystal mounted in its lead shield on the old hospital cart. The G.M. scans along the length of the bed showed the relative position of the radioactivity as a whole and the relative positions of each of the isotopes in the sandbed were established by means of the scintillation detector and pulse-height analyzer. Frequent scanning of the sides was continued until the position of the radioactivity in the bed stabilized. During this time, the effluent was continuously collected in new plastic gallon bottles and a determination of the radioactivity of the water samples, both quantity and type, was made. When it became obvious that most of the radioactivity was firmly retained by the sand bed and further leaching with distilled water was not likely to produce any additional significant movement of the isotopes, the flow of water was terminated and the sand bed allowed to stand idle

for several months. During this time, several scans of the sides were made to establish retention boundaries of the ^{46}Sc and ^{86}Rb as the 18.7 day half-life ^{86}Rb decayed away leaving the 84 day half-life ^{46}Sc alone in the sandbed.

The lid was lifted off the sand pack and the sand allowed to dry as much as it would during the idle period. After the bed had dried for 273 days* distilled water was again introduced. Once the bed had again become saturated and flow was initiated from the effluent manifold, a dilute solution of radioactive iodide, ^{131}I , obtained from Mallinckrodt as "carrier free" sodium iodide was made up. The five millicuries obtained were diluted to one gallon with distilled water. After introduction of the radioactive solution to the bed as a "slug", a continuous flow of water was maintained until the iodide too had stabilized in position in the sand bed.

The next action with the bed was taken for the purpose of determining the stability of the position of retained radioisotope (I^{131}) in the sandbed as the carrier salinity was raised incrementally. This was accomplished by raising the sodium chloride concentration of the influent water by magnitudes from E-7 to E-1 molar. Each solution was made up as twenty liters and a scan of the side of the sandpack made after each 20 liters had passed into the bed. Detection of ^{131}I in the effluent during this period was noted but was not studied in detail.

This terminated the first experiment and the sand container was broken open, the sand removed and placed in sealed barrels for disposal, and the interior surfaces of the box wiped down, vacuumed, washed with distilled

*Approximately three half-lives of ^{46}Sc or one magnitude in activity.

water and dried. After drying the doors were resealed, new polyurethane wicks placed over the face plates and the bed pressure-tested for leaks by filling half full of water. After rinsing again with distilled water and drying thoroughly, the sand container was repacked with fresh sand.

Experiment Two

Realizing that the salinity front that builds up at the leading edge of the input water into a dry sand bed must play a large part in the release of particles from the sand (especially the bacteria) the newly packed sand was not prewet before adding the next radioactive isotope. Instead, a solution of the very soluble ammonium bromide was activated in the Georgia Tech Nuclear Research Reactor to obtain a radioactive isotope $^{82}\text{Br}^-$ chemically and physically very much like the iodide but which had a different gamma spectrum and shorter half life. These isotope characteristics would make it possible not only to distinguish the two radioactive isotopes when present in the same volume together but also to be rid of most of the ^{82}Br by decay before the iodide was added to the sand bed again.

In the part of the experiment using the ^{82}Br the leading portion of water used to wet the bed was tagged with $^{82}\text{Br}^-$ and the passage of the isotope through the bed followed, as before, by scanning along the sides. The bromide passing through the sand bed was collected and the quantity received compared to the input in order to obtain an estimate of the loss to the bed. The flow of water was continued until movement of the bromide in the bed stopped.

At this point a new supply of radioactive iodide was purchased. Instead of introducing it directly to the sand bed as had been the bromide,

the iodide was mixed with a suspension of kaolin using about the same quantities as had been used before with the following exceptions. The kaolin particles were reduced in size range by successive filterings. All particles used in this part of the experiment were larger than 0.1 micron and smaller than 0.45 micron in diameter. Also, a small quantity of radioactive rubidium was mixed with the iodide-kaolin suspension for the purpose of comparing the relative rate of movement of the monovalent anion and cation. Unfortunately, the rubidium received was activated in too weak a flux in the reactor. Consequently, once this isotope was introduced to the sand bed its radiation could not be clearly distinguished. After determining the degree of retention of the iodide-kaolin combination by the sand bed, the salinity of the input solution was again raised in magnitude steps from E-7 to E-1 molar NaCl. Each input consisted, as before, of 20 liters of solution. This movement was continued until the iodide began to break through into the effluent, then it was terminated.

With the sand bed filled with salt water, it seemed pertinent to determine what effect the salinity would have on the retention of such a strongly adsorbed ion as the scandium ion. The next input to the sand-bed was, therefore, a mixture of radioactive scandium, salt solution and kaolin clay particles. The particles had been prepared in the same way as those used for the iodide tagging above except that they had been allowed to dry down onto the millipore filter used to collect them prior to re-suspension. This scandium solution was made up with E-1 molar brine in order to maintain the right density of the input solution relative to that that existed at that point in time in the pores of the sand bed.

The final series of input solutions had essentially the same sodium content and the same density of solution as the 0.1 Molar NaCl. However, they did have different anions. The particular anions were chosen because they represented a common group used in industry and in the home as dispersants. In sequence then, the last series of influent solutions were sodium tetrphosphate, followed by plain brine, next a solution of the mixture of the sodium phosphate-sodium carbonate-soda ash that makes up the product "calgon", and finally more plain brine. Scanning of the sides was carried out in detail during this procedure. Effluent samples were collected and analyzed for radioactivity, particle identity, and particle association with the radioactivity recovered from the effluent. These final procedures involved use of the laser for scattering studies, fine filtration for particle-radioactivity association, and electron microscopy for particle identification. Since these techniques were incidental to the experimental process, the minor procedures followed will be considered along with the data they provided in the next chapter, RESULTS.

The energy of interaction of cations with mineral surfaces is generally taken to be stronger than that of anions because of relative charge and size differences of the two ion types. The procedures used in this experimental work were designed to take advantage of such differences in order to dramatize changes in retention characteristics of the sand bed.

CHAPTER IV

RESULTS

Experiment One

The shielded NaI(Tl) scintillation crystal mounted on the mobile carrier was used to scan the side of the sand bed during the first few hours while the radioactivity was moving into the bed. An energy spectrum of the simultaneous presence of the three radioisotopes is shown in Figure 6 using 100 channels of the TMC 401. The peak of highest energy (the ^{140}La at 1.6 MeV) is seen furthest to the right and labeled I. Peak II combines both the ^{86}Rb (1.08 MeV) and the ^{46}Sc (1.12 MeV) gammas. The third peak, III, is the ^{46}Sc gamma at 0.89 MeV. The lack of resolution of the two gamma energies combined in peak II provided no particular difficulty because the amount of scandium present could be estimated from peak III and the rubidium taken by difference. Except at the beginning of the experiment, the problem of resolution did not really arise; because the two isotopes assumed such different locations in the sand bed their spectra did not interfere with one another very much.

Figure 7 shows the position of the radioactivity shortly after addition to the bed (curve I). The relative position of the retained radioactivity is shown by the sketch of the bed in cross section at the top of the figure. The apparent peak at the left of both curves is due to an edge effect in the scanning procedure and only occurs where the detector cone

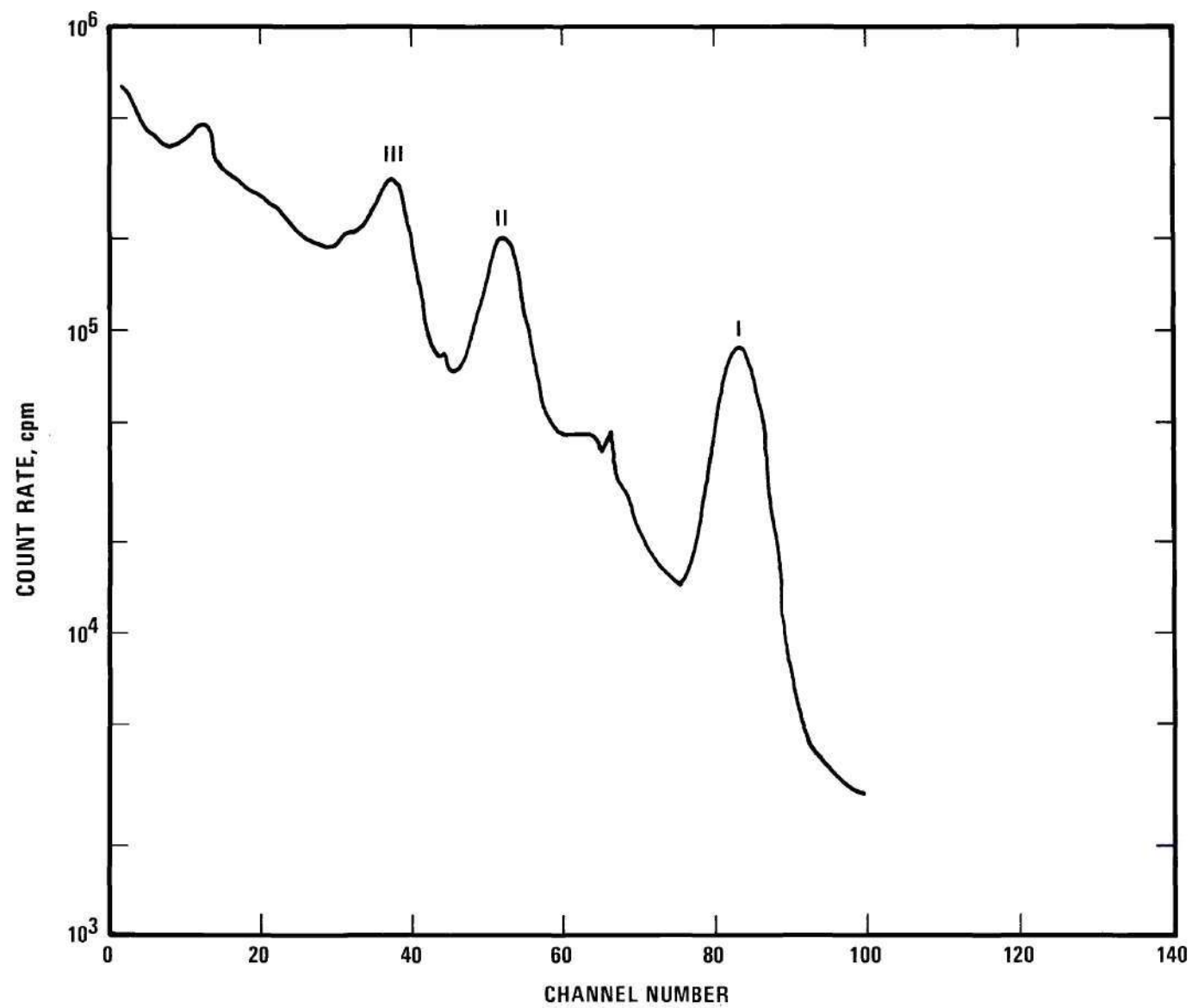


Figure 6. Combined Energy Spectrum of ^{46}Sc , ^{86}Rb , ^{140}La

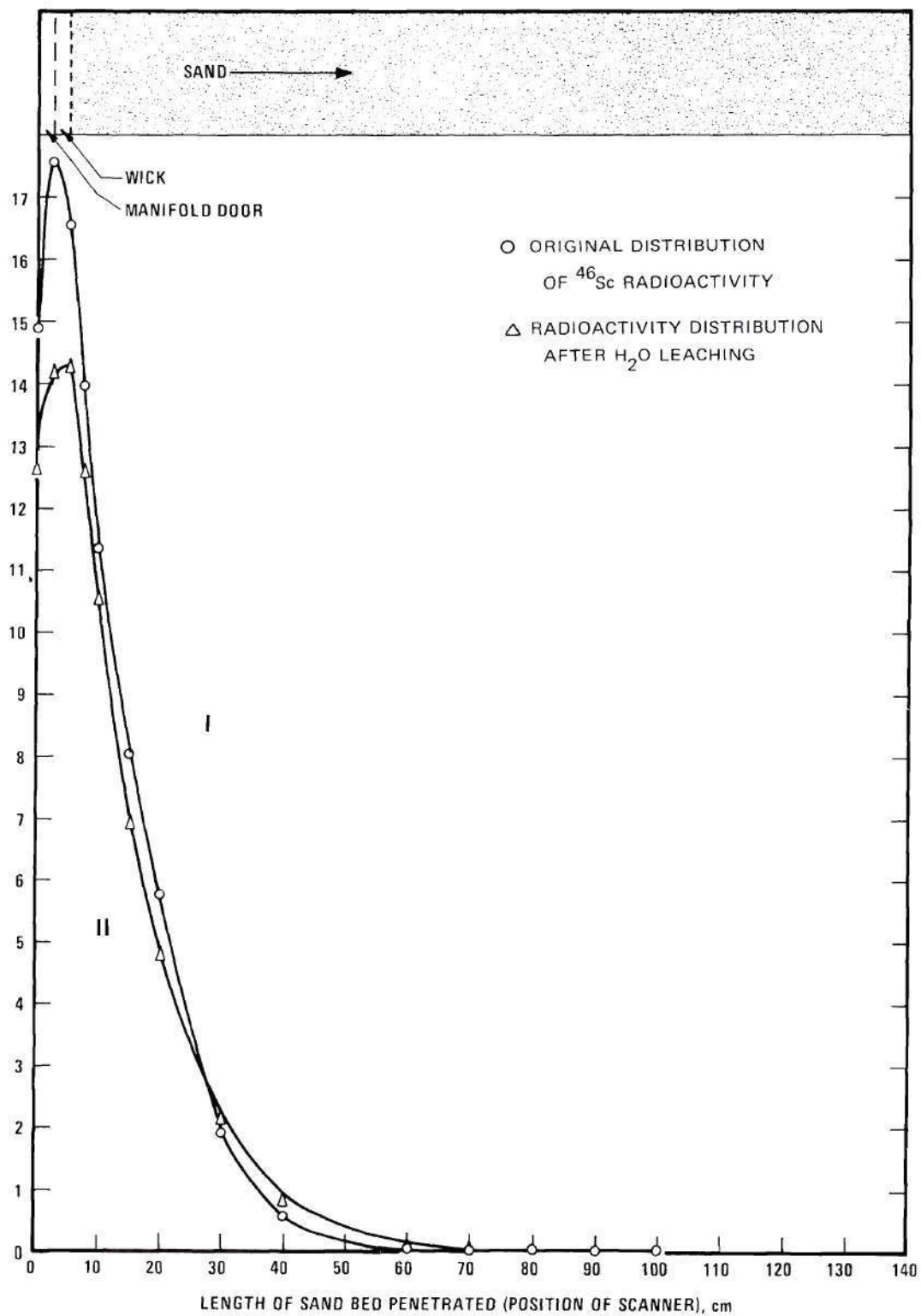


Figure 7. Deposition of Radioactivity Relative to Aquifer Construction

of sensitivity intersects non-radioactive void space in the door. Curve II shows the radioactivity distribution after two days of continuous distilled water flow through the bed at the rate of about 1 cc per second. As may be seen, the apparent distribution of radioactivity (determined by Geiger-Müller tube scanning) had not changed markedly, although the water interface moves through the bed at a rate of about 5-7 cm per hour.

Figure 8 shows the isotopic distribution determined by scintillation crystal scanning after about a week of continuous leaching with distilled water following the addition of the activity to the bed. Although much of the lanthanum had decayed in the time interval, its clear and well defined peak in the energy spectrum permitted easy definition of that isotope leading to the determination of its distribution. The position of the lanthanum-labeled bacteria is shown by the lower left hand curve marked I. Plotted on semilogarithmic paper, as shown, the distribution of the lanthanum in the sand approximates an exponential very closely. Curve II shows the retention of the scandium-labeled kaolin clay particles. Curve III shows the activity due to rubidium calculated from the peak II, Figure 6, after numerically removing the scandium component. Limited interaction of the Rb front is indicated by the almost flat slope of Curve III up to about 60 cm. Beyond 70 cm the interaction of the rubidium appears nearly as strong as that of the polyvalent cations, Curves I and II.

After the radioactivity distribution in the sand bed had essentially stabilized, the bed was allowed to sit idle for a number of months. After 273 days the bed was rewet with distilled water and ^{131}I , in the form of

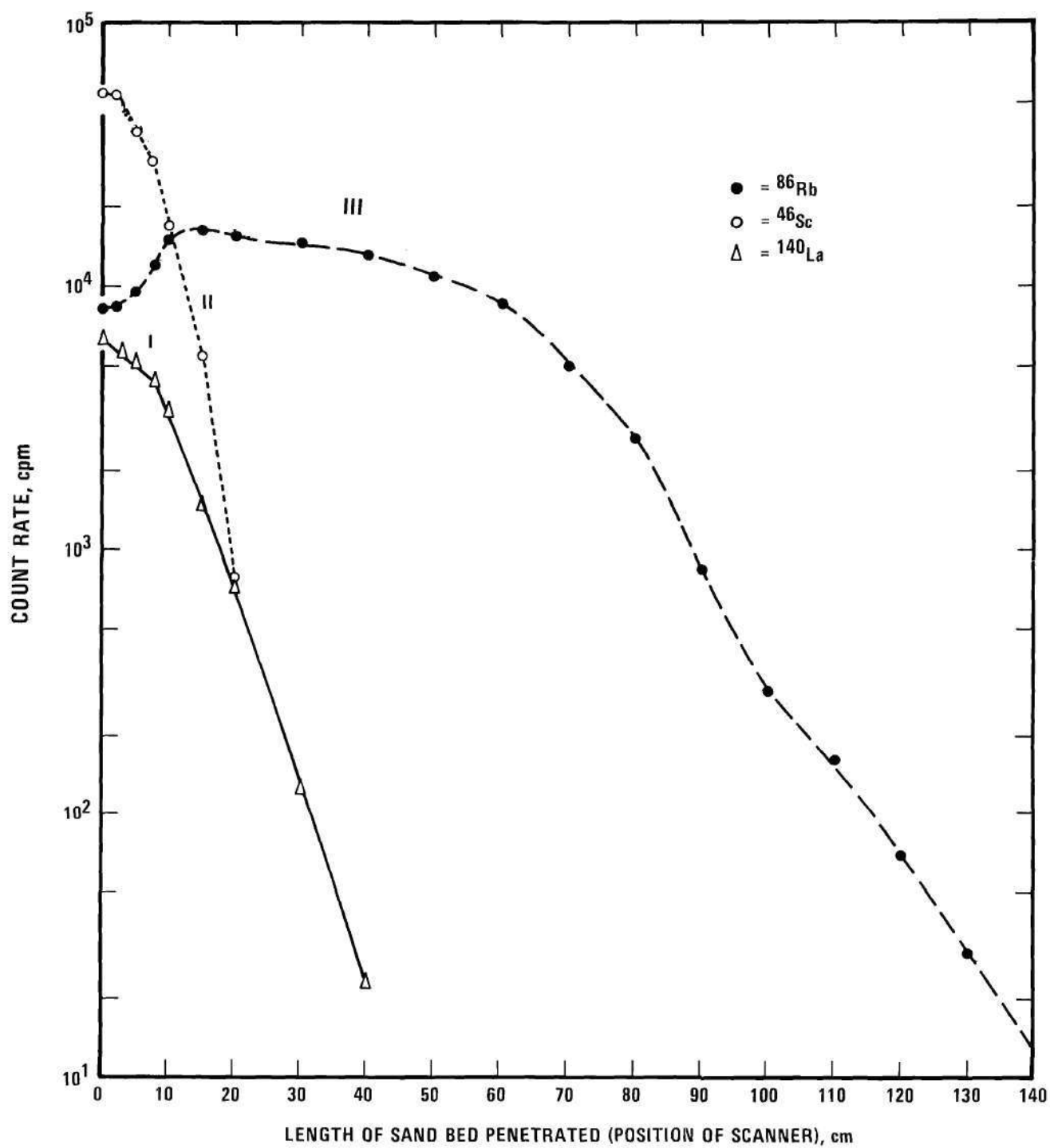


Figure 8. Relative Deposition of ^{46}Sc , ^{86}Rb , ^{140}La in Sand Bed

the iodide, was passed into the bed at a high specific activity and low carrier concentration. The distribution of the iodide in the sand is shown, curve II in Figure 9. The last known positions of the scandium and lanthanum-labeled particles are also shown in the figure. Once inside the bed proper, the distribution of the iodide was found to follow the slope of the lanthanum, curve I, so closely that their distributions were difficult to distinguish along the first quarter meter of the bed. After about 40 cm, the ^{131}I showed much less tendency to be retained by the sand.

The final step of this portion of the study was an attempt to estimate the optimum sodium chloride concentration in the infiltrating water that would bring about iodide release from its position of highest concentration in the sand bed. This was done by increasing the molar concentration of NaCl in the input water in steps by orders of magnitude in lots of 20 liters each. Figure 10 shows the change in radioiodide distribution from the stabilized position in the bed acquired using distilled water as an influent to the position at the end of the 0.1 molar NaCl input.

The change in distribution of the radioiodide with rising NaCl concentration showed two things of significance. First, the iodide moved from the input area to approximately the same region last occupied by the rubidium while it could still be detected. Second, the distribution seemed to change in nature as well as in location. The high concentration at the input merely seemed to decrease in area proportionally with increasing NaCl molarity. After allowing for the time decay of the ^{131}I , and adjusting the gross count under the peak for the contribution of the remaining scandium,

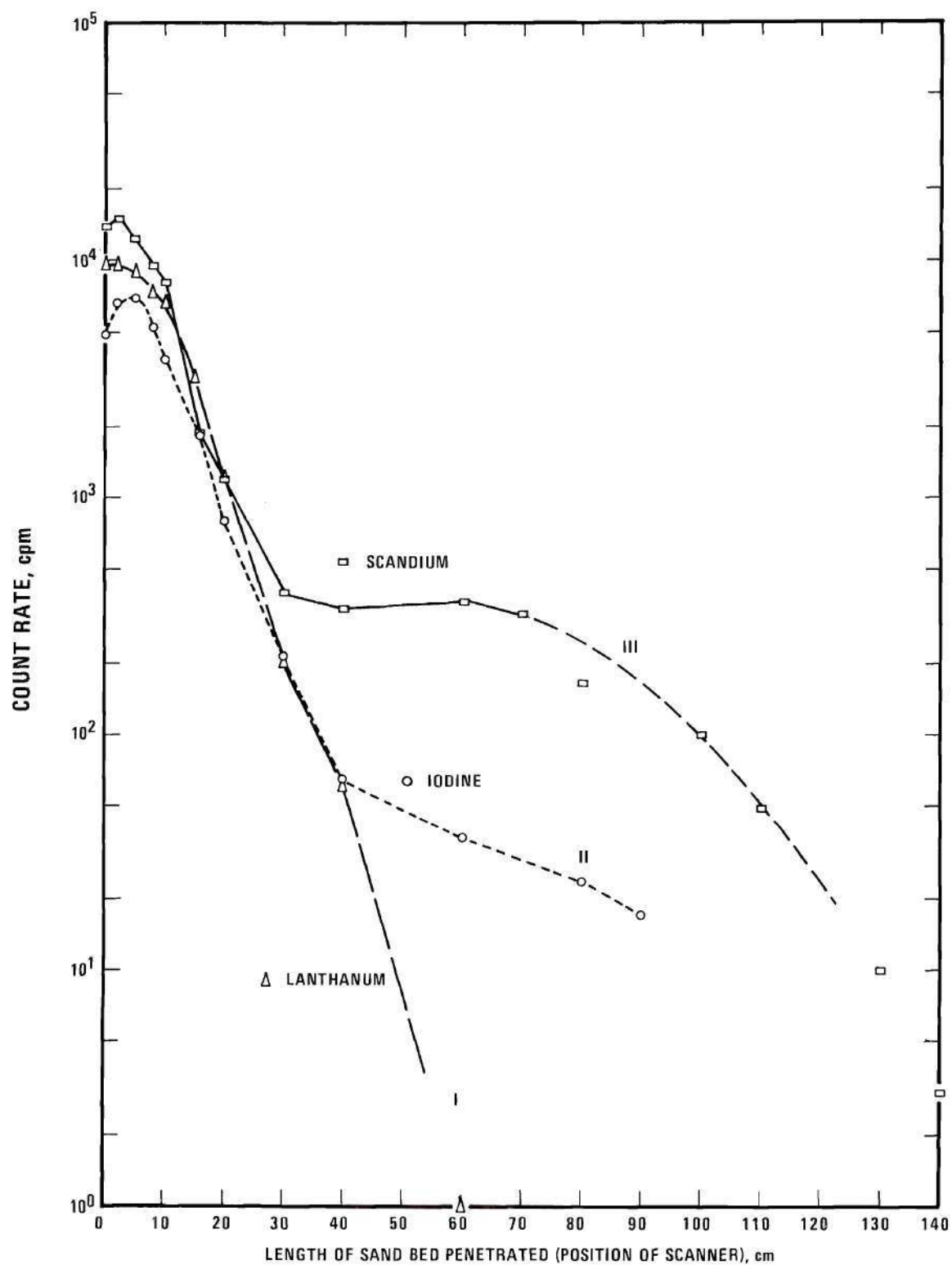


Figure 9. Similarity in Radioactivity Retention of First 40 cm for ^{45}Sc , ^{131}I , ^{140}La

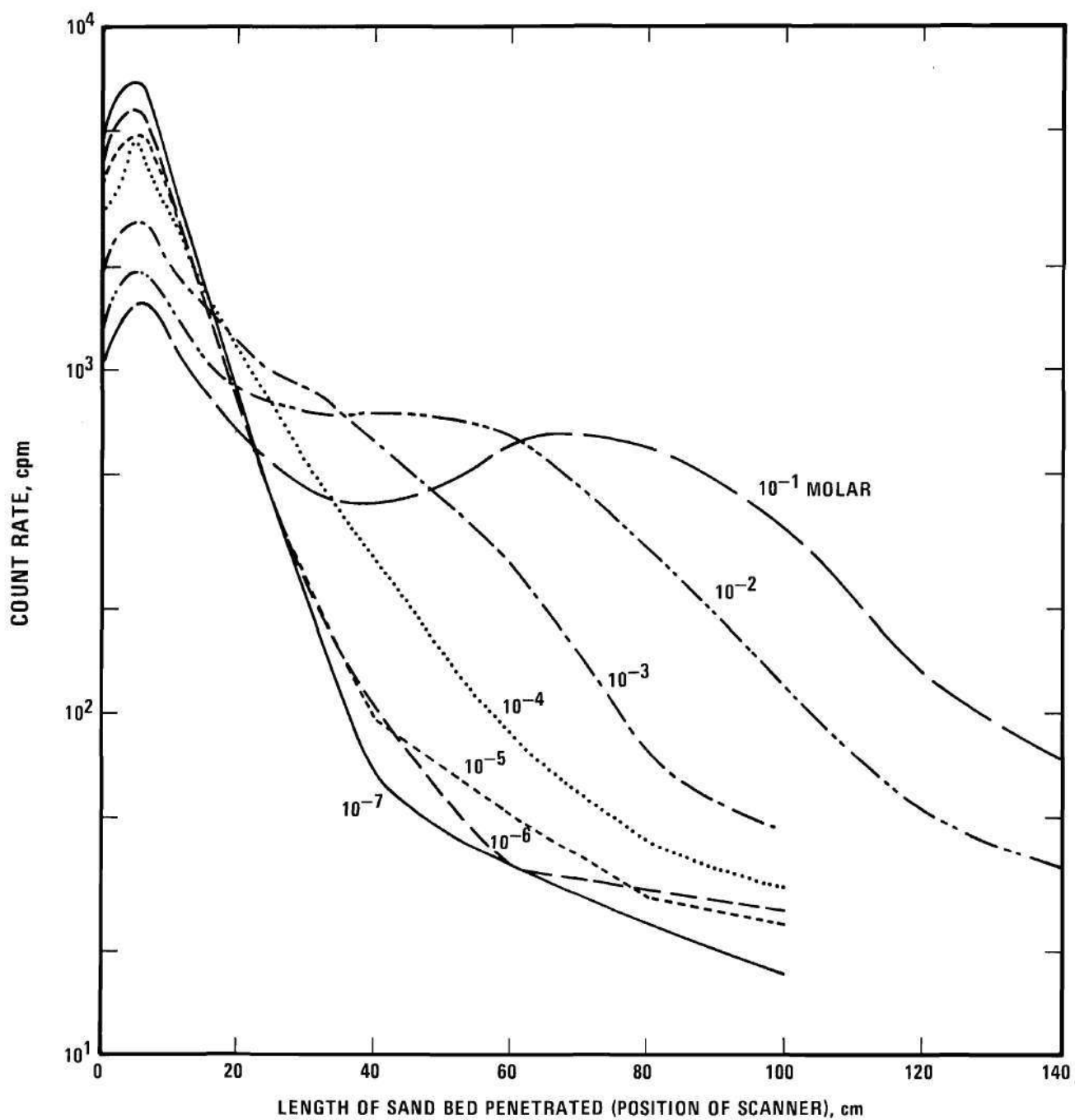


Figure 10. Displacement of ^{131}I in Sand Bed by NaCl Solutions

it was possible to compare the change in area under the main distribution peak of the ^{131}I to the concentration of the solution passing through. Figure 11 indicates optimum elution from the sand bed for the ^{131}I to be about 10^{-3} molar NaCl. The apparent data rise at the left is a calculational uncertainty due to lack of knowledge of the absolute concentration of the original influent solution made up from the "carrier free" sodium iodide obtained from Mallinckrodt.

An additional point of interest is the relative change in the distribution of the scandium still traceable from the earlier studies. Figure 12 shows the change in the distribution of that isotope as the result of the sodium chloride leaching by comparing the distribution at the beginning of the 273 day delay period, and that at the end of the NaCl solution series. The latter data were corrected for decay back to the same day the data for the first curve (I) were obtained. The distribution at the left part of curve II remains essentially the same as that for curve I except for total concentration. Deeper into the bed, however, the radioactivity distribution of the ^{46}Sc became almost constant at a higher concentration than for curve I. It appears that the change in ion concentration did remobilize some of the particles carrying the ^{46}Sc tracer, although the degree of mobilization was small compared to that of the ^{131}I .

Experiment Two

The second experiment was designed primarily to study the mobility or retention characteristics of the two anions, Br^- and I^- using the two cations, Sc^{+3} and Rb^{+1} as controls for an already "established" system. A fresh sand bed was prepared by vibration packing 2300 pounds of the

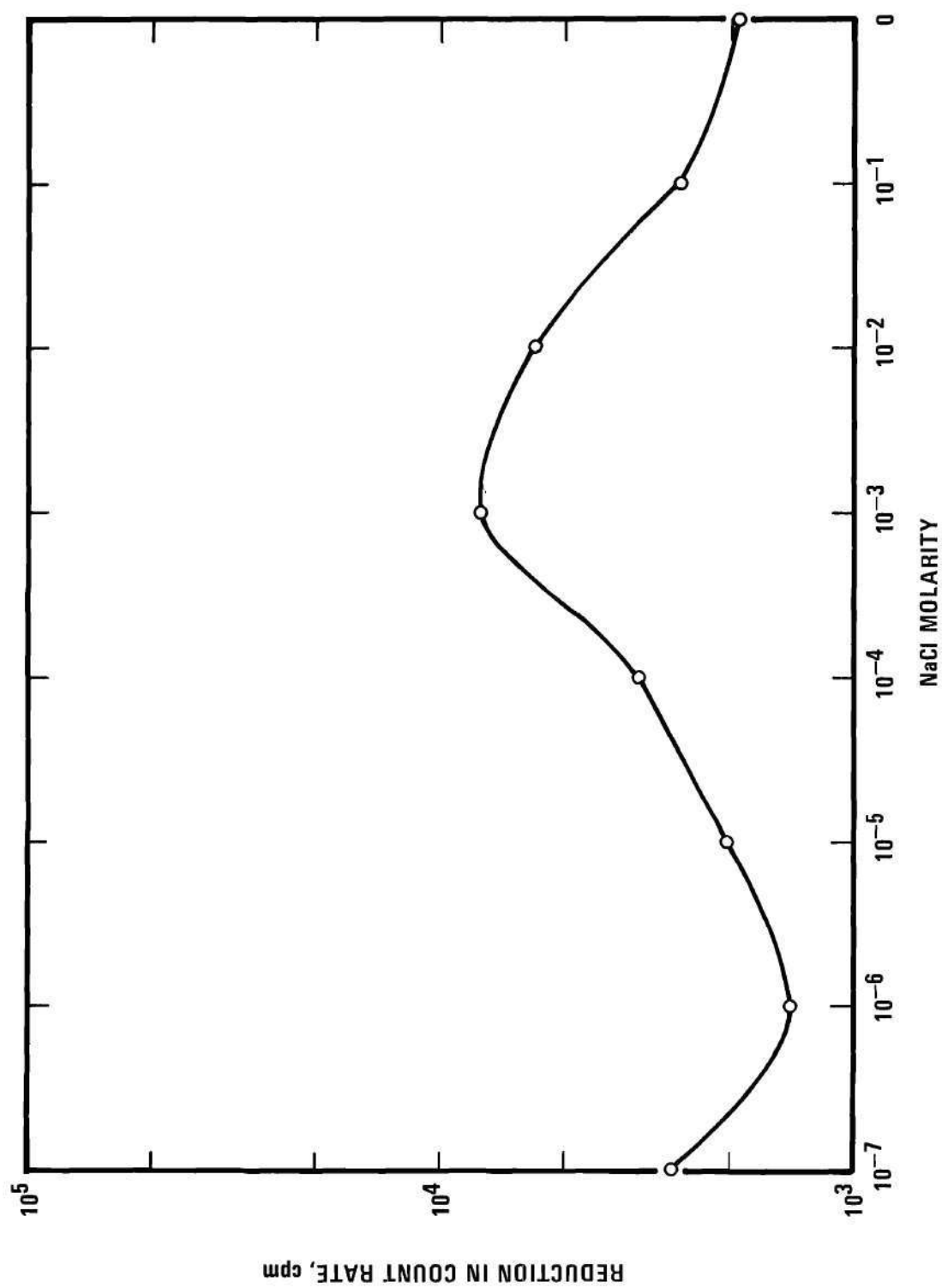


Figure 11. ^{131}I Displacement Relative to NaCl Molarity

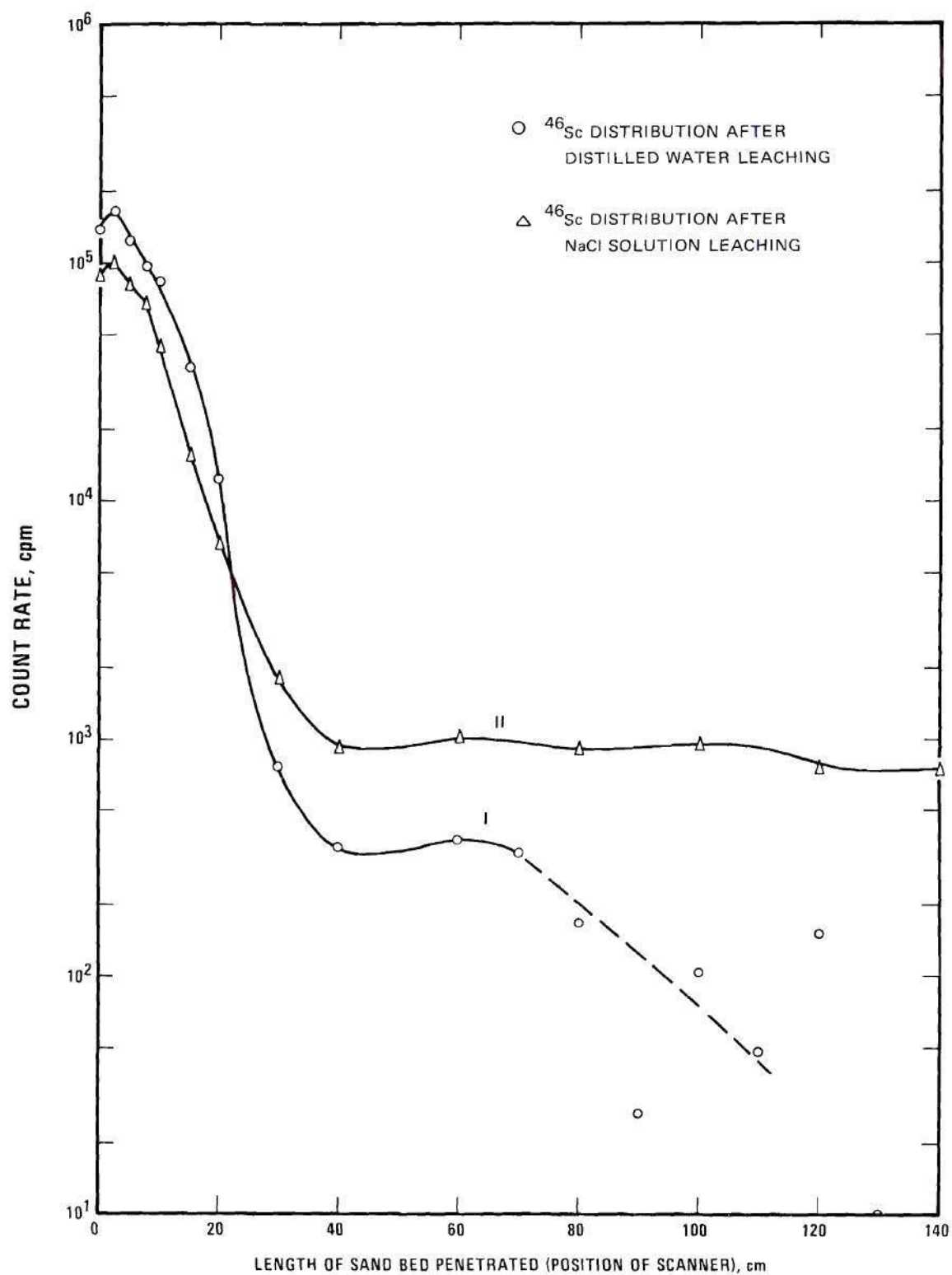


Figure 12. ^{46}Sc Redistribution in Sand Bed as a Result of NaCl Solution Leaching

Pennsylvania Glass sand into the test box, giving a sand pack 30 cm thick. A 0.25 ppm solution of radioactive Br^- was prepared to match the approximate mean of the dissolved salt concentration observed in the effluent leaching water obtained from other sand packs using distilled water influents. The initial solution was made up in 3700 ml of distilled water giving a concentration of about 30 micromoles per liter.

Instead of prewetting this newly prepared sand bed with distilled water as was the normal procedure, the NH_4Br solution described above was introduced to the bed and followed by distilled water. Curve I, Figure 13, shows the position of the radioactivity after all the ^{82}Br had entered the bed. Following the movement of the ^{82}Br by scanning the side with the Geiger-Müller scanning tower, the arrival of the activity at the end of the bed (Curve II) was observed to coincide with the first portion of effluent water collected. Curve III shows the radioactivity retained by the sand bed after the ^{82}Br recovery in the effluent had become as close to 100 percent as the significant figures in the original influent could account for. The results showing the recovery of the ^{82}Br are shown in Figure 14. As may be seen in the latter figure the bulk of the bromine activity was recovered in the first 30 liters of effluent, approximately 10-15 percent of the total fluid volume required to fill the sand bed, roughly 200 liters. Although the bulk of the bromine passed through the sand bed with the water front, considerable trailing and broadening of the distribution peak was noted. In addition, after most of the bromine had passed from the bed, a minor amount was observed retained at the beginning of the sand bed with an exponential distribution

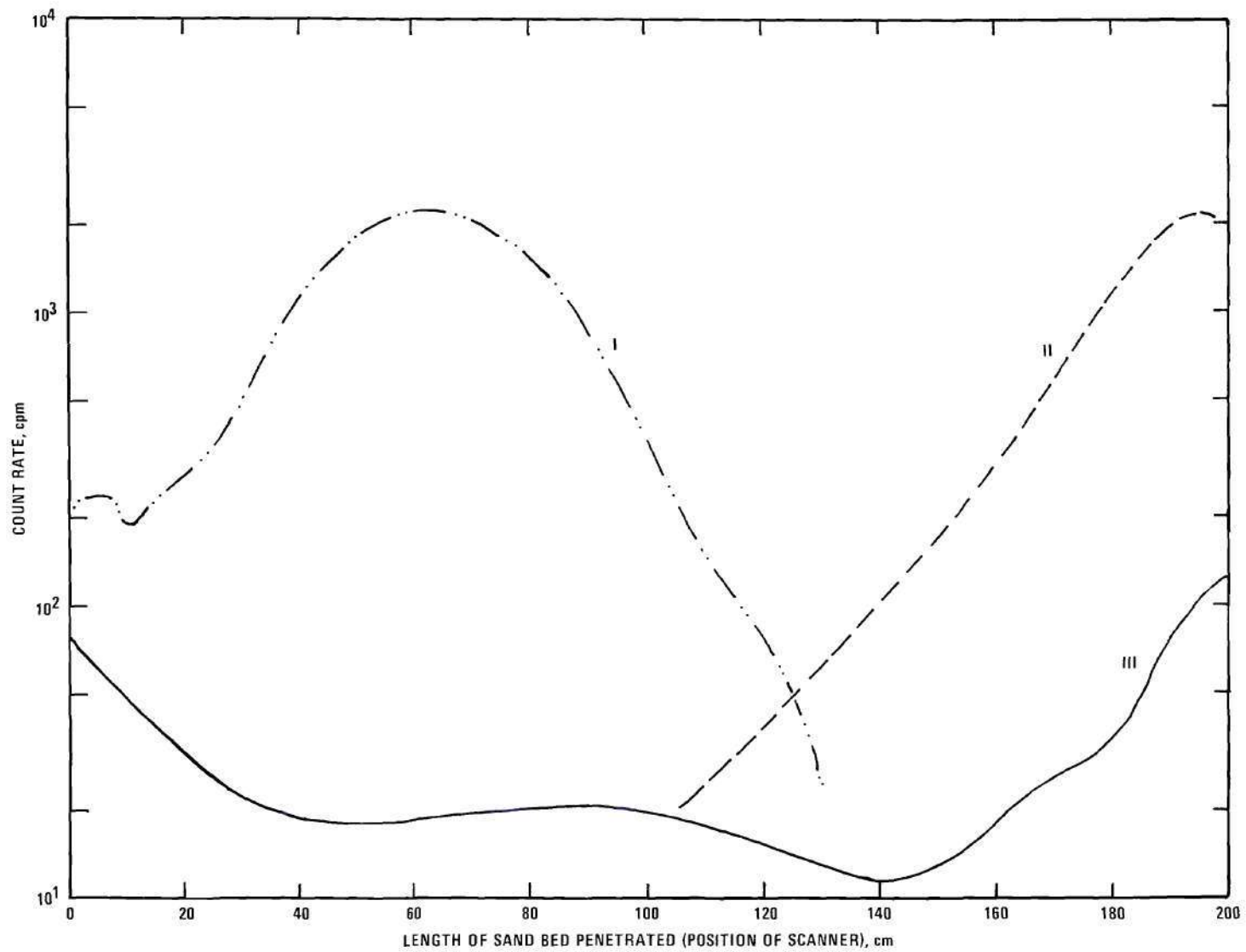


Figure 13. Bromide-Bacteria Release Profile

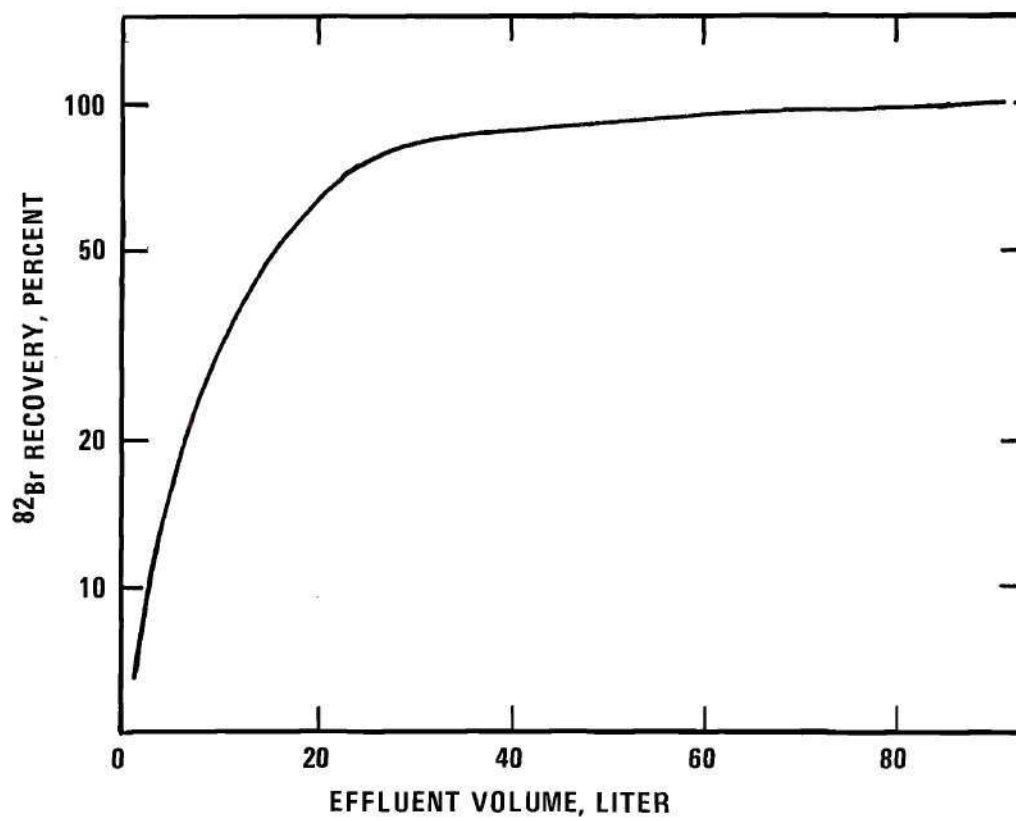


Figure 14. ^{82}Br Recovery in Effluent Water

very similar to that observed earlier for the other isotopes, ^{140}La , ^{46}Sc , ^{131}I .

Following the introduction and recovery of the bromine from the sand bed, a mixture of $^{131}\text{I}^-$ and $^{86}\text{Rb}^+$ labeled kaolin particles were added to the bed. Unfortunately, the rubidium isotope was too weak to be detected well at the dilutions necessary for the study, so the detection of its presence in the various analyses was somewhat uncertain. The iodine distribution is shown in Figure 15 at the left. This figure also shows the effect on that distribution of increasing the NaCl content, as was done previously. Again, the main release point of NaCl concentration can be seen to be at about 10^{-3} molar. Displacement of the iodide by NaCl solutions was continued until ^{131}I could be detected in the effluent.

Finally, the clay suspension made up with scandium was mixed with sodium chloride solution of the same concentration as that last used for the iodide displacement, 0.1 molar, and passed into the sand bed. The scandium labeled clay particles assumed the same deposition distribution in the sand bed as the iodine-labeled clay had. This position was held by the particles regardless of the continued introduction of 0.1 molar NaCl solution.

After the introduction of the ^{46}Sc -labeled kaolin in 0.1 molar sodium chloride suspension, forty liters of plain 0.1 molar NaCl solution were passed into the sand bed with no particular effect on the distribution of the radioisotope, ^{46}Sc . Next a solution of sodium tetraphosphate was made up with the same weight dry phosphate as that of the

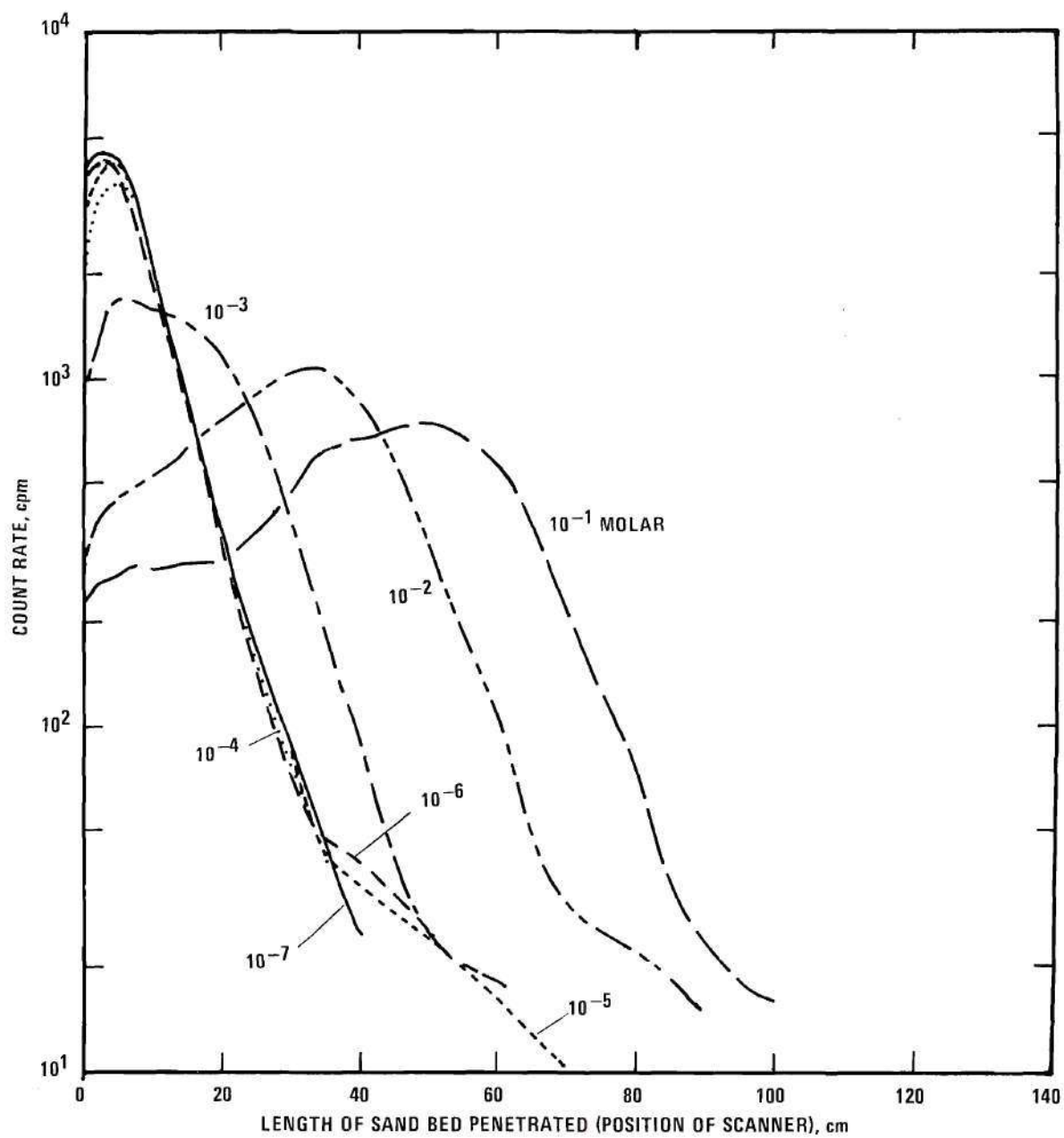


Figure 15. Iodide-Kaolin Release Profile
(NaCl Eluent)

NaCl (0.1 molar). As this new solution passed into the sand bed, the retained scandium moved with it. Figure 16 shows the displacement for each of two 20-liter inputs of sodium tetraphosphate solution. The forward movement of the peak area approximated the movement of the water itself. Permeability difficulties were experienced with the bed during this time so the water was supplied to the bed much more slowly until the permeability increased again.

Following the introduction of the 40 liters of sodium tetraphosphate, 80 liters of plain NaCl were introduced behind the phosphate in the bed. Following this was 60 liters of "calgon" solution prepared in the same way as the tetraphosphate. The "calgon" solution was followed in turn by 100 liters more of NaCl solution. By this time essentially all the scandium had been displaced from the sand bed into the effluent. Figure 17 shows the leading edge of the scandium position in the sand bed after each progressive 20 liter input of the solutions described above. The distribution of the scandium, once it was free of the input area was nearly symmetric about the peak, as Figure 18 shows. This symmetry about the peak area was maintained all along its movement through the sand bed even though the peak broadened somewhat as it moved. This displacement of the scandium isotope from the sand bed terminated the experimental work with the bed itself.

The results of the rest of the work in Experiment Two involved investigations of the influent and effluent samples. It was of interest to determine the physical nature of the particles in suspension that would influence their rate of movement through the sand. Hence, a series of

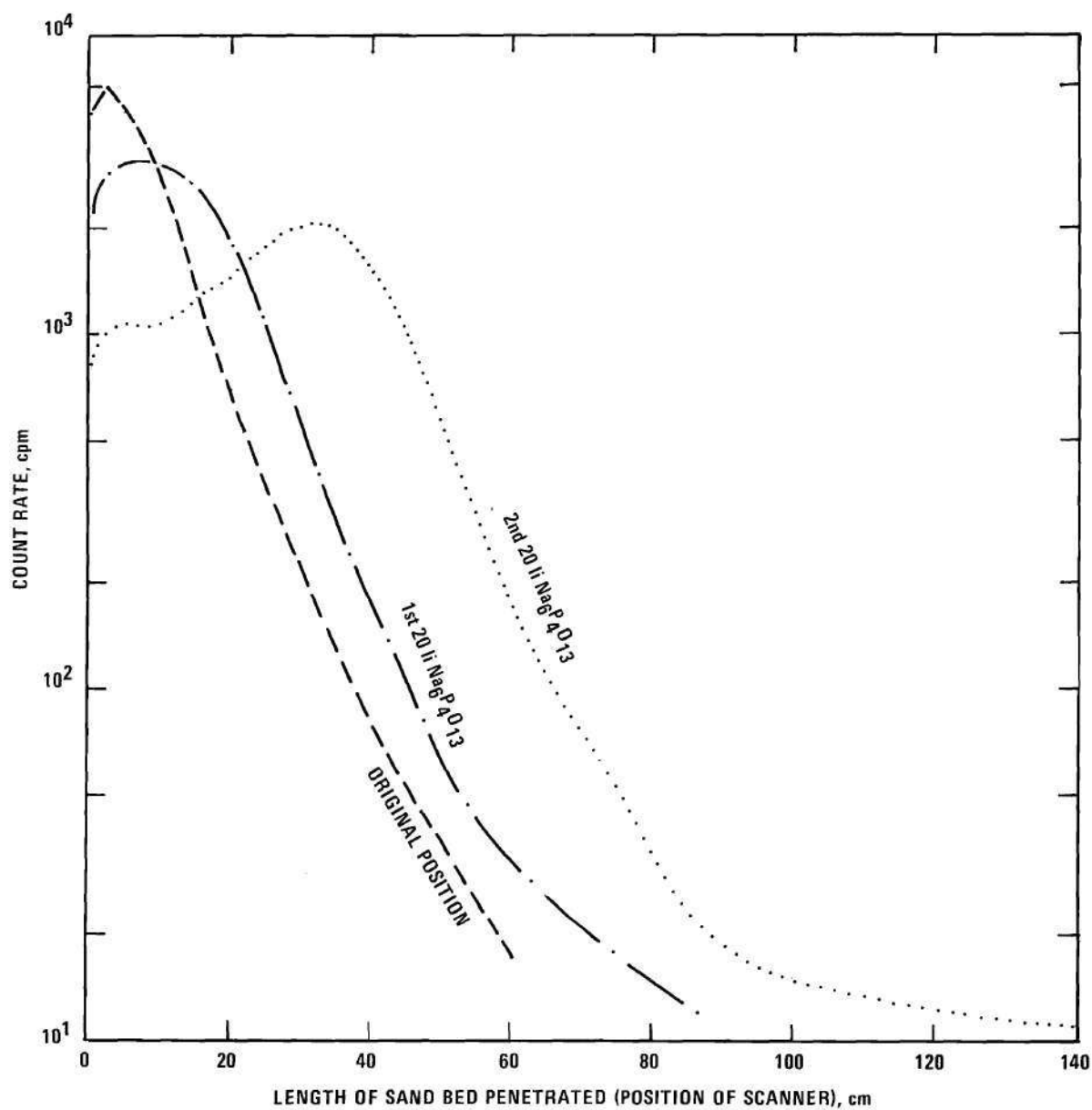


Figure 16. ^{46}Sc -Kaolin Displacement by Sodium Tetraphosphate Solutions

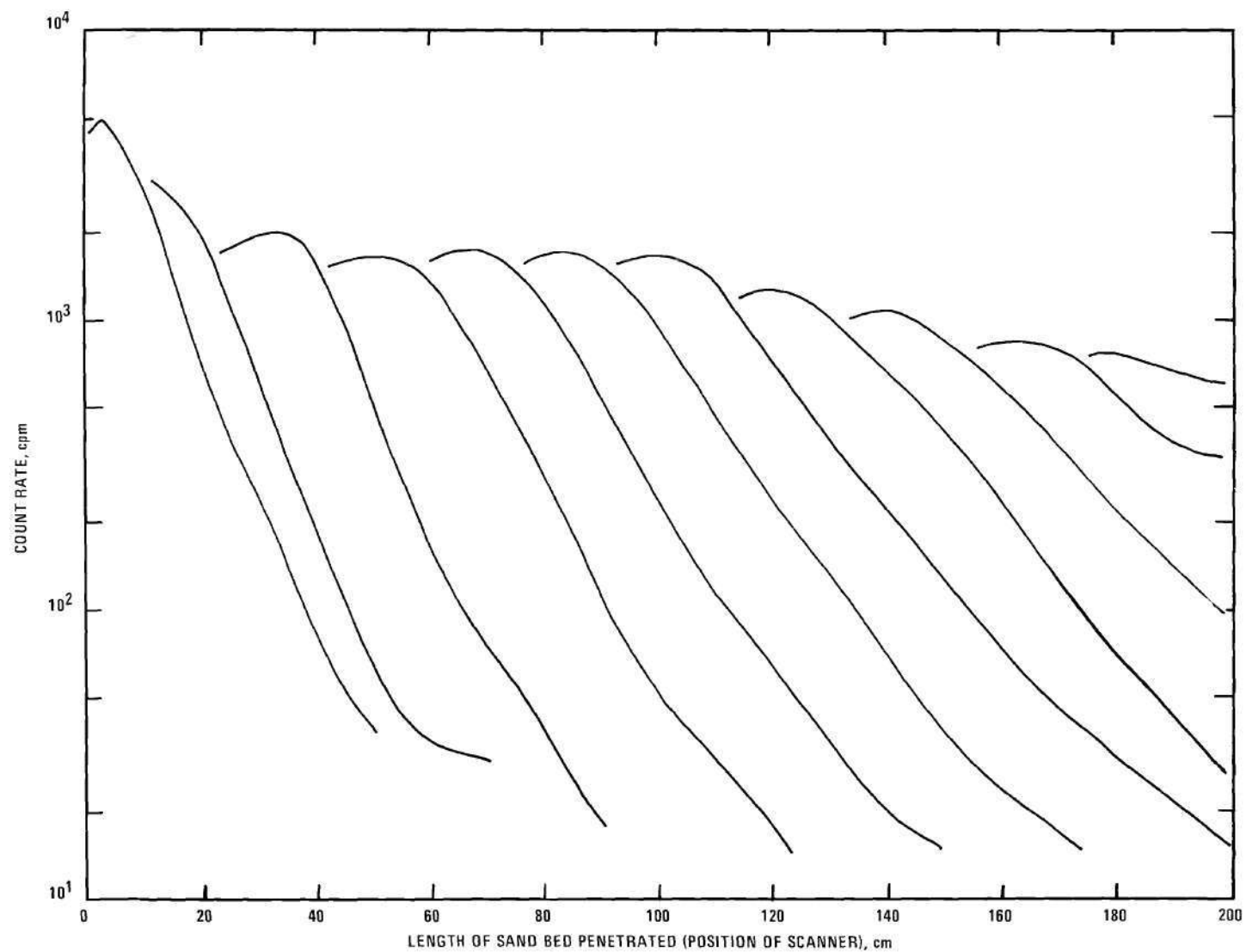


Figure 17. ^{46}Sc -Kaolin Front Showing Near Parallel Displacement After Each 20-liter of Influent

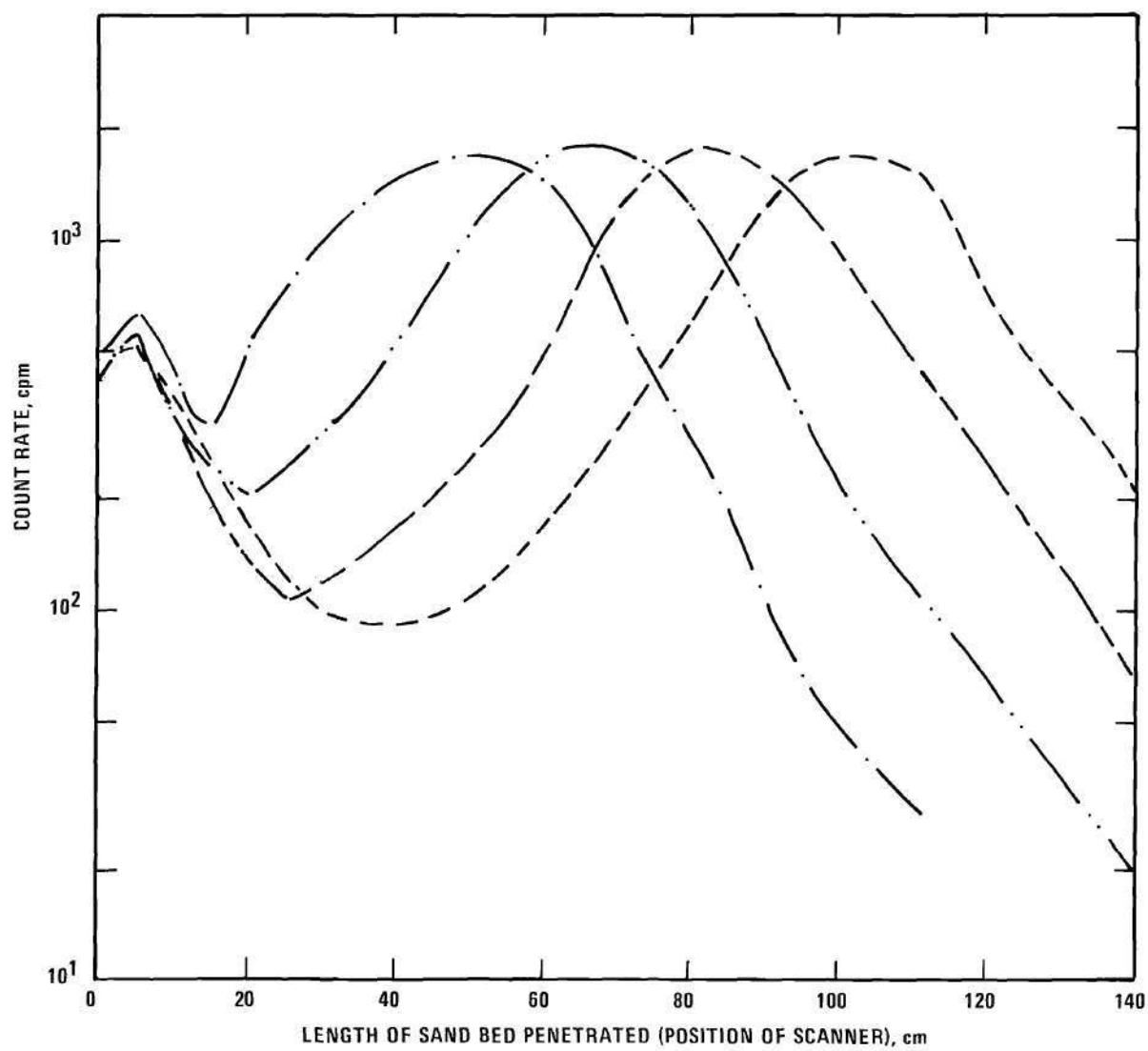


Figure 18. Symmetric Displacement of ^{46}Sc -Kaolin

scattering determinations were made using a Neon (He) laser as a light source, a photomultiplier as a detector and a nanoampmeter as a readout device. Figure 19 shows the degree of scattering of selected representative samples of the series, including the influent materials and some standards.

The polystyrene standard showed scattering which was almost isotropic from about two degrees to 35 degrees. The distilled water standard showed very low scattering with small angle forward scattering about a magnitude higher in intensity than that at 10° . The scattering response of other samples examined fell between these two standards from 15-35 degrees, but showed some sharp differences from them in the smaller angles. Most different was the input sample of kaolin that was tagged with ^{46}Sc . This sample's response (scattering) decreased three magnitudes as the angle of detection was varied from two to 35 degrees. Two of those magnitudes of change were in the first 15 degrees.

The forward scattering of the ^{46}Sc -tagged kaolin was especially pronounced, appearing to project an image of the suspended particles forward against a wall. The intensity and width of this projection out from the central beam was much larger for the ^{46}Sc -kaolin than that of any of the others, especially that of the polystyrene standard (0.5 micron diameter). Photographs of some of these images are shown in Figure 20. Most notable was the pattern difference between the spherical polystyrene particle projected image and that of the clays, Figure 20B and C respectively. In the former, the image is of a continuous fixed pattern very similar to that of a fabric. In the latter, the pattern was random, less clearly defined,

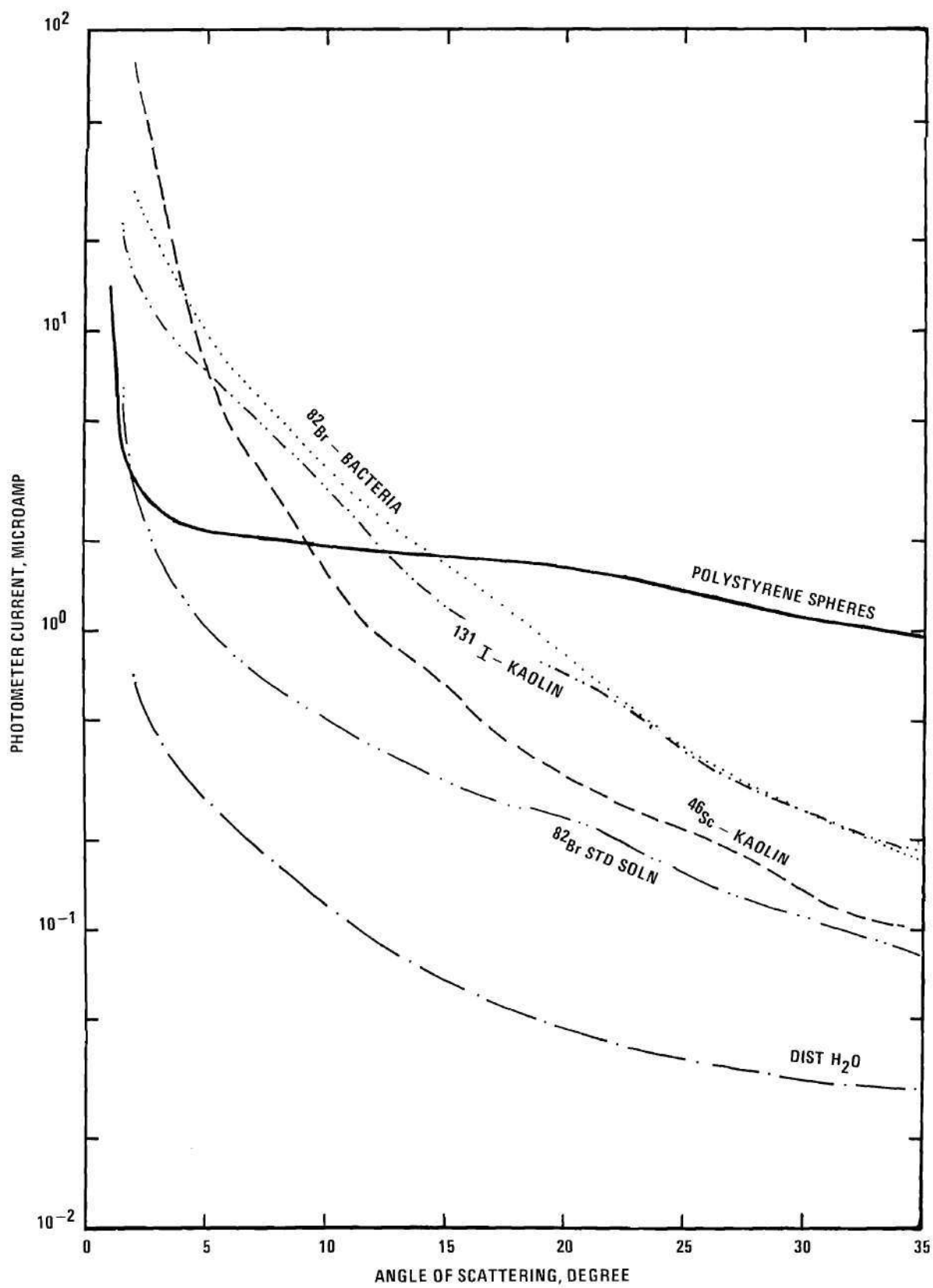
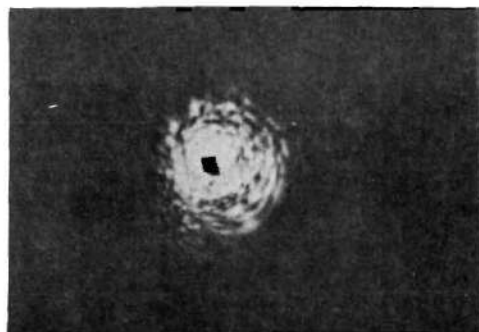
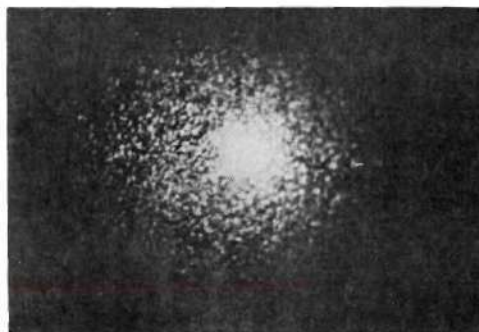


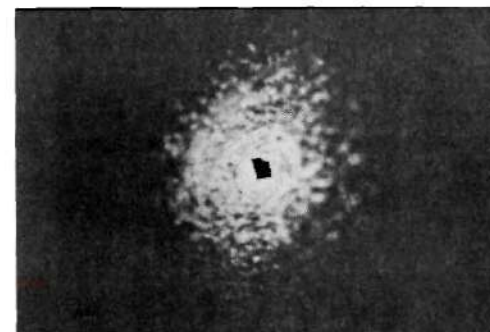
Figure 19. Laser Scattering (Angular Dependence) by Aqueous Suspensions



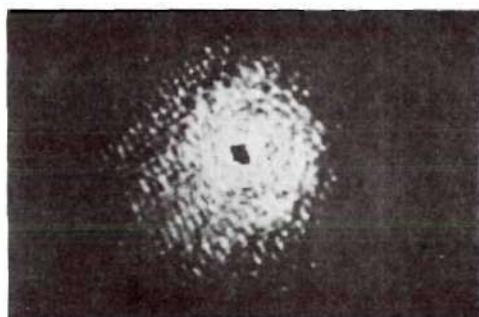
(a) Distilled water



(c) ^{46}Sc labeled kaolin influent



(e) ^{82}Br bacteria effluent



(b) 0.5μ polystyrene spheres



(d) ^{131}I labeled kaolin influent



(f) ^{131}I kaolin effluent

Figure 20. Laser Scatter Patterns of Aqueous Suspensions

and larger in projected area. Dynamically, the major difference was that the pattern of the clay projection was continuously moving, each of the spots scintillating, so to speak. The image of the polystyrene spheres was steady and had a secondary phenomenon of parallel shadows running across it.

Also shown on Figure 20 is the scattering pattern of the iodide-kaolin clay input showing a star reflection effect, Figure 20D, caused by the laser beam touching an edge of the collimator hole through which it was passing. This star pattern seemed to accentuate the scatter pattern at a considerable distance from the center of the beam, even where the individual points of light seemed too dim to register on the film. Figure 20E shows the scatter pattern of the water received in the effluent at the peak of the radioactive bromine release. Its pattern was weak relative to that of the scandium-kaolin, but larger in area than that of the polystyrene spheres. It was random, like that of the clays, but seemed to have a cotton-ball pattern that the clay suspensions did not show. While difficult to show in the photographic print, some of this odd pattern may be seen toward the bottom of the picture, beyond the interference rings.

Figure 20F shows the scatter pattern of the effluent water as the ^{131}I -kaolin was being released into the effluent. Its pattern was similar to that of the polystyrene spheres except for being somewhat more random and the fabric pattern instead of being rectangular (i.e. like that of the spheres) was spiral with the center acting as a point of origin for the rays. Marked parallel shadows were noted crossing the scatter pattern for this sample also. It showed a general difference from the input iodine

clay scatter pattern.

Considering the results shown in Figure 19 the angle of three degrees was chosen to measure the relative difference in scattering by suspended forms in the effluent samples. Each of the ^{82}Br -labeled suspensions were placed in the optical cell and a measurement of the scattering intensity at 3° was taken. Figure 21 shows this response graphically. The initial very high response shown at the left corresponds closely with the high content of the bromine radioisotope in the first portion of the effluent. The rest of the samples showed relatively constant scattering intensity increasing slightly with continued volume displacement.

Additional studies were made to support the laser data by filtering portions of the most important samples or standards to obtain some information about the size distribution of the tagged particles that could be used to correlate with the scattering data. In Figure 22 is shown the particle size distribution of the ^{131}I -kaolin influents suspension. This clay had all been passed through a 0.45 micron Millipore filter and caught on a 0.10 millipore filter before resuspension in the radioactive solution used for tagging the particles. Note that the distribution is still largely that of the finer particles, but a significant number were caught on the five microns pass filter. By contrast the ^{46}Sc -kaolin influent shows a marked difference in distribution. This sample was prepared just like the other except that the clay was allowed to dry down on the filter for several hours before resuspending in the ^{46}Sc solution. It was then mixed with 0.1 molar sodium chloride. As can be seen the ^{46}Sc -kaolin suspension was characterized by large particles, most of them larger than 5 microns.

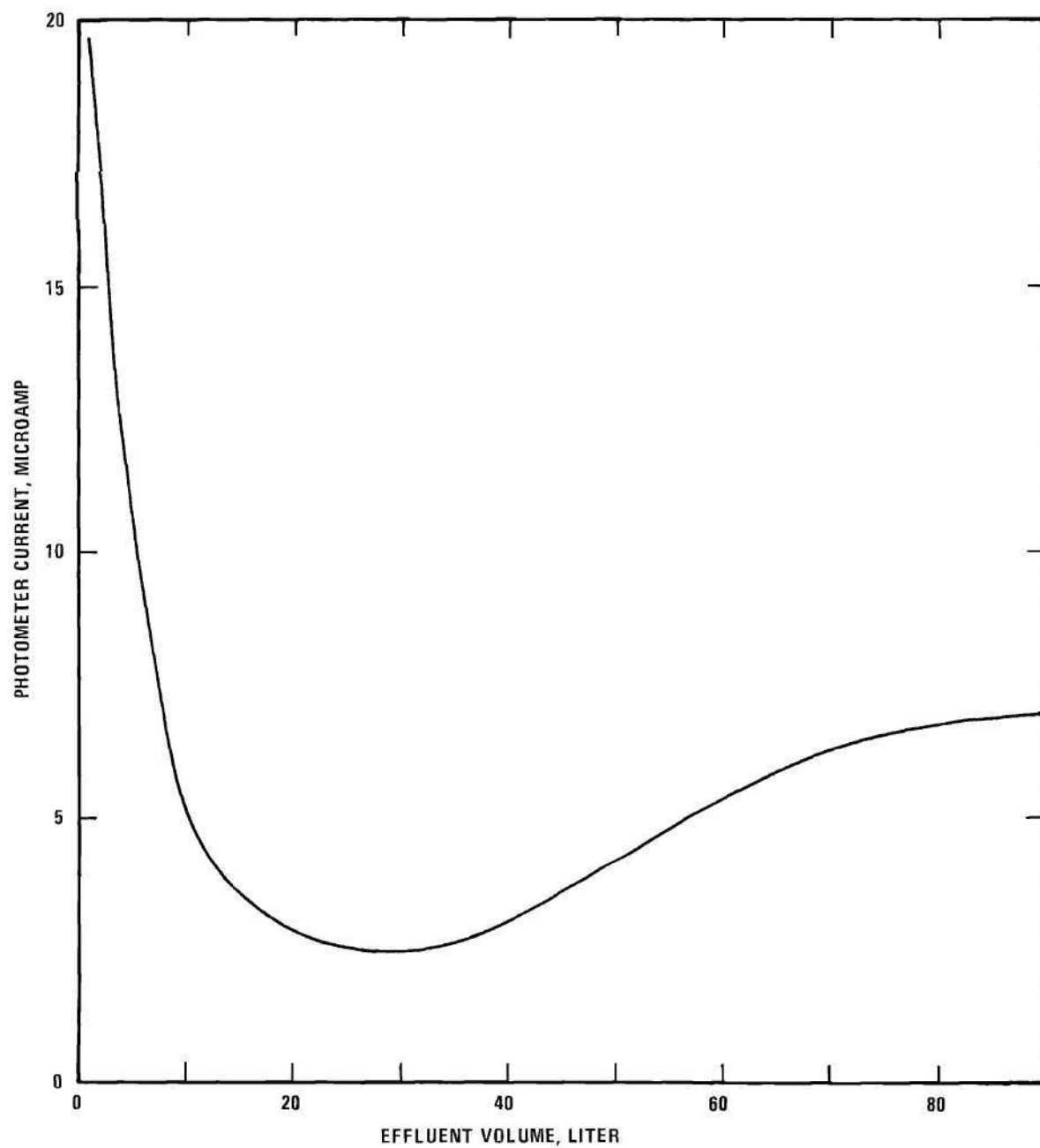


Figure 21. Scattering Intensity of ^{82}Br -Bacteria Effluent Samples at 3°

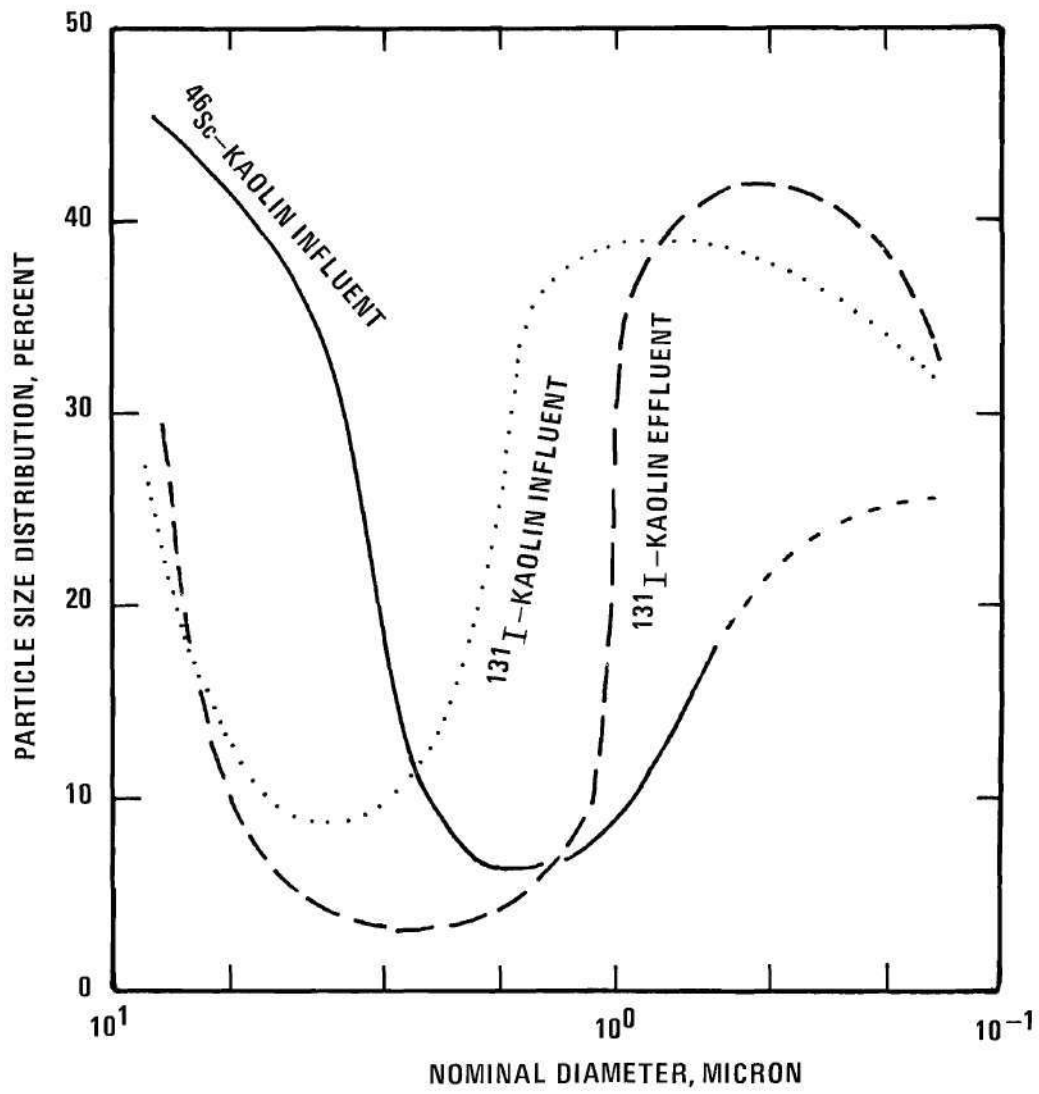
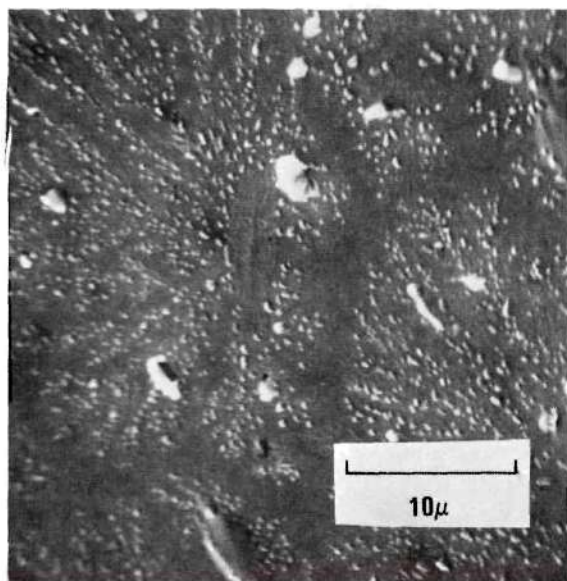


Figure 22. Fractional Distribution of Particle Sizes in Kaolin Suspensions

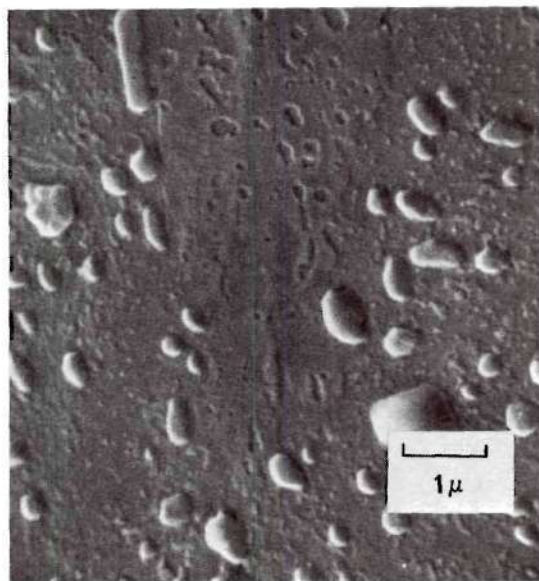
The third curve shown in Figure 22 is that of the sample taken from the effluent which was carrying radioactive iodine (and probably rubidium). Note that its distribution is most like the original solution, although an emphasis of the smaller sizes can be seen.

Figure 23 A and B are electron scanning microscope exposures of the particles contained in the ^{82}Br effluent from the sand bed prepared by smearing the liquid on a glass slide, drying, shadowing etc. The larger magnification shows bacteria-like particles very similar to those shown in Figure 5 which were cultured from samples taken from a previous effluent. Figure 23 C and D show similar particles obtained from the iodide effluent but trapped on a Millipore filter. The detail in Figure 23D is especially sharp, showing the nature of the filter surface as well as that of the particles. Figure 24 A and B show the nature of the 5 micron and 0.1 micron filters. This "welded dumb-bell" type of surface seems to be typical of the larger pore filters used. Figure 24C shows the kaolin used in the ^{131}I -kaolin input trapped on a 0.1 micron filter membrane. Note that while the perfect hexagonal shape is not always present for a given particle, the interplanar angle serves to identify the kaolin. Figure 24D shows an electron silhouette of kaolin particles trapped on a 0.01 micron pass filter. Technical difficulties with trying to replicate this filter surface required this determination to be made on the actual particles rather than the replica normally formed by carbon deposition. This sample was the iodide-kaolin effluent from the sand bed for which the laser scattering pattern was determined, Figure 20F.

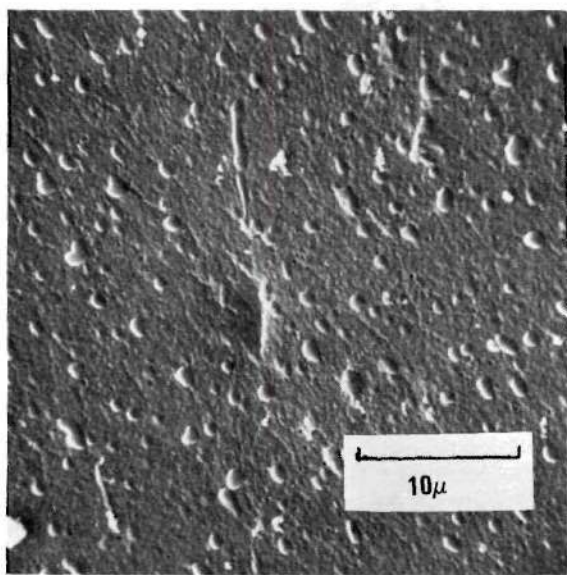
Figure 25A shows the location of particles of kaolin adsorbed to



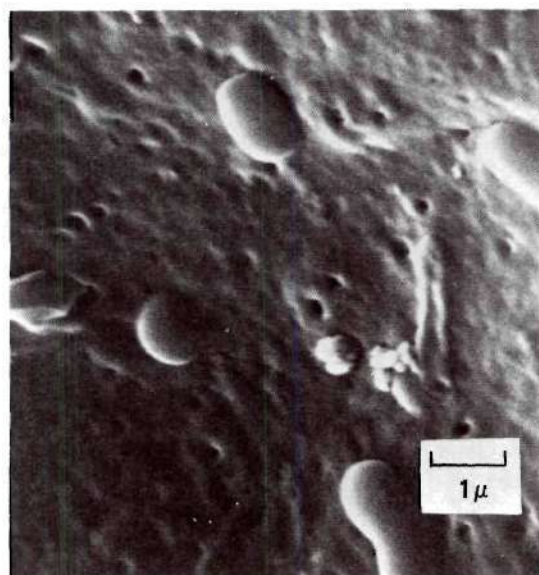
(a) Particles from ^{82}Br effluent smear on glass slide



(b) Detail on ^{82}Br smear

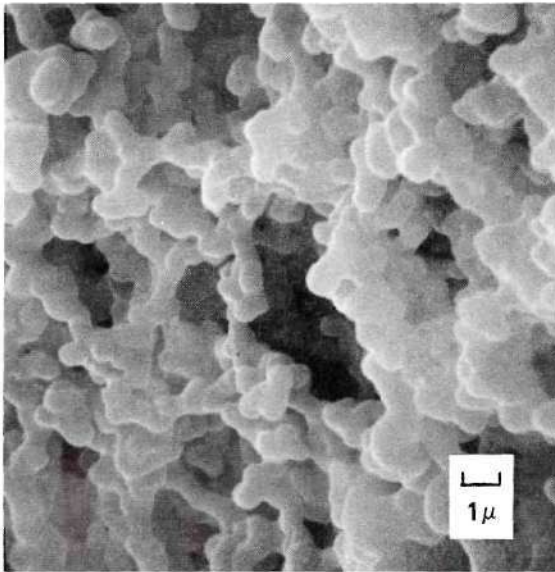


(c) Particles from ^{131}I effluent trapped on millipore filter

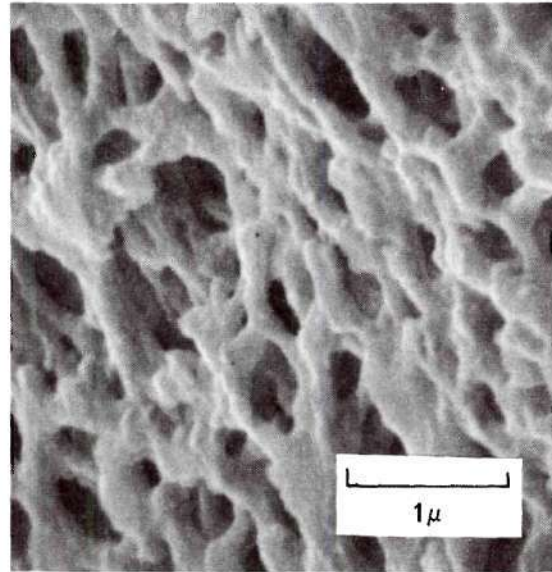


(d) Detail on ^{131}I filter

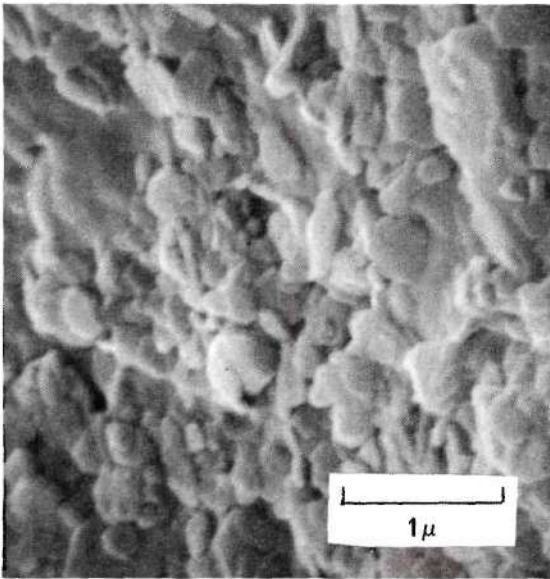
Figure 23. Bacterial Particles in ^{82}Br Effluent



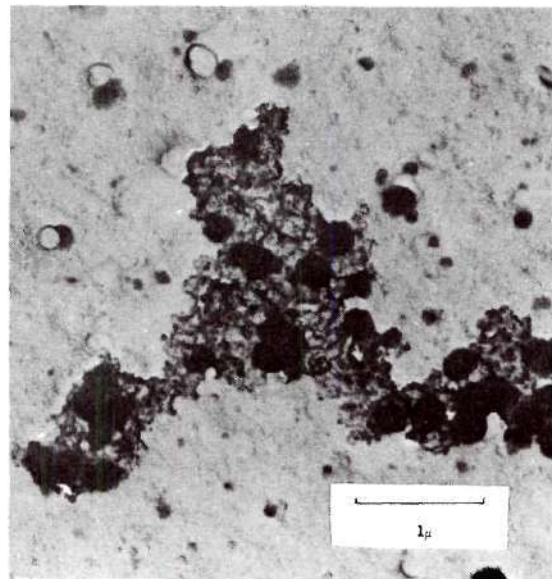
(a) Surface of 5 μ membrane filter



(b) Surface of 0.1 μ membrane filter

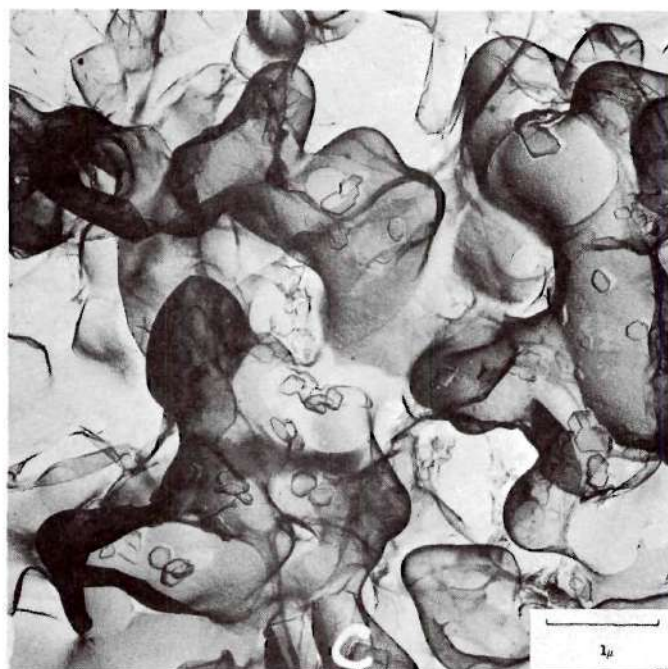


(c) ^{131}I -labeled kaolin 0.1 μ -0.45 μ diameter particles

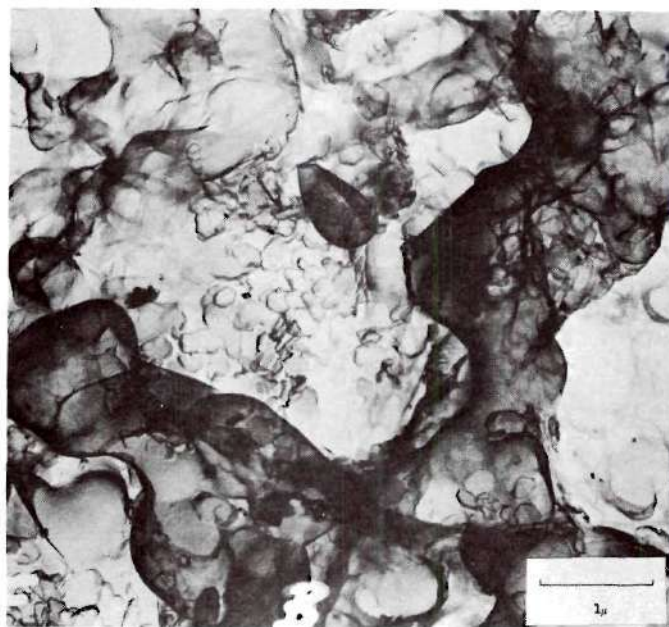


(d) Silhouette micrograph of kaolin particles trapped by 0.01 μ pass filter

Figure 24. Electron Photomicrographs of Filter Surfaces, ^{131}I Labeled Influent and Effluent Clays



(a) Individual ^{131}I kaolin particles on membrane filter



(b) Agglomerated ^{46}Sc kaolin particles on membrane filter

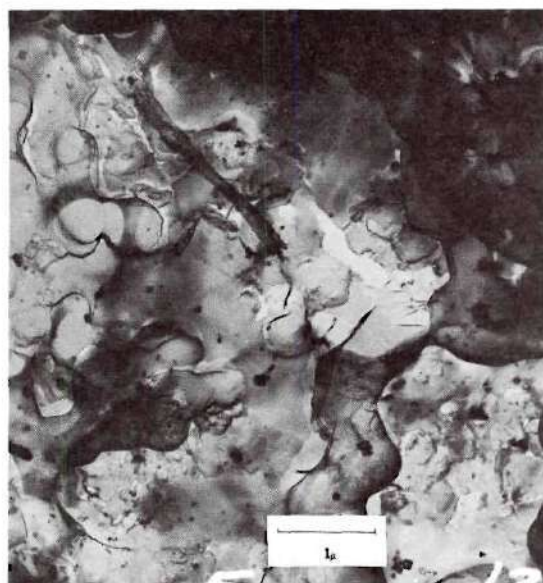
Figure 25. Comparison of ^{131}I -Kaolin and ^{46}Sc -Kaolin on 5μ Membrane Filters

the surface of a filter with little accumulation in the pores. This sample was the I^{131} -kaolin influent mixture showing individual particle action for the most part. Figure 25B shows the kaolin filtered from the ^{46}Sc -kaolin input suspension. Note the large mats of kaolin particles that have caught in the pores. Stereo exposures of these filters confirmed the presence of these mats that seem to have formed by edge to edge attachment between kaolin crystals.

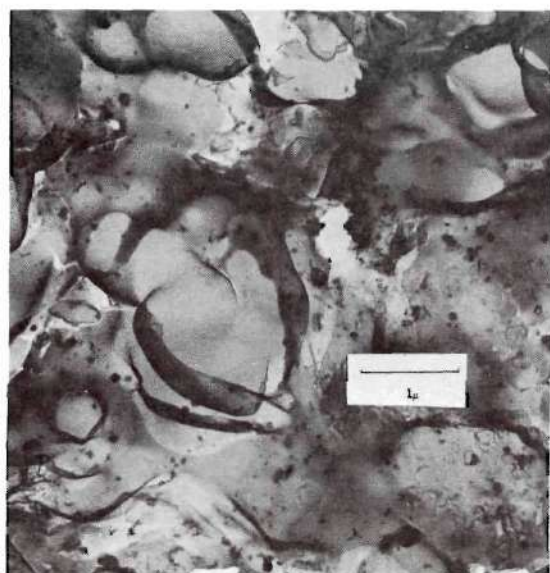
The effect of the dispersant solutions added to the bed in the effort to move the scandium was clearly demonstrated in the effluent as the displaced radioisotope (noted in Figures 16 etc.) began to discharge from the bed. The clear effluent slowly turned greenish, amber, and then dark rouge, with the darkness of the effluent color approximating the radioactivity intensity. Figure 26 shows the filtered material taken from one of the effluent samples during the release of ^{46}Sc radioactivity and strong color. In each of the pictures A, B and C, kaolin particles are seen associated with widespread coatings of finely divided material. The kaolin shapes seem blurred in some cases because of it. This material, which had the color of ochre, deposited on the filters leaving the filtrate almost colorless. After successive filtering through $5\ \mu$, $1.2\ \mu$, $0.45\ \mu$, $0.1\ \mu$ and $0.05\ \mu$ the material shown in Figure 26D was trapped on the $0.01\ \mu$ filter and the large particles shown in 26D are fragments of the filter cake this material formed. After drying the cake seemed to have little adhesion to the filter and it broke loose into shivered fragments. One of these fragments was ground in a mortar and suspended in collodion for the



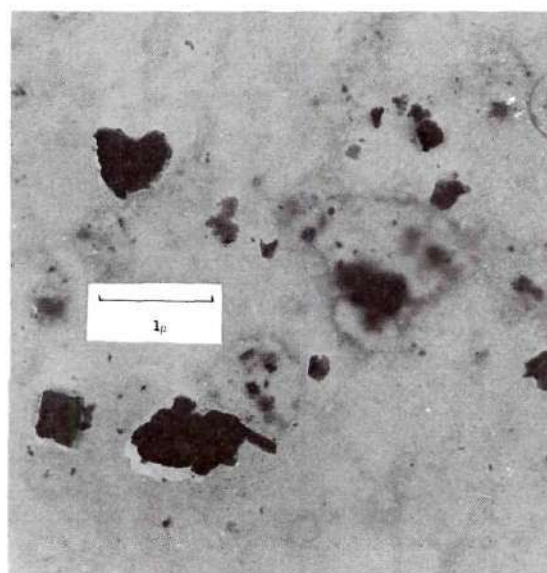
(a) Filter surface showing edge-absorbed kaolin



(b) Kaolin and filter coated with fine ochre-like material



c



(d) Detail of bed-derived particles filter cake (crushed)

Figure 26. Electron Photomicrograph of ^{46}Sc -Kaolin Effluent Suspensions on Membrane Filters

electron microscopic examination. Around these flakes are some small particles of fairly uniform size. These small particles are on the order of 70 Å in diameter.

Figure 26A shows one and possibly two examples of the clay particles attached to the filter by an edge. Note also the blurred outlines of the other kaolin particles held tight to the filter surface by their large flat sides. Figure 26B shows kaolin particles and the coating of fine material in some detail, especially in the lower center where it appears some of the fine particle coating may have broken off the buried clay particles. Figure 26C shows kaolin agglomerated with other particles. In addition little dark flakes and agglomerates can be seen that may be iron hydroxides.

CHAPTER V

DISCUSSION

It is pertinent at this point to summarize the results of this experimental work. Radioactive ions were passed in solution or dilute clay or bacteria suspensions into a simulated aquifer of carefully packed sand. Retention of all the ions in the first part of the bed was shown to fall off with distance exponentially. The degree of retention appeared to be somewhat dependent on the salinity of the water and strongly dependent on the ability of the anion of the dissolved salt to induce dispersion of finely divided particulate matter present either in the influent water or in the sand bed. By and large when the salinity of the influent water was very low, the ions and particles were strongly retained by the sand. When the salinity was high and the anion dispersive both ions and particles passed through the two meter length of the packed sand with apparent ease. Under no circumstances in these experiments was the movement of radioactive tracer ions observed without associated particulate movement.

Three different particle types were involved in the experimental work. First was a finely divided pure kaolin of restricted size range used as a special tracer. This material was labeled with scandium,⁴⁶Sc, and with iodide, ¹³¹I, at different times. Although the release of the labeled material from the sandbed differed somewhat in the two cases, the pattern of movement for the scandium-labeled clay and the iodine-labeled

clay through the packed sand, after release was obtained, was quite similar. Bacteria labeled with lanthanum, ^{140}La , showed much the same retention pattern in the beginning of the sand bed as did the labeled kaolin. No subsequent movement of the labeled bacteria was shown during the lifetime of the lanthanum isotope. However, subsequent retention of dissolved iodide ions by the sand bed so closely resembled the pattern of the lanthanum-labeled bacteria that it could be assumed the iodide was taken up by the same particles.

Later, during a stepwise increase in salinity of the influent solutions it was found that the iodide moved forward with the water as soon as the salinity approached that of a millimolar solution of NaCl . Since this is approximately the concentration of the self-made solution* that carried the bromide (^{82}Br) through the bed, associated with large quantities of suspended bacteria, it is reasonable to assume that the iodide-lanthanum labeled particles were moving forward with the water also.

With the exception of the removal of the scandium-labeled clay by use of the dispersant phosphates and carbonates, the movement of the isotopes through the sandbed was always associated with such low concentrations of dissolved salts that it would seem unlikely that the isotope movement was due to ion exchange. Rather, it would seem that the movement of the isotopes primarily was due to the movement of suspended particles that had become released from the sand bed through the influence of the increased ion concentration. Even when the scandium isotope was observed to move in the bed with solutions of 0.1 molar NaCl there seemed to be little indication that the scandium was desorbing as an ion from its

*Formed by solution of soil salts in the distilled water.

base particle through the action of the saline solution. On the contrary, such movement as was observed was associated with the movement of the tagged particles themselves.

The preparation of the clay for scandium labeling in the second experiment and that for iodine labeling differed in two important details. In removing the water during the clay concentration after careful size restrictions by filtration procedures, the clay to be used for the scandium labeling was dried down on the filter by vacuum. Although it did not reach dryness, its desiccation was much more complete than that of the clay prepared for the iodine. The iodide was dispersed by agitation in distilled water and the scandium labeled clay dispersed by agitation in 0.1 molar brine. In the theoretical section it was pointed out that distilled water dilution should tend to cause aggregation. Indeed, if the iodide-clay was ever completely dispersed, the filtering studies and laser scattering studies showed that a significant amount of the iodide clay had aggregated into sizes on the order of 1-5 microns. By like comparison, however, the presence of salt solutions should cause subsequent dispersion. However, both filter studies and laser scattering showed that the presence of particles 1-5 microns in size was common in the scandium clay in brine. Electron microscopy showed some of these particles to be mats of kaolin seemingly with the little crystals attached edge to edge.

It is difficult to say, at this point, whether the relative ease of release for the iodide-clay from retention by the bed was due to its initial better degree of dispersion than that of the scandium-clay, or if it was due to the fact that the polyvalent ions such as scandium act

to bind the particles to the surfaces of the sand through some chain like connection by means of their multivalence. Conceivably, divalent and trivalent ions could take a position between two particles or between a particle and a grain with some kind of an adsorption bond to each of them. This type of adhesion of the particles to each other or to the sand grains could only be released by replacement of the scandium by another ion which would bind the surfaces together even more tightly or by introduction of an anion that would restrict the activity of the scandium to such a degree that it was no longer capable of reacting with either or both surfaces.

In view of the fact that the iodide-clay and iodide-bacteria were released under essentially the same conditions and the knowledge from filtering and scattering studies that a significant number of large aggregates were present in the influent iodide-kaolin suspension, it is difficult to justify the assumption that the scandium is not influential in the degree of retention of the particles to which it is attached. If the two iodide release figures are compared, it can be seen that although the iodide-kaolin released at approximately the same salt concentration as the iodide presumed to be adsorbed on the lanthanum labeled bacteria, the pattern of subsequent movement is substantially different. The iodide-labeled clay moved forward as a peak with the leading edge held constant in slope very much like the scandium-clay release pattern. The iodide-bacteria particles did not move as a front but moved with little apparent inclination to readorb until the center of the bed was reached. However, the iodide-kaolin release differed from that of the scandium-kaolin in

the rapid spreading of the iodide retention peak. Data were unavailable to determine whether the iodide-kaolin peak remained symmetric as did the scandium-kaolin peak when it was moving through the sand bed.

Since the iodide-kaolin was observed to release from the sand bed at a moderate salinity, and the influent material had been shown to contain agglomerates that might have been retained by the sand bed by straining, the higher salinity must have either disassembled those agglomerates or so reduced their ability to react with the sand bed that they moved forward with the salt water. On the other hand, the scandium-labeled particles were shown to be present not only as large, labeled particle aggregates but also as significant numbers of fine particles whose size was the same as that in the original, fractionated clay. The fact that no scandium could be observed moving in the bed despite efforts to leach it with 0.1 molar salt water, and that none was observed in the effluent prior to the release by the introduction of phosphate to the bed indicate that the primary removal mechanism of the scandium-labeled particles by the sand bed was not straining but sorption. Indeed, either the two mechanisms, straining and sorption, have the same approximate retention rate or the effect of the former (at least for very fine particles)* is very overrated in the literature. The observations made on the filter membrane which (it might be presumed) effectively reproduced the same phenomenon as that produced on the sand grain surfaces would certainly support the contention that sorption was the predominant process for these

* That is, particles that are less than one percent of the size of the grains making up the sand pack.

particles of micron size or smaller.

One must consider, therefore, that the van der Waals forces holding the clay particles to the sand grains are active over a relatively large range as predicted in the theoretical section. Presumably, the only difference between the iodide-labeled and scandium-labeled clay particles (except for relative distribution of agglomerates) is the relative ability of iodide and chloride and of scandium and sodium to adsorb to surfaces. This factor controls the relative charge-induced repulsion between particles and between particles and grains.

If the assumptions made about the charge distribution on particles and the variations of that charge caused by the adsorption of ions in the theoretical section are valid, then it is pertinent at this point to consider more carefully the probable state of the material as it entered the sand bed. Approximately 10 mg of kaolin was in suspension at 2.3×10^{-16} g per particle. Roughly, that represented 4×10^{13} particles; the edge area of each being 0.2×10^{-10} cm². The total number of charge sites per particle was previously determined to be about 3000, consequently the total number of charge sites in the 10 mg would be about 1.2×10^{17} . Assuming the adsorption energy of scandium to be approximately that of aluminum, 0.75 eV, the probability of a scandium ion being away from the charge site would be 3×10^{-5} percent. Five milligrams of $\text{Sc}(\text{NO}_3)_3$ contains about 1.3×10^{19} atoms to be adsorbed on about 1.2×10^{17} sites. With its adsorption energy there would seem little question about the ability of the scandium to effectively mask the charges of the kaolin particles quite effectively.

At the time the clay, radioactive scandium salt, and sodium chloride solution were mixed, the concentration of the sodium chloride solution was 100 millimolar and the scandium nitrate was 7 micromolar. If the ratio of the number of sites occupied by the two cations is approximately equal to the ratio of their concentrations in solution raised to the reciprocal of their own respective valence, then

$$\frac{C'_{\text{Na}}}{C'_{\text{Sc}}} = \frac{[\text{Na}]^{\frac{1}{1}}}{[\text{Sc}]^{\frac{1}{3}}} \approx 5/1$$

At 3000 charge sites per particle, then 2500 would be occupied mostly by sodium ions and at any given time the number of sites unoccupied would be determined, by the Arrhenius equation, to be 8 percent or two hundred sites. This is approximately equivalent to $1 \text{ E}+13$ charges per cm^2 . Calculation of the repulsion energy between two identical particles at 80 angstroms yields about $5 \text{ E}-14$ ergs per particle compared to a predicted van der Waals attractive energy of $14.3 \text{ E}-12$ ergs/particle.

Even if all the charge sites were balanced by sodium ions instead of scandium ions, giving 8 percent of 3000 sites, the repulsion forces would not be enough to overcome the effects of the van der Waals attraction. In fact, as the range of the repulsive forces is effectively shortened by the increased salinity of the water, the probability that the van der Waals forces will be predominant over a much larger range becomes greater. Note that in Figure 3 the van der Waals forces are predominant over a wide range for high salt concentrations and over a relatively restricted range for dilute solutions. At $\text{E}-7$ molar, the separation distance over

which van der Waals forces predominate is from 0 to 160 Angstroms.

Figure 3, however, shows curves for energy of repulsion for surfaces whose charge density is about $3 \text{ E}+4 \text{ esu/cm}^2$. A particle of kaolin whose edge area (total) is $0.2 \text{ E}-10 \text{ cm}^2$ and whose total charge is 3000 charges must have a maximum of $7.2 \text{ E}+4 \text{ esu/cm}^2$. This makes a relatively minor difference in the position of the data curve for 0.1 molar. (The difference between $2.6 \text{ E}-3$ and $3.6 \text{ E}-3$ at a half distance of 40 angstroms). The total repulsion energy for such a particle would be $7.3 \text{ E}-14$ ergs or nearly double that of the thermal kinetic energy but not significantly higher than the value previously obtained. If, instead of using Lawrence's charge distribution exclusively at the edges of the particles, a lateral surface charge distribution is used, then the charge density would be even smaller and the repulsion energy, calculated by Van Olphen's equation, smaller too. As long as the total amount of charge on the particles is a constant, it is not clear from Figure 3 how dispersion could occur at a 0.1 molar concentration of salt in water solution.

Such a dispersion did occur, however, and in such a great degree that not only were the kaolin particles redispersed but so also were the very fine particles which formed the films on the sand grains. If the assumption is valid that the balance between fixed charge repulsion and van der Waals attraction is the cause of dispersion or agglomeration as one or the other predominates, then the resultant dispersion produced by the substitution of polyphosphates for the chloride ions in the influent solutions must permit the van der Waals attraction to be overcome.

If the phosphate is attracted to the lateral surfaces of the clay and contained within the first 10 angstroms of the particle surface at a concentration equal to that of the bulk solution, that would represent 260 ions per particle. With multiple negative charges on the phosphate this might increase the total particle charge by 25-30 percent. In figure 3 it can be seen that the energy gain by the introduction of the new charges might bring about repulsion at close ranges of 15 to 25 angstroms but the bulk of the curve would still underlie that of the van der Waals forces.

Figure 27 shows the relative magnitudes of the energies due to van der Waals forces and that due to coulombic forces for particles such as the model kaolin particle. As may be seen even at close range the attractive energy is a magnitude larger than the repulsive energy. The maximum range over which the van der Waals forces could be effective is shown to be the intersection of the van der Waals curve with the so-called thermal energy cut-off. It is clear from this diagram that even though the charge on the particle was increased by a magnitude, the attraction between particles and grains over most of the range would not be significantly affected.

According to the equation (45) used to determine the repulsive energy, the only place for the effect of increased charge to enter into the picture is through the term $(\gamma)^2$. For most of the calculated results shown, the value for this term ranged about 0.5 to 0.75 in Figures 3 and 27. At the most, this value could approach unity. Doubling the energy of repulsion would be most effective in the E-3 molar range. This increase might be effected by allowing either for an increased charge density on the particles themselves or by assuming a change in the water-structuring

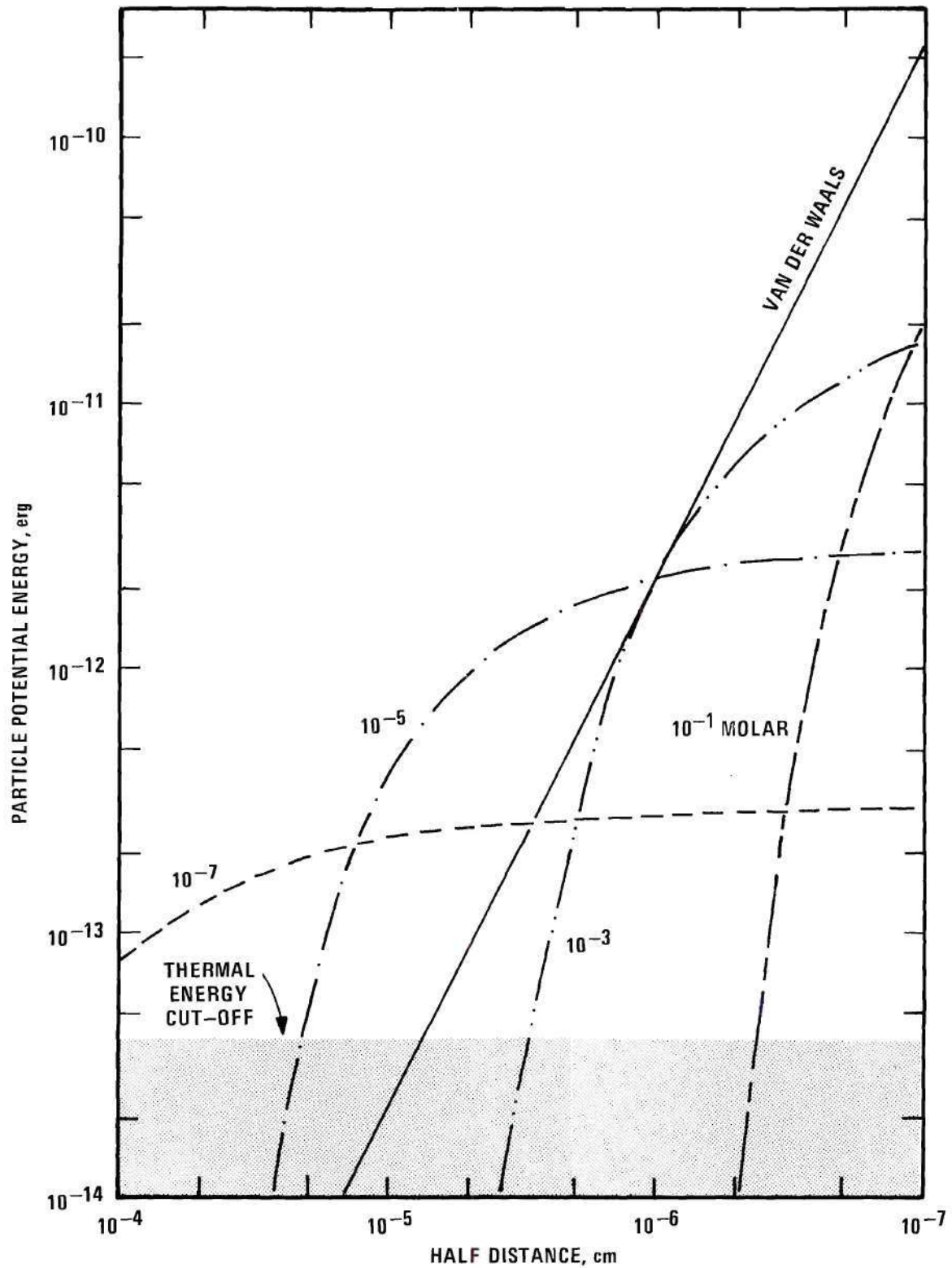


Figure 27. Energies of Interaction Conformed to Mean Particle Size of Kaolin Used in Sand Bed

brought about by the presence of strong ions in solution. The change in water structure would lower the effective value of the dielectric constant from that of the bulk solution and give rise to a larger charge effect. However, as noted above, the potential effect of this (assuming van Olphen's equations are valid) would be limited at the most to doubling the energy value.

Figure 27 shows a complex of possible interactions between the particles themselves and the particles and the quartz grains are possible, depending on distance, salt concentration, particle size and flake thickness etc. It does not explain, however, the fact that really great dispersion can be obtained at 0.1 molar concentrations if the anion of the salt used is a polyphosphate. As indicated above, the assumption of the phosphate interacting with the scandium ions is an inadequate explanation. This would also be true of the suggestion that phosphate adsorption onto the lateral surfaces of the clay gives rise to extra charges. There is a limit to the effectiveness of this charge increase and for the calculations presented in Figure 27, it is inadequate to account for the dispersion observed.

The reaction of the bed to the introduction of the phosphate solutions was to release great quantities of all kinds of particles including the special kaolin tracers. Unless some other factor was active that is not adequately accounted for here, then the only remaining possibility for this effective dispersion and displacement is for a change to have taken place in the ability of the van der Waals forces to sum and be effective over relatively large distances.

Since only the London force is being considered in the curve for van der Waals force energy in Figure 27, the effect of the phosphate would have to be through some reaction that caused the atomic oscillations in the opposing surfaces to be out of phase. This might be accomplished by the phosphate in superimposing an electromagnetic field between the surfaces that interferes with the transmission of the field resulting from the "zero-point" oscillations of the surface atoms. Or perhaps the adsorption of the phosphate to the surfaces causes changes in the oscillations themselves so that the electric fields do not sum well.

Of the two possibilities, the former would seem somewhat more likely. The action of the phosphate might be through the amplification of the retardation reaction offered as a correction to the London attraction by Casimir⁹⁷. This retardation correction normally becomes important at distances for which the time required for an electromagnetic wave to pass from one to another of two interacting atoms is on the same order as or larger than the time of revolution of the electrons. In essence when the distance between the atoms becomes comparable to the wave length of the London frequency, the London force will be markedly smaller. In flat plate interactions this amounts to the van der Waals attraction energy varying as $1/d^3$ instead of $1/d^2$. Normally this correction would become important beyond separation distances of 1000 Å, which is, as Figure 27 shows, beyond the range of effective van der Waals attraction for these particles anyway. However, the phosphate ions through their large polarizability may induce sufficient retardation to the electromagnetic fields of the

silicate surface atoms to sharply curtail the effective energy of attraction due to London-van der Waals forces. Unfortunately there is insufficient evidence here, with the present understanding of the problem to do more than speculate that this may be the answer to the effectiveness of the phosphate salts. It would seem a profitable field for further research, however.

When phosphates and other like salts are not present, Figure 27 shows that the range, over which the London-van der Waals force of attraction is either dominant or significant in reducing the repulsive forces, extends to a distance of separation of about 1500 Å ($d = 750$ Å). Because of the limiting effect of the thermal forces, this would be the maximum range of the attractive forces under the most favorable circumstances. If the probability of a particle being trapped by a unit of the sand bed is proportional to the fractional area of a pore occupied by this van der Waals attraction, then an estimation of the range of the particle in the sand bed could be obtained.

Since the probability will be greatest for the average pore of greatest restriction (obtained for example by the intersection of three spheres) in a bed of fairly homogeneously sized grains, then a mean hydraulic radius of that pore can be calculated by dividing its area by its perimeter. For this sand bed, this value of pore mean hydraulic radius is about 8.5 microns. Assuming this to be the radius of a theoretical straight smooth capillary, the ratio of the area of cross-section of the whole capillary to the area of the toroidal section in which van der Waals forces are effective gives a rough estimate of the magnitude of the mean

path length of the kaolin particles in the sand bed. For the circumstances described, this value is 28.6 cm which compares well to the value obtained from Champlin's Masters thesis of 30-35 cm.

Figure 27 suggests that particles of limited charge capacity must be especially subject to van der Waals adsorption from suspension. For a given lateral area of a kaolin particle, therefore, a thick kaolin fragment would have many more charges than a thin particle. This would have two effects. First, thicker particles would tend to "grow" at the expense of thinner ones. Second, the relative range of smaller particles suspended in ionic solutions would be less in the sand bed. Champlin's data were based on the empirically determined size range of kaolin particles from 2 microns down. The present data, based on the restricted size range of 0.1 to 0.45 micron particles, show a somewhat shorter mean path length, as might be expected from the above discussion. However, there are too many variables present in these experiments to make a specific determination of these interaction parameters useful at this time.

While kaolin particles were used in this thesis as the principal model particle, it is noteworthy at this point that the bacteria used also gave satisfactory results. In distilled water, labeled with ^{140}La they were rapidly removed by the sandbed. Being larger than the individual kaolin flakes they might have been expected to have a higher retention rate than the tiny clay particles and they did. Subsequent tagging "in-place" in the bed with ^{131}I provided the means to further consider their movements. Raising the salinity of the incoming water by steps, the bacteria were displaced at a NaCl concentration which corresponded closely

to that obtained from the fresh beds by allowing distilled water to infiltrate them⁴.

Placing $^{82}\text{Br}^-$ in the front of such an influent of distilled water showed that this was indeed the case. The ^{82}Br traveled with the water front as long as the bacterial count was high. This high bacterial count corresponded to a certain NaCl content etc. Later experiments with kaolin labeled with iodide showed similar dependency on the NaCl concentration. Consequently the general approach that the kaolin interreactions could be interpreted as being closely similar to those of the bacteria seemed justified.

The balance considered between the opposing forces and attractive forces between the particles were not intentionally restricted to van der Waals and electrostatic interactions. As shown by the more complete considerations taken up in the theoretical section, Chapter II, only these two types of interactions appeared truly significant. All the others were so much smaller that, except for completeness, they could have been covered by a single sentence or two. In addition, the results seem to substantiate that these are the two main *opposing forces* involved with these particles.

The effect of the phosphate on the system of particles adsorbed on quartz grains in water was so dramatic that essentially all the radioactivity and fine particles were removed from the bed. Subtleties of the interreactions of ions, particles and grains still remain to be interpreted, hopefully with additional experimentation and further development of basic microphysical theory. From an applications standpoint, one cannot help

noting the obvious importance of the interpretation of these experimental results in terms of waste migration in many fields, especially in the effects of massive pollution of streams and lakes.

CHAPTER VI

CONCLUSIONS

The results of these experiments clearly showed that large amounts of radioactivity can be caused to pass through a sand bed through control of the chemistry of the influent water by addition of relatively common and seemingly innocuous chemicals commonly associated with water treatment. The radioactivity passing through the sand bed was always associated with particles. In fact there seems to be little justification to any hypothesis that much of the radioactive material passed through the bed in solute form. To the contrary, the evidence is very strong that all the radioactivity passed through the sand beds used in these experiments was associated with, absorbed to, or chemically bonded to particulate matter.

The control of the movement of radioactivity through porous soils and sandy reservoirs appears to lie first with the nature of the particles themselves, secondly with the cation and anion concentrations of the suspending solutions, and lastly with the pore size distribution of the aquifer. For particles of kaolin to which could be assigned certain reasonable limits of charge repulsion and van der Waals attraction it is clear that the sand bed attraction for the particles was strong under almost all conditions of salinity. For bacterial bodies, the retention rate appeared to be similar to that of the particles of kaolin. Both types of particle were shown to be easily displaced by saline solutions and the radioactive particles migrated at nearly the same rate

through the sand bed as the water.

Stepped increases in salinity showed the greatest quantity of iodide-labeled particles to be displaced at a concentration (E-3 molar NaCl) which suggests the separation distance for the bound kaolin particles from each other or from the sand grains to be about 200 angstroms. Subsequent studies with scandium-labeled particles at a higher salinity showed it was not possible to displace particles from the bed under those conditions unless special anions such as the phosphates were used. In the presence of phosphates, not only did the introduced particles move (carrying with them the radioactivity) but also the fine films covering the quartz grains were displaced in such large numbers that the effluent was colored a dark blood red.

Comparing the van der Waals range at the thermal cut off with some measure of the capillary size in the sand pack used for the experiment seemed to be a reasonable approach to establishing a rough value for the mean free path of the particles through the sand. Under dilute and saline conditions of the water in the sand bed, this seemed to give about the same result for particle retention rate for either of the two particles used under the different conditions. Even the leading edge of the scandium-labeled clay distribution (moving through the bed as a result of the phosphate intrusion) maintained a parallel orientation to that which it had had on first being retained by the bed. This suggests that the resultant of forces acting on the particles were not materially different at low and high salinity. This parallel front represented the effect of a chemical gradient on the interaction between attractive and repulsive forces.

The results of these experiments can be viewed several ways. First they show quite conclusively that radioactivity can be and is transported through porous aquifers by the movement of particulate matter. They also show that those aquifers represent a significant restraint on the movement of particulate matter of any finite size through the action of van der Waals attractive forces. That this retention of the radioactive particles is dependent on the chemical nature of the solution passing through the bed is perhaps the most significant result of all. For through the effect of relatively dilute solutions of salt and phosphate additions, all the radioisotopes were caused to penetrate 2 meters of packed sand with negligible losses.

The importance of this observation lies in two places. First, the leakage of radioisotopes from the nuclear production and power plants into the environment may depend very strongly on the degree of addition of clay-sized minerals in the treatment of the effluent water and the overall balance and total concentration of ions in the finished product. Certainly, the combination of effects obtained by adding powdered clay and phosphates to the low level wastes at Oak Ridge (and probably elsewhere) as a final effort to try to reduce the release of strontium and cesium isotopes to the river, must be viewed critically as a result of these experiments.

Secondly, the fact that radioisotope carrying particles can be caused to pass through a sand aquifer with relatively little permanent retention strongly supports the contention that these particles could be effectively used for many hydrologic studies in which the use of tritium

is undesirable or inconvenient. The relative ease of chemical control of this movement using chemicals that are readily available everywhere and that are among the cheapest chemicals available makes the aspect of hydrologic use appear very favorable.

The results of these experiments bring to mind the paradoxical plugging problems in the secondary recovery operations in the oil fields of Wyoming, Colorado and other northern Plains States. The importance of salinity gradients pointed out here and the effectiveness of van der Waals forces under strong saline conditions have many times been borne out empirically in field investigations of the oil fields.

Several experimental techniques were used in these experiments as a means of support for the basic study. Some gave results that were frankly exciting in their potential for future research. Of these the use of laser-scattering is perhaps the most outstanding. The power of the monochromatic light in the scattered wavefronts is sufficiently high to permit many experiments on the nature of the particles and the change of the degree of aggregation with chemical conditions. Work with the electron microscope produced pictures of bacteria and clay particles of considerable clarity and detail. Under careful control of chemical conditions, the interaction of these particles with surfaces could be explored and values of interaction energies determined. The potential of the sandbed itself in studies with fine colloids, transition metal sesquioxides, lignins etc. is great, especially in the determination of how to get soils to work most effectively in the decontamination of water.

It has been said of research that it brings more questions to light than it answers. If that is the criterion, then the research that provided the supporting data for this thesis was indeed a success. Certainly, it has opened the avenues of study to many problems of sediment microphysics and chemistry. Without question, the use of radioisotopes in soil physics was a very important part of the success obtained here. Observation of particulate movement became possible through the great sensitivity with which the radioactively tagged particles can be detected.

These results are those of the examination of a phenomenon. The theory offered helps explain what was originally observed and was useful in the design of experiments that would amplify the phenomenon of particle movement and make it unquestionable. That particle movement with the radioactivity takes place has been shown. The remaining work lies in more thorough testing of the theory to develop a better one that more completely fits the facts. From such studies, hopefully, will come a major improvement in the quality of the water resources of the world as well as the fundamental physics of microparticle interactions.

BIBLIOGRAPHY

1. Templin, L. J., ed., Reactor Physics Constants, ANL-5800, 2nd edn. U.S. Atomic Energy Commission, Washington, D. C., 1963.
2. Amphlett, C. B., Treatment and Disposal of Radioactive Wastes, Pergamon Press, New York, 1961.
3. Straub, C. P., Low-Level Radioactive Wastes, Treatment, Handling, Disposal, USAEC, Division of Technical Information, U. S. Government Printing Office, Washington, D. C., 1964.
4. Champlin, J. B. F., "The Movement of Micron-Size Particles Through a Sand Bed," Georgia Tech Water Resources Report WRC-0867, December 1967.
5. Christenson, C. W., E. B. Fowler, G. L. Johnson, E. H. Rex, and F. A. Virgil, "Soil Adsorption of Radioactive Wastes at Los Alamos," Sewage and Industrial Wastes 30, 1478-1489, 1958.
6. Jacobs, D. G. and T. Tamura, "Mineral Reactions Pertinent to the Treatment and Disposal of Radioactive Wastes," USAEC TID-7613, 691-718, 1960.
7. Jacobs, D. G. and T. Tamura, "Soil Disposal of Intermediate Level Waste," USAEC Rept. ORNL-2590, 1958.
8. Honstead, J. F., J. L. Nelson, B. W. Mercer, and W. A. Haney, "Waste Fixation on Minerals," Fixation of Radioactivity in Stable, Solid Media, USAEC TID-7613, 623-640, 1960.
9. Ames, L. L., Jr., L. B. Sand, and S. S. Goldich, "The Hector California Bentonite Deposits," Economic Geology 53, 22-37, 1958.
10. Ames, L. L., Jr., "Zeolitic Extraction of Cesium from Aqueous Solutions," USAEC HW-62607, 1959.
11. Ames, L. L., Jr., "The Cation Sieve Properties of Clinoptilolite," American Mineralogist 45, 689-700, 1960.
12. Auerbach, S. I., D. A. Crossley, Jr., P. B. Dunaway et al., "Radioactive Waste Area and Radiation Effects Studies," USAEC Rept. ORNL-3492, 81-95, 1963.

BIBLIOGRAPHY (Continued)

13. Christenson, C. W. and R. G. Thomas, "Movement of Plutonium Through Los Alamos Tuff," Second Ground Disposal of Radioactive Waste Conference, USAEC TID-7628, 248-281, 1962.
14. Hawkins, D. B., "Mineral Reaction Studies at National Reactor Testing Station," The Use of Inorganic Exchange Materials for Radioactive Waste Treatment, USAEC TID-7644, 151-175, 1963.
15. Lomenick, T. F., "Movement of Ruthenium in the Bed of White Oak Lake," Health Physics 9, 835-845, 1963.
16. Fletcher, O. M., I. L. Jenkins, F. M. Kever, et al., "Nitrate and Nitrocomplexes of Nitrosyl Ruthenium," Journal of Inorganic and Nuclear Chemistry 1, 378-401, 1955.
17. Jones, R. F., "The Accumulation of Nitrosyl Ruthenium by Fine Particles and Marine Organisms," Limnology and Oceanography 5 (3), 312-325, 1960.
18. Iwashima, K. and N. Yamagata, "Environmental Contamination with Radioruthenium," Journal of Radiation Research (Japan) 7, 91-111, 1966.
19. Larson, K. H., J. W. Neel, et al., "Distribution Characteristics and Biotic Availability of Fallout, Operation Plumbob," UCLA Lab of Nuclear and Radiation Biology, Rept. WT-1488, 1966.
20. Anonymous, "Final Report of an Investigation on the Degree of Activity Associated with Particulate Solids of Different Particle Size Removed from Large Volume, Low-Level Radioactive Process Waste at ORNL," USAEC Rept. ORO-453, 1961.
21. Perkins, E. J. and B. R. H. Williams, "The Biology of the Solway Firth in Relation to the Movement and Accumulation of Radioactive Materials. II: The Distribution of Sediments and Benthos," United Kingdom Atomic Energy Authority, Production Group Rept. PG-587(CC), 1966.
22. Johnson, V., N. Cutshall and C. Osterberg, "Retention of ^{65}Zn by Columbia River Sediment," Water Resources Research 3 (1), 99-102, 1967.
23. Eichholz, G. G., T. F. Craft and A. N. Galli, "Trace Element Fractionation by Suspended Matter in Water," Geochimica et Cosmochimica Acta 31, 737-745, 1967.

BIBLIOGRAPHY (Continued)

24. Black, A. P. and C. Chen, "Electrophoretic Studies of Coagulation and Flocculation of River Sediment Suspensions with Aluminum Sulfate," Journal American Water Works Association 57 (3), 354-362, 1965.
25. Black, A. P. and A. L. Smith, "Suggested Method for Calibration of Briggs Electrophoresis Cells," Jour. AWWA 58 (4), 445-454, 1966.
26. Nelson, R. W. and D. B. Cearlock, "Analysis and Predictive Methods for Groundwater Flow in Large Heterogeneous Systems," Proceedings of the National Symposium on Ground-Water Hydrology, American Water Resources Association, Urbana, Illinois, 301-318, 1967.
27. Champlin, J. B. F., "Research on Field Problems on Injecting Solutions Into Permeable Rocks," USAEC Rept. TID-7628, 324-346, 1962.
28. Champlin, J. B. F. and R. D. Thomas, "Separation by Ultrasonic Elutriation and Analysis of the Fine Particles in Sandstone," Journal of Sedimentary Petrology 36, 1152-1156, 1966.
29. Camp, T. R., "Theory of Water Filtration," Journal of the Sanitary Engineering Division, Proceedings of the American Society of Civil Engineers 90, 1-30, August 1964.
30. Warner, D. L., "Deep Well Waste Injection - Reaction with Aquifer Water," Jour. San. Eng. Div., Proc. Am. Soc. Civ. Eng. 92, 45-69, August 1966.
31. Davis, E. and J. A. Borchardt, "Sand Filtration of Particulate Matter," Jour. San. Eng. Div., Proc. Am. Soc. Civ. Eng. 92, 47-60, October 1966.
32. O'Melia, C. R., "Sand Filtration of Algal Suspensions," Ph.D. Thesis, University of Michigan, Ann Arbor, Michigan, 1963.
33. Hall, W. A., "An Analysis of Sand Filtration," Jour. San. Eng. Div., Proc. Am. Soc. Civ. Eng. 83, Paper 1276, 1957.
34. Stanley, D. R., "Sand Filtration Studied with Radiotracers," Jour. San. Eng. Div., Proc. Am. Soc. Civ. Eng. 81, Paper 592, 1955.
35. Bush, A. F. and J. D. Isherwood, "Virus Removal in Sewage Treatment," Jour. San. Eng. Div., Proc. Am. Soc. Civ. Eng. 92, 99-107, February 1966.
36. Robeck, G. C., N. A. Clarke and R. A. Dastal, "Effectiveness of Water Treatment Processes in Virus Removal," Jour. AWWA 54, Part 2, 1275-1290, 1962.

BIBLIOGRAPHY (Continued)

37. Pelczar, M. J., Jr. and R. D. Reid, Microbiology, 2nd. edn., McGraw-Hill Book Co., Inc., New York, 1962.
38. Eliassen, R., P. Kruger, and W. Drewry, "Studies on the Movement of Viruses in Groundwater," Annual Progress Report, Water Quality Control Research Laboratory, Stanford University to the Commission on Environmental Hygiene of the Armed Forces Epidemiological Board, U. S. Army Medical Research and Development Command, Dept. of the Army, Washington, D. C., Contract No. DA-49-193-MD-2324, February 1964 to March 1965.
39. Corey, G. L., A. T. Corey and R. H. Brooks, "Similitude for Non-Steady Drainage of Partially Saturated Soils," Hydrology Paper No. 9, Colorado State University, Fort Collins, Colorado, August 1965.
40. Filmer, R. W. and A. T. Corey, "Transport and Retention of Virus-Sized Particles in Porous Media," Sanitary Engineering Paper No. 1, Colorado State University, Fort Collins, Colorado, June 1966.
41. Brooks, R. H. and A. T. Corey, "Hydraulic Properties of Porous Media," Hydrology Paper No. 3, Colorado State University, Fort Collins, Colorado, March 1964.
42. Champlin, J. B. F., and G. G. Eichholz, "The Movement of Radioactive Sodium and Ruthenium Through a Simulated Aquifer," Water Resources Research 4 (1), 147-158, 1968.
43. Dvyagintsev, D. G., "Adsorption of Microorganisms by Soil Particles," Soviet Soil Science 13, 140-144, 1962.
44. Krone, R. B., G. T. Orlob and C. Hodgkinson, "Movement of Coliform Bacteria Through Porous Media," Sewage and Industrial Wastes 30 (1), 1-13, 1958.
45. Carlson, G. F., Jr., F. E. Woodard, D. F. Wentworth and O. J. Sproul, "Virus Inactivation on Clay Particles in Natural Waters," Journal of Water Pollution Control 40 (2) part 2, R89-R106, February 1968.
46. Bailey, G. W. and J. L. White, "Review of Adsorption and Desorption of Organic Pesticides by Soil Colloids, with Implications Concerning Pesticide Bioactivity," Agricultural and Food Chemistry 12, 324-332, 1964.
47. Bailey, G. W., "Entry of Biocides into Watercourses," Proceedings of The Symposium on Agricultural Waste Waters, Water Resources Center, University of California, Davis, Calif. Rept. No. 10, 94-103, 1966.

BIBLIOGRAPHY (Continued)

48. Bailey, G. W., "Role of Soils and Sediment in Water Pollution Control: Part I, Reactions of Nitrogenous and Phosphatic Compounds with Soils and Geologic Strata," U. S. Department of the Interior, Federal Water Pollution Control Administration, Southeast Water Laboratory, March 1968.
49. Bailey, G. W., J. L. White and T. Rothberg, "Adsorption of Organic Herbicides by Montmorillonite: Role of pH and Chemical Character of Adsorbate," Soil Science Society of America Proceedings 32, (2), 222-234, 1968.
50. Scalf, M. R., V. L. Hauser, L. G. McMillion, W. J. Dunlap and J. W. Keeley, "Fate of DDT and Nitrate in Ground Water," U. S. Dept. of Interior Robert S. Kerr Water Research Center and U. S. Dept. of Agriculture, Southwestern Great Plains Research Center, April 1968.
51. Essington, E. H. and H. Nishita, "Effect of Chelates on the Movement of Fission Products Through Soil Columns," Plant and Soil XXIV (1), 1-23, 1966.
52. Nishita, H. and E. H. Essington, "Effect of Chelating Agents on the Movement of Fission Products in Soils," Soil Science 103 (3), 168-176, 1967.
53. Lawrence, W. G., ed., Clay-Water Systems, The Ceramic Association of New York, Alfred University, Alfred, New York, 1965.
54. Moeller, T., Inorganic Chemistry, John Wiley and Sons, New York, 1952.
55. Weast, R. C., S. M. Selby, C. D. Hodgman, Handbook of Chemistry and Physics, 45th edn. The Chemical Rubber Co., Cleveland, Ohio, 1965.
56. London, F., "The General Theory of Molecular Forces," Transactions of The Faraday Society 33, 8-26, 1937.
57. Bernal, J. D. and R. H. Fowler, "A Theory of Water, with Particular Reference to Hydrogen and Hydroxyl Ions," Journal of Chemical Physics 1, 515-548, 1933.
58. Gaudin, A. M., Flotation, 2nd edn. McGraw-Hill Book Co., Inc., 1957.
59. Pauling, L., The Nature of the Chemical Bond, 3rd edn. Cornell Univ. Press, Ithaca, New York, 1960.
60. Bernal, J. D., "The Structure of Liquids," Scientific American 203, 124-134, August 1960.

BIBLIOGRAPHY (Continued)

61. Sebba, F., Ion Flotation, Elsevier Publishing Co., New York, 1962.
62. Anonymous, Flotation Fundamentals, The Dow Chemical Company, Michigan, 1958.
63. Danielli, J. F., K. G. A. Pankhurst, and A. C. Riddiford, Recent Progress in Surface Science I and II, Academic Press, New York, 1964.
64. Plaksin, I. N., Flotation Properties of Rare Metal Minerals, Primary Sources, New York, 1967.
65. Muskat, M., Physical Principles of Oil Production, McGraw-Hill Book Co., Inc., New York, 1949.
66. Eichholz, G. G., R. B. Hughes, and A. E. Nagel, "Adsorption of Ions in Dilute Aqueous Solutions on Glass and Plastic Surfaces," Georgia Institute of Technology, Nuclear Engineering Series, Technical Report NE-2, September 1964.
67. Robinson, R. A. and R. H. Stokes, Electrolyte Solutions, 2nd edn., Academic Press, Inc., New York, 1959.
68. Brown, R. A., "Additional Remarks on Active Molecules," Philosophical Magazine VI (Series 2), 161-166, 1829.
69. Perrin, J., Atoms, Translated by D. L. Hammick, Constable and Co., Ltd., London, 1923.
70. Kruyt, H. R., ed., Colloid Science I, Elsevier Publ. Co., New York, 1952.
71. Sheludko, A., Colloid Chemistry, Elsevier Publ. Co., New York, 1966.
72. Lapple, C. E., Fluid and Particle Mechanics, University of Delaware, Newark, Delaware, 1951.
73. Keesom, W. H., "Die van der Waalsschen Kohäsionskräfte," Physikalische Zeitschrift 22, 129-141, 1921.
74. Debye, P., "Die van der Waalsschen Kohäsionskräfte, Molekularkräfte und ihre elektrische Deutung," Phys. Z. 21, 178-187, 1920; 22, 302-308, 1921.
75. de Boer, J. H., "The Influence of Van der Waals' Forces and Primary Bonds on Binding Energy, Strength and Orientation, with Special Reference to Some Artificial Resins," Trans. Farad. Soc. 32, 10-38, 1936.

BIBLIOGRAPHY (Continued)

76. Prock, A. and G. McConkey, Topics in Chemical Physics, (The Harvard Lectures of Peter Debye), Elsevier Publ. Co., New York, 1962.
77. Pitzer, K. S., "Inter-and Intramolecular Forces and Molecular Polarization," Advances in Chemical Physics II, Interscience Publ. Inc., New York, 1959.
78. Klassen, V. I. and V. A. Mokrousov, An Introduction to the Theory of Flotation, Butterworth and Co., (Publishers) Ltd., London, 1963.
79. Goldschmidt, V. M., "Crystal Structure and Chemical Constitution," Trans. Farad. Soc. 25, 253-283, 1929.
80. Stern, O., "Zur Theorie der Elektrolytischen Doppelschicht," Zeitschrift für Elektrochemie 30, 508-516, 1924.
81. Grim, R. E., Clay Mineralogy, McGraw-Hill Book Co., Inc., New York, 1953.
82. van Olphen, H., Clay Colloid Chemistry, Interscience Publishers, New York, 1963.
83. Hamaker, H. C., "A General Theory of Lyophobic Colloids. I," Recueil des Travaux Chimiques des Pays-Bas, 55, 1015-1026, 1936.
84. Hamaker, H. C., "A General Theory of Lyophobic Colloids. II," Rec. Trav. Chim. 56, 3-25, 1937.
85. Hamaker, H. C., "The London-Van Der Waals Attraction between Spherical Particles," Physica IV, (10), 1058-1072, 1937.
86. Hamaker, H. C., "The London-Van Der Waals Forces in Colloidal Systems," Rec. Trav. Chim. 57, 61-72, 1938.
87. Robie, R. A. and Bethke, P. M., "Molar Volumes and Densities of Minerals," U. S. Dept. of the Interior, Geological Survey Rept. TEI-822, July 1962.
88. Weaver, C., Dept. of Geology, Georgia Institute of Technology, Atlanta, Georgia, Personal Communication, 1969.
89. Hasted, J. B., D. M. Ritson, and C. H. Collie, "Dielectric Properties of Aqueous Ionic Solutions," The Journal of Chemical Physics 16 (1), 1-21, 1948.

BIBLIOGRAPHY (Concluded)

90. Button, D. D. and W. G. Lawrence, "Effect of Temperature on the Charge on Kaolinite Particles in Water," Journal of the American Ceramic Society 47 (10), 503-509, 1964.
91. Stout, E., ed., Isotope Techniques in the Hydrologic Cycle, Geophysical Monograph Series No. 11, American Geophysical Union, NAS-NC Pub. 1488, William Byrd Press, Inc., Richmond, Va., 1967.
92. Welcher, F. J., The Analytical Uses of Ethylenediamine Tetraacetic Acid, D. Van Nostrand Co., Inc., Princeton, New Jersey, 1957.
93. Lawrence, W. G., Alfred University, Alfred, New York, Personal Communication, 1969.
94. Fyfe, W. S., Geochemistry of Solids, McGraw-Hill Book Co., Inc., New York, 1964.
95. Latimer, W. M., K. S. Pitzer and C. M. Slansky, "The Free Energy of Hydration of Gaseous Ions, and the Absolute Potential of the Normal Calomel Electrode," J. Chem. Phys. 7, 108-111, 1939.
96. Merten, U., ed., Desalination by Reverse Osmosis, The M.I.T. Press, Cambridge, Massachusetts, 1966.
97. Casimir, H. B. G. and D. Polder, "The Influence of Retardation on the London-van der Waals Forces," Physical Review 73, (4), 360-372, 1948.

VITA

Jerry B. Francis Champlin was born in Salamanca, New York on April 27, 1928, and resided with his parents in Little Valley, New York until 1942. He attended prep school at Peddie, Hightstown, New Jersey, graduating in 1945. After one year of college at Massachusetts Institute of Technology, he served two years in the U. S. Navy with duty in the harbor of Tsing Tao, China. Returning to M.I.T. in 1948, he majored in quantitative biology and minored in geology. Graduating from there in 1951 he did post-graduate work in geology and geophysics. He was subsequently employed with Standard Oil of New Jersey in Columbia, South America as an assistant geologist. Later he worked as a geophysicist for Geophysical Service Inc. of Dallas, Texas, as a physics instructor at The Citadel, Charleston, S.C., and as a geochemist for the U. S. Bureau of Mines, Petroleum Research Center, Bartlesville, Oklahoma, where he performed research on the "origin of petroleum", rock core analysis, corrosion, and "nuclear waste disposal in the geologic depths". He came to Georgia Institute of Technology as an employee of the Engineering Experiment Station in 1964 to work in radio-isotope applications research. He completed his Master of Science degree in 1968 in the School of Nuclear Engineering at Georgia Tech while developing the topic for his Degree of Doctor of Philosophy.

Mr. Champlin is married and has five children. He has authored several papers on diverse topics concerned with his fields of interest and

has reviewed several books on hydrologic uses of radioactivity. He is a member of the Society of Sigma Xi and won the Sigma Xi award for best engineering thesis for the MS degree at Georgia Tech in 1968.